4 - 9017

Golder Associates
CONSULTING GEOTECHNICAL AND MINING ENGINEERS

REPORT TO
CANMET

DEVELOPMENT AND USE OF TRIAXIAL ROCK TESTING PROCEDURES FOR SAMPLES OF THE SYDNEY COALFIELD PHASES ONE AND TWO

SYDNEY NOVA SCOTIA

DSS CONTRACT NO. OSQ84-00214

Distribution:

10 copies - Cape Breton Coal Research Lab.
Sydney, Nova Scotia

1 copy - Univeristy of Toronto
Toronto, Ontario

2 copies - Golder Associates
Mississauga, Ontario

MICROMEDIA

186 pp

March 1985 841-1287

GOLDER ASSOCIATES (EASTERN CANADA) LTD. • 3151 WHARTON WAY, MISSISSAUGA, ONTARIO, CANADA L4X 2B6 • TELEPHONE (416) 625-0094 • TELEX 06-961136
OFFICES IN CANADA • UNITED STATES • UNITED KINGDOM • AUSTRALIA

REPORT TO
CANMET

DEVELOPMENT AND USE OF TRIAXIAL ROCK TESTING PROCEDURES FOR SAMPLES OF THE SYDNEY COALFIELD PHASE ONE

SYDNEY NOVA SCOTIA

DSS CONTRACT NO. OSQ84-00214

March 1985

841-1287

TABLE OF CONTENTS

		Page No.
1.0	INTRODUCTION	1
2.0	BACKGROUND DATA	2
3.0	TEST PROGRAM	5
4.0	LABORATORY EQUIPMENT	6
4.1	Reference Material	6
4.2	Testing Machine and Equipment	6
4.3	Instrumentation	7
4.4	Servo-Controlled System for Simultaneous Loading and Unloading	8
5.0	TEST PROCEDURES AND RESULTS	10
5.1	Aspect No. 1 - Strength Characteristics of Pier Cap Sandstone and Rate Effect	10
5.2	Aspect No. 2 - Multistage Triaxial Testing	11
5.3	Aspect No. 3 - Calibration of the Procedures for Simultating Stress Changes	14
5.4	Aspect No. 4 - Effects of Stress Paths on Strength and Failure Mode	15
5.5	Aspect No. 5 - Introduction of Pore Gas Pressure	16
6.0	DISCUSSION OF TEST RESULTS	18
6.1	Strength Characteristics of Pier Cap Sandstone and Rate Effect	18
6.2	Establishment of a Multistage Testing Procedure	19
6.3	Effect of Stress Path	20
6.4	Effect of Gas Pressure	20
7.0	CONCLUSIONS AND RECOMMENDATIONS FOR PHASE 2	23
	ACKNOWLEDGEMENTS	26
	REFERENCES	27

LIST OF TABLES

1. Testing Program for Phase 1

2. Physical Properties of Pier Cap Sandstone and Dimensions of Test Specimens

3. Summary of Test Results, Intact Samples, Aspect No. 1, Slow Stress Rate

4. Summary of Test Results, Intact Samples, Aspect No. 1, Moderate Stress Rate

5. Summary of Test Results, Intact Samples, Aspect No. 1 Rapid Stress Rate

6. Summary of Test Results, Failed Samples, Aspect No. 1

7. Summary of Test Results, Strain Measurements, Samples 5 and 13, Aspect No. 2

8. Summary of Test Results, Determination of Failure Envelope (MST), Aspect No. 2

9. Summary of Test Results, Multistage Tests, Samples 29 and 30, Aspect No. 2

10. Summary of Test Results, Aspect No. 3

11. Summary of Test Results, Stress Change Simulation, Aspect No. 4

12. Summary of Test Results, Rapid Confining Pressure Reduction, Aspect No. 4

13. Summary of Test Results, Strength Characteristics of Samples with Pore Gas Pressure, Aspect No. 5

14. Summary of Test Results, Uniaxial Compression, Aspect No. 5

15. Summary of Test Results, Rapid Reduction of Confining Pressure, Samples with Pore Gas Pressure, Aspect No. 5

16. Proposed Test Program for Phase 2

LIST OF FIGURES

1. Proposed MTS σ_3 Servo Controlled System

2. Strength Envelopes of Intact Specimens of Pier Cap Sandstone at 3 Stress Rates

3. Strength Envelope of Failed Specimens of Pier Cap Sandstone

4. Stress Paths of ISRM and Proposed Multiple Stage Triaxial Tests

5. Stress-strain Relationship of Pier Cap Sandstone

6. Examination of Various Imminent Failure Criteria - Specimen 5

7. Examination of Various Imminent Failure Criteria - Specimen 13

8. Strength Envelopes of Pier Cap Sandstone Single Stage and Multistage Triaxial Tests

9. Stress Path of Calibration Tests

10. Stress Changes Simulations

11. Rapid Reduction of Confining Pressure

12. Strength of Specimens with Pore Gas Pressure

13. Rapid Reduction of Confining Pressure Specimens with Pore Gas Pressure

14. Correlation Between Failure Mode and Stress Condition at Failure, Specimens with Pore Gas Pressure

LIST OF PLATES

Plate 1 MTS Testing Equipment

Plate 2 Special Platens for Testing Samples with Pore Gas Pressure

Plate 3 Strain Gauges on Specimen 29

Plate 4 Flaky Broken Pieces of Specimen 48 after Bursting. (Intact Specimen Shown for Comparison Purpose)

Plate 5 Specimen 14

Plate 6 Specimen 18

Plate 7 Specimen 56

Plate 8 Specimen 49

1. INTRODUCTION

Golder Associates, in association with the University of Toronto, was awarded a research contract from the Department of Supply and Services (DSS Contract No. OSQ-84-00215) to develop a triaxial rock testing procedure for testing samples from the Sydney Coalfield which has experienced difficulties in the development of access roadways due to outburst phenomena.

The specific factors required to be addressed in the program include:

(a) the behaviour of the rock strata under the dynamic stress regime (stress changes) around the underground opening

(b) the effect of gas pressure within the pores of the rock material, and

(c) the rate effects of (a) and (b)

The project is divided into two phases. Phase 1 entails the development of the triaxial testing equipment and techniques based on samples from a "reference material" and Phase 2 consists of testing samples from No. 26 or other Colliery using the procedures developed in Phase 1.

This report summarizes the results of the Phase 1 study including the experimental procedure and the techniques developed, and the problems encountered while testing the reference material. A suggested program for Phase 2 is also presented.

2. BACKGROUND DATA

In connection with the outburst problems in No. 26 Colliery, the Cape Breton Development has compiled outburst records based on field observations and measurements. The salient points that we have noted from these records are summarized below.

- A total of 37 outbursts of various scales have occurred in No. 26 Colliery to date. The first burst occurred in 1977 at a depth of 703 m below seabed. All the outbursts occurred between 703 m and 790 m depth.

- The number of occurrences appeared to increase with depth.

- In the earlier events (prior to June 1983) gas was neither detected nor recorded but in recent events, a substantial volume of gas was detected.

- The bursting formation is invariably sandstone with interbeds of siltstone when it occurs on coal or within 3 m of coal. The failed material was generally pulverized or consisted of small flakes. The failure surfaces, as exposed after the most recent outburst at the main deeps, were typical of surfaces resulting from intense shear failure.

- Sandstone appeared intact when cored but core disking was noted in the holes drilled into the pillar adjacent to the main deeps.

- No correlation with respect to the type of material fired. Bursting generally occurred upon creation of the opening. All but one of the outbursts were induced by shotfiring.

- All outbursts took place in development roadways with no preferential directions.

- All outbursts appeared to have been initiated away from the face (i.e. above or ahead of the face).

- The mechanical properties of the strata are as follows:
  Sandstone = 83 MPa (12,000 psi)
  Siltstone = 55 MPa (8,000 psi)

Rock Burst as a Result of Overstress

The condition necessary for a burst requires that the stresses in the rock exceed its strength. Following the excavation of an underground opening, the ground stresses are redistributed around the opening due to the presence of the fracture zone and inelastic zone; the point of maximum stress concentration moves away from the face.

The stress concentration factor may be as high as four times the insitu stress values[1] . At the depth where rock bursts were observed in No. 26 Colliery, the insitu stress ranged from about 20 MPa (2,900 psi) to 24 MPa (3,500 psi). Hence, the maximum stress concentration may amount to 80 to 96 Mpa (11,600 to 14,000 psi), which is close to the intact strength of the sandstone of about 83 MPa (12,000 psi). Since the rock mass strength of sandstone would be lower than the intact strength determined from laboratory samples, rock failure is therefore imminent at the point of maximum stress concentration.

The phenomenon of core disking is also indicative of a high stress regime around the drillhole. The critical stress level for core disking to occur is a function of the stresses around the drillhole and the shear strength of the rock.

Gas Outburst

Gas outburst occurs when, in the course of mining, gas under pressure is released in substantial quantity*. The event is often accomplished by a rock failure which in many instances

* To be a true outbrust, gas pressure must contribute to failure. This distinguishes "bursts" from "blowers"

is violent. Gas outbursts are most commonly experienced in mining coal. The gas is absorbed primarily in the pore structure of coal, but migrates only through fractures, partings, joints, cleats, etc. Since coal is relatively impermeable, attempts to drain (bleed off the gas through boreholes) have been relatively ineffective except in a small area.

The outburst phenomena in No. 26 Colliery might be initiated by rock failures at some point ahead and above the face. This, when coupled with the presence of pressurized gas in the bursting formation would, in general, aggravate the situation by causing more violent expulsion of the material.

The strength characteristics of the bursting formation under the pertinent field stress conditions, the effect of gas pressure in the formation and their interacting effects are, therefore, fundamental parameters which have to be addressed in order to further understand the mechanism of outbursts at No. 26 Colliery. The program of triaxial tests undertaken in this study is designed to provide the necessary data base for a broader research frame work in this area.

3. TEST PROGRAM

The central purpose of the project is to study the strength characteristics of the rock burst prone strata at the No. 26 Colliery and other mines in the Sydney Coalfield. In Phase 1 of this research project, a reference material was tested in order to refine and/or develop the procedures that would be used in the second phase. The aspects to be studied in the Phase 1 test program are outlined below.

(a) the development of suitable testing techniques to meet the specific requirements of the project on the basis of established triaxial testing procedures;

(b) The calibration of a multi-stage testing technique to optimize the number of samples for the second phase;

(c) the calibration of a procedure for simulating the dynamic stress regimes resulting from the development of underground openings in the rock burst prone strata; and

(d) the development of a suitable testing system whereby gas pressure could be introduced into the pores of the specimens under various triaxial loading/unloading conditions.

Table 1 presents the details of the testing features for each of the above aspects of the program. All the laboratory tests were carried out at the rock mechanics laboratory of the University of Toronto by Mr. D. Lau under the overall direction of Dr. A. Crawford.

4. LABORATORY EQUIPMENT

This section describes the reference material and equipment used for the first phase of the testing program.

4.1 Reference Material

The reference material used in this phase of the research project is a light-grey, homogeneous, medium grained, Pier Cap Sandstone obtained from a local stone supplier. The sandstone was supplied in the form of a slab about 700 x 700 x 76 mm (27 x 27 x 3 inches) in dimensions.

The slabs were cut into beams of 700 x 176 x 76 mm (27 x 7 x 3 inches). Specimens of NX size (54 mm, 2.125 inches dia.) were cored from these beams, in accordance with ISRM* Standards[2] (L/D ratio ranging between 2 to 3). All cores were cut to a length of about 125 mm (5 inches), yielding an aspect ratio (L/D) of approximately 2.35. The ends were prepared using a Harig 612 automatic grinder. The length of the specimens was designed to match the dimension of the Hoek triaxial cell. For the tests with internal gas pressure, the specimens were cut to about 115 mm (4.5 inches) in length (L/D=2.11) in order to accommodate the special platens. Table 2 summarizes the physical properties and dimensions of the specimens tested.

4.2 Testing Machine and Equipment

For tests performed using slow (300 seconds to failure) or moderate (2 MPa/s) loading rates, the 1.2 MN Louis Small C-CP250 Concrete Tester was used. For tests with loading rates of 21.9 to 43.7 MPa/s, the 5.0 MN capacity servo-controlled MTS machine was used (Plate 1).

---

* International Society of Rock Mechanics

The Hoek triaxial cell was used in all cases. The maximum core size that can be accommodated in the cell is 57 mm dia. x 127 mm. Two special platens were fabricated to facilitate testing with internal gas pressure. These platens are 57 mm dia. x 127 mm right circular steel cylinders with a passage drilled through the centre and an exit from the side (see Plate 2). Circular grooves were cut at one end (the end in contact with the specimen) for even distribution of gas pressure which was supplied via a nitrogen bottle. High pressure tubings were used for conducting the gas and all connections were checked for leakage using soap solution prior to any testing.

4.3 Instrumentation

For the slow and moderate rate tests, the axial and confining stresses were measured using pressure gauges. Prior to testing, the pressure gauge in the Louis uniaxial compression rig was calibrated using a load cell. The calibration indicated that the pressure gauge was accurate to within ±1%. For tests performed via the MTS machine, the axial load was measured by a load cell that was built in within the actuator.

Resistance wire strain gauges were used to monitor the axial, lateral and the volumetric strains in the samples during the multi-stage triaxial tests. For each sample, two sets of strain gauges were installed at the mid-height and diagonally opposite to each other. Each set consists of two gauges with one along and the other prependicular to the axis of the core. (Plate 3).

Gas pressure was measured by pressure transducers at both ends of the sample. These transducers have a capacity of 34 MPa (5000 psi) and can measure pressure to ±7 kPa (1 psi).

The duration for each test was recorded by a stop-watch which is accurate to within 1/10 of a second. For tests using the MTS, the timing device was not necessary as the loading rate was an input function.

As indicated in Table 2, the sandstone used in this study has a high porosity (porosity = 19%), special procedures were taken to prevent gas leakage through the surface of the specimens under very low confining stress (σ_3 close to zero). A thin (<<1 mm) araldite epoxy coating was put on the surface of the specimen and the ends were sealed with silicon chaulking compound to provide a closed system. These results indicated that the epoxy coating did not have any significant effects on the strength and failure characteristics of the specimens. There was no evidence of crumbling of specimen due to higher bearing stresses on the edges of the special platens.

4.4 Servo-Controlled System for Simultaneous Loading and Unloading

In order to simulate the stress changes around an underground excavation, tests were scheduled in Phase 1 (see Aspects 3 and 4 in Table 1) to incorporate simultaneous changes in the principal stress (σ_1 and σ_3) applied to the specimens. Such changes were achieved by manually controlling the applied stresses.

In order to improve on the procedure of controlling the applied stress levels, a servo-controlled system for regulating the confining pressure in the triaxial cell was designed, and would be ready for Phase 2 of the project. An illustration of the main design features of this device is given on Figure 1.

The controller which will be used to regulate the confining pressure in the triaxial cell takes the command signal from the MTS controller (for example, a voltage ramp function), inverts it, and adds a d.c. voltage to it. The fixed d.c. voltage will represent some positive pressure, the amount of confining pressure at the start of the test.

As the test starts, and the axial pressure increases, the confining pressure will decay at the same rate or at a greater or lesser rate (by increasing or decreasing the gain of the amplifier). The controller regulates the confining pressure by monitoring the pressure to the Hoek cell and dumping the excess oil from the pump into the storage reservoir.

5. TEST PROCEDURES AND RESULTS

This section describes the procedures adopted and the results obtained for each aspect of the test program as outlined in Table 1. In general, the methods suggested by ISRM were followed. Modifications to these methods and special techniques were developed to meet the objectives of the test program as required.

5.1 Aspect No. 1 - Strength Characteristics of Pier Cap Sandstone and Rate Effect

The first series of tests was performed to define the strength characteristics of the Pier Cap Sandstone and to examine the effect of loading rates on the rock strength.

Brazilian tensile, uniaxial and triaxial compression tests were carried out on individual specimens in accordance with the procedures suggested by ISRM (see Appendix 1). The specimens were tested under a slow and constant loading rate (axial stress) to produce failure within 5 to 10 minutes. In triaxial compression, the confining stress remained constant during the test.

To examine the rate effect, the loading rate for the axial stress (σ_1) was increased to 2 MPa/sec (moderate rate) and 43.7 MPa/sec (fast rate). The latter was carried out using the MTS testing equipment.

In addition, the lower bound of the strength envelope was obtained by testing the failed (fractured) specimens from the slow tests under different confining stresses at the ISRM standard loading rate.

The results of this series of tests are summarized in Tables 3, 4, 5 and 6. Figure 2 presents the strength envelopes of the Pier Cap Sandstone with the axial stress (σ_1) plotted against the confining stress (σ_3) for three loading rates. Curves A, B and C respectively represent the strength envelopes of the slow (IRSM standard), moderate and fast loading rates. Curve R depicts the strength envelope for the failed specimens on Figure 3.

It may be noted that the strength of the rock increases with increasing loading rate. Regardless of the stress levels at which the samples were failed, the strength of the failed specimens, when retested at different confining stresses, follow consistently the strength envelope represented by curve R.

5.2 Aspect No. 2 - Multistage Triaxial Testing

One of the main aspects of the study in Phase 1 was the development of a multistage triaxial testing procedure which would allow an approximate strength envelope to be derived by testing a single specimen. This was compared with the strength envelope derived from the testing of individual samples to assess the validity of the test procedure.

The ISRM suggested methods of determining the strength of rock by multi-stage triaxial compression were described in detail by Kovari et. al (3,4,5). Two types of tests were proposed, termed the "multiple failure state test" and "continuous failure state test".

In the multiple failure state test, the specimen is tested under stepwise increase in confining and axial stresses and the peak strength is used as the criterion to define the end of each stage of shearing. In the continuous failure state test, the specimen is initially tested to peak strength to establish the stress strain relationship of the test material.

The confining and axial stresses are then increased continuously such that the stress strain curve is following the same slope determined during the first stage of the test.

The stress paths to be followed by the test specimens and the test procedures suggested by ISRM for these two types of tests are illustrated on Figure 4.

The above procedures were reviewed on the basis of the test results from aspect No. 1. It was noted that the Pier Cap Sandstone exhibited a brittle behaviour within the stress levels tested. The samples simply failed when peak strength was reached (Figure 5, Table 7). It was impossible to perform any multiple failure state tests according to the ISRM methods.

To permit the testing of brittle materials and to avoid a situation in which the sample is subjected to excessive damage at the end of each of the stages, the stress levels have to be kept within a reasonable limit, although they should be high enough so that the strength of the specimen would not be under-estimated. Ideally, in this state, the growth and propagation of micro-cracks have been initiated but the specimen is still stable and has very little permanent deformation. The term "imminent failure" is used herein to define this particular state in the specimen and the stress level lies in between the yield stress and the peak strength levels. Obviously, using the yield stress as the imminent failure criterion would significantly under-estimate the peak strength; and to define imminent failure as a percentage of peak strength is impossible since the peak strength is undefined.

Two samples (No. 5 and 13) were tested under triaxial compression with strain monitoring to examine possible imminent failure criteria on the basis of the stress strain characteristics of the material. The results of these preliminary tests (Figures 6 and 7) indicated that amongst the various

stress-strain relationships, the point at which the volumetric strain ($\Delta v/v$) returns to zero, on the $\Delta v/v$ vs. ε_a plot, appeared to be an appropriate criterion for imminent failure for the present test material. It may be noted from Figures 6 and 7 that the stress level at which this occurs is about 95% of the peak strength.

In order to verify the practicality and validity of this criterion of imminent failure, 2 multi-stage triaxial tests (No. 29 and 30) were performed at standard ISRM loading rate following the procedure outlined below.

Stage 1 [σ_3 = 0 MPa]

° increase σ_1 until the volumetric strain ($\Delta v/v$) is equal to zero

° reduce σ_1 to 0 MPa

° record permanent deformation (if any)

Stage 2 [σ_3 = 10 MPa]

° increase σ_1 and σ_3 to 10 MPa simultaneously at the same stress rate

° zero all strain gauges

° maintain σ_3 constant and increase σ_1 until $\Delta v/v$ = 0

° reduce σ_1 to 10 MPa

° record permanent deformation (if any)

Stage 3 [σ_3 = 20 MPa]
Stage 4 [σ_3 = 30 MPa]

° repeat steps as outlined in Stage 2 in Stages 3 and 4 with the initial values of σ_1 and σ_3 at 20 and 30 MPa respectively.

- at the desired final stage of testing, σ_1 is increased to failure

The stress paths followed by these two multistage test specimens are illustrated on Figure 4. The results are presented on Tables 8, 9 and the strength envelope estimated from these tests are shown on Figure 8.

It may be noted that the multistage tests provide a very close approximation of the strength envelope of the test material obtained from individual triaxial tests shown on the same plot.

5.3 Aspect 3 - Calibration of the Procedures for Simulating Stress Changes

As a result of the development of an underground opening, the stress field in the surrounding area is changed. For example, at the crown of a tunnel, the trangential stress (σ_1) would increase whereas the radial stress (σ_3) would decrease near the excavation boundary. In order to calibrate a procedure that can simulate these changes in the stress field in triaxial testing, two preliminary tests were performed. In the first test (sample No. 31), the test specimen was initially loaded to a hydrostatic pressure of 20 MPa. The axial stress σ_1 was then increased and the confining pressure σ_3 reduced simultaneously at uniform rates (σ_1 increased at 2 MPa/s and σ_3 decreased at 0.5 MPa/s). The test was carried out until the sample failed and the final values of σ_1 and σ_3 were recorded. In the second test, (sample No. 32), the test specimen was loaded axially to σ_1 = 100 MPa at a confining pressure of 30 MPa. While keeping σ_1 constant, σ_3 was reduced at a rate of 1 MPa/sec to failure. The final values of σ_1 and σ_3 were recorded. The tests results are detailed in Table 10 and shown on Figure 9.

These tests showed that changes in the stress conditions applied on a sample can be performed manually at slow to moderate rates. The rate of changes in the field however is much faster (probably less than one second). Therefore, the modelling of these conditions would require an automatic servo-controlled system that permits the simultaneous variations in σ_1 and σ_3 at a very fast rate. This servo-controlled loading-unloading system is presently under construction at the University of Toronto and will be ready for operation by January 1985.

5.4 Aspect No. 4 - Effects of Stress Paths on Strength and Failure Mode

Based on the procedures established in Section 5.3, 2 series of stress path tests were performed to study the effect of stress changes on the failure mode. The rates at which loading and unloading can be applied were governed by the limitation of the equipment available for this phase of the study.

The first series of tests were concerned with the simultaneous changes in σ_1 and σ_3. Eight samples (samples no. 33 to 40) were tested at slow to moderate rates along predetermined stress paths as shown on Figure 10. The initial stress levels and the rates at which the stresses were changed for these test specimens are summarized in Table 11. The test results are plotted together with the results of the preliminary test described in Section 5.3.

The second series of tests were performed to simulate the rapid changes in the stress field. Since it was not possible at this time to simultaneously increase σ_1 and reduce σ_3 at a very fast rate, the samples were loaded to a predetermined level of axial load (σ_1) under a confining pressure (σ_3) of 30 MPa. Keeping σ_1 constant, the confining pressure was then reduced rapidly by opening up the bleeding valve of the hydraulic jack controlling σ_3. The

value of σ_3 at failure was recorded. A total of five tests were carried out at five different initial σ_1 stress levels. The test results are summarized in Table 12 and plotted on Figure 11.

In both of the above series of tests, the results obtained from stress path tests agreed closely with the strength envelope derived from individual tests at the corresponding loading rates.

5.5 Aspect No. 5 - Introduction of Pore Gas Pressure

This aspect of the test program deals with the testing of rock samples with pore gas pressure. The procedure and equipment for the introduction of pore gas pressure to the samples are described in Section 4. Of prime importance in this aspect of study is the determination of the strength characteristics and the observation of the failure mode of the specimens with pore gas pressure.

Three different types of tests were undertaken on samples subjected to pore gas pressure. In the first series of tests, 8 individual uniaxial and triaxial tests were performed under stress rates of 2, 21.9 and 43.7 MPa/s. The confining pressures ranged from 5 to 30 MPa. The samples were initially loaded hydrostatically to the stress level of the confining pressure (σ_3). Pore gas pressure was then introduced and the sample was loaded to failure under increasing axial stress (σ_1).

The pore gas pressure was maintained at 3.1 MPa in all the tests except the one performed at a stress rate of 2 MPa/s in which the pore gas pressure was 5 MPa. Table 13 details the test data. The results are shown on Figure 12 indicating the failure envelopes with respect to both total and effective stresses.

In the second series of tests, an axial and constant seating load (σ_1) was applied on the specimens with no confining pressure (σ_3=0). Pore gas pressure was then introduced within the specimen until failure occurred. Three samples were tested in this series with axial stresses (σ_1) ranging from 7.8 to 55 MPa and pore gas pressure of 1.4 to 2.6 MPa. The test data are presented in Table 14 and the results are plotted on Figure 12. The results of this series of tests are of particular interest since all the specimens failed in tension. One of the specimens (Sample 48) was virtually disintegrated (Plate 4) producing flaky fragments similar to those recovered from the recent outburst area in No. 26 Colliery.

The third series of tests were undertaken to examine the failure mode of the samples when the axial stress (σ_1) at failure is close to and higher than the unixial compressive strength of the samples. The samples were initially subjected to a system of confining and axial stresses with gas pressures ranging from 4 to 5 MPa. The confining pressure was then reduced at a very fast rate to bring the sample to failure in a manner similar to the stress change simulations (aspects No. 3 and 4). A total of four tests were performed with initial axial stresses ranging from 65 to 115 MPa and confining pressures of 10 to 35 MPa. Table 15 summarizes the test data and the results are plotted on Figure 13.

6.0 DISCUSSION OF TEST RESULTS

The procedures and results of the tests for various aspects of the study have been presented in Section 5. This section provides further discussion on the results and considers their implications on phase 2 of the test program.

6.1 Strength Characteristics of Pier Cap Sandstone and Rate Effect

The reference strength envelope of the Pier Cap Sandstone was determined from a series of individual tensile, and uniaxial and triaxial compression tests. Because of the homogeneity of the test material, very consistent results were obtained under similar testing conditions. The lower bound of the strength is defined by the strength envelope derived from testing the fractured specimens.

Under triaxial compression at moderate to high confining pressures, failure of the samples was generally characterized by shear failure along single, inclined failure surface (see Plate 5). Under uniaxial compression or low confining pressures, inclined shear failure surfaces are often accompanied by vertical cracking (see Plate 6). While the samples exhibit brittle behaviour extensive disintegration of the samples was not observed at failure.

Based on the test results, it is apparent that the strength of the Pier Cap Sandstone is rate dependent; the faster the loading rate, the higher is the failure strength. The effect appears to be more pronounced under low confining pressures.

6.2 Establishment of a Multistage Testing Procedure

As discussed in Section 5.2, the ISRM suggested method of multiple or continuous failure triaxial testing could not be applied to the Pier Cap Sandstone which exhibits brittle behaviour. A review of the ISRM procedure[5] and preliminary test results revealed that repeated or continuous loading of the specimen at peak strength would not yield the actual failure envelope, but rather substantially underestimated the actual strength of the intact material as the number of stages (or range of continuous testing) increased. This has necessitated the use of a correction factor to correlate the estimated and actual strength[5].

In this study, a comprehensive evaluation of the procedure for multistage triaxial testing of brittle material results in the determination of a criterion of imminent failure that permits the test to be stopped prior to the onset of unstable conditions within the specimen.

The sample was considered to be in the state of imminent failure when the volumetric strain ($\Delta v/v$) returned to zero on the $\Delta v/v$ vs. ε_a curve. Testing of the Pier Cap Sandstone under multistage uniaxial and triaxial conditions yields a failure envelope that approximates closely the single stage failure envelope within ±5%. As the discrepency is within experimental accuracy for triaxial testing, no correction is considered necessary.

The establishment of this testing procedure for the Pier Cap Sandstone has significant implications on the Phase 2 testing program in that this procedure could provide a means of approximating the strength envelope of the material from No. 26 Colliery and other mines with the minimum number of samples.

6.3 Effect of Stress Path

Despite the limitation of the testing equipment available for this phase of the program, the stress path tests have been successfully accomplished. The results generally indicated that within the natural variations of laboratory testing, the strength of the Pier Cap Sandstone is independent of the initial stress level (below 30 MPa) and the stress paths to failure when tested at a given loading (σ_1 increase) rate. That is, the failure state of intact samples of Pier Cap Sandstone is adequately defined by its strength envelope.

The use of a servo-controlled system for stress path testing as discussed in Section 5 would enhance the experimental procedure and enable rapid changes in stress levels to take place within the specimens.

6.4 Effect of Gas Pressure

The effect of gas pressure on the strength and the mode of failure of Pier Cap Sandstone was studied under various uniaxial and triaxial testing conditions. The following points are of particular interest in the overall context of the study of outburst under gassy conditions.

(a) When a rock sample is subjected to internal pore gas pressure and a system of externally applied axial and confining stresses, the effective stresses in the sample are given by the following expressions.

$$\sigma_1' = \sigma_1 - p$$
$$\sigma_3' = \sigma_3 - p$$

where σ_1, σ_1' = total and effective axial stresses respectively

σ_3, σ_3' = total and effective confining stresses (pressure) respectively

p = pore gas pressure (hydrostatic)

It is the effective stress system which governs the strength of the sample. It was noted that at the same loading rate, at low confining pressure, the effective strength envelope agreed closely with the total stress envelope obtained with no pore gas pressure. At high confining pressure, slight reduction in strength was observed.

(b) Samples of the Pier Cap Sandstone were tested at different initial stress levels and along different stress paths to examine the range of failure mode under the effect of pore gas pressure. Three different modes of failures were observed during the tests and they generally occurred within the following range of stress levels.

Mode of Failure	Stress Levels	Ref. Plate
(i) single or multiple inclined failure planes with or without signs of axial cracks	$\sigma_3' >$ 5 MPa $\sigma_1' >$ uniaxial compressive strength	7
(ii) single or multiple, inclined failure planes accompanied by intense vertical cracking of sample	$\sigma_3' \geq 0$ but less than approx. 2 MPa	8
(iii) tensile failure by intense vertical splitting. Violent explusion of fractured material resulting in flaky rock fragments	$\sigma_3' \leq 0$	4

The above observations are approximately delineated on Figure 14. In summary, bursting of the sample occurred when, due to the presence of pore gas, the effective confining pressure became negative and exceeded the tensile strength of the rock as defined by the strength envelope. At low confining pressure, intensive vertical splitting was

indicative of the potential of bursting, but manifestation of the phenomenon was probably restricted by the confinement from the membrane within the Hoek cell.

The similarity between the shape of the rock fragments from the laboratory tests and the site of the recent outburst at No. 26 Colliery has provided some insights to the possible mechanism of the bursting phenomenon.

7.0 CONCLUSIONS AND RECOMMENDATIONS FOR PHASE 2

In connection with the study of the outburst problem in the Sydney Coalfield in Nova Scotia, a program of laboratory tests was undertaken to investigate the strength characteristics of the burst prone strata and the effect of pore gas pressure.

Phase 1 of the program was directed towards the testing of a reference material to establish the testing procedures and calibrate the equipment required to undertake the Phase 2 testing program. The conclusions derived from Phase 1 are summarized below:

(a) The reference material is a homogeneous, relatively porous sandstone which yielded consistent test results. The strength of this material is rate dependent; the strength being higher when tested at faster loading rate.

(b) Stress path testing procedures at low to moderate loading rates have been established to simulate stress changes in the field by predetermining the stress paths along which the samples have to follow.

The Pier Cap Sandstone was used to calibrate the test procedure developed and it was noted that the strength of this material is independent of the stress paths to failure.

A servo-controlled unit is under construction and will be used in Phase 2 to refine the test procedure and to better control the rapid stress changes in the sample.

(c) A multistage triaxial testing procedure was successfully developed to estimate the strength envelope of the Pier Cap Sandstone which exhibits brittle

behaviour. By using an imminent failure criterion (based on the point at which the net volume strain becomes zero within each stage of testing) the complete failure envelope was derived from a single sample.

There is close agreement between the multistage and single stage (individual tests) strength envelopes. This finding has significant implications on the Phase 2 program in that this procedure could enable the strength envelope of other materials to be estimated with the use of minimum number of samples.

(d) The procedure and equipment for testing rock samples with the introduction of pore gas pressure have been established through the Phase 1 test program. Pore gas pressures of up to 5 MPa could be introduced into the specimen under various loading conditions.

It is possible to cause bursting of the sample by inducing tensile failure which was manifested in violent explusion and intense fragmentation of the test material at failure. At very low confining pressure there is a potential for the material to burst, but the manifestation of this phenomenon is restricted by the confinement from the membrane within the triaxial cell. At high confining pressure (σ_3 exceeds the gas pressure), failure is only characterized by shear failure. Some vertical cracking was observed.

With the presence of the pore gas pressure, the strength of the material is governed by the effective stress system in the sample.

(e) It must be emphasized that while the test procedure and the general concepts developed in Phase 1 can be used as a basis for developing the Phase 2 program, the strength characteristics pertaining to Pier Cap Sandstone may not directly reflect the mechanical behaviour of the material from No. 26 Colliery or other mines of the Sydney Coalfield.

(f) Based on the findings of Phase 1, a program of laboratory tests for Phase 2 was developed and presented in Table 16. Two aspects will be emphasized in the Phase 2 test program. The first is the effect of rapid stress changes. Of particular interest is the mode of failure of the sample associated with the final stress state near the tensile region of the strength envelope. The second is the effect of pore gas pressure on the mode of failure under various stress conditions.

In view of the limited availability of the samples from No. 26 Colliery, it is suggested that samples recovered from the same rock unit in other operating mines (e.g. Lingan Colliery) be used for the second phase to provide enough specimens for completing the proposed test program. For this purpose, some tests have been included in the Phase 2 program to relate the properties of the materials available from two different sources.

ACKNOWLEDGEMENTS

Golder Associates wishes to thank Dr. A. Crawford and Mr. D. Lau of the University of Toronto for their contributions and assistance in the preparation of the Phase 1 report. Helpful discussion of Dr. Peter Cain of the Cape Breton Coal Research Laboratory during the course of the study was also gratefully acknowledged.

GOLDER ASSOCIATES

for Guy LeBel

Clement M.K. Yuen, P. Eng.

REFERENCES

1. Brown, E.T., Rock Characterization Testing and Monitoring, ISRM Suggested Methods, Pergamon Press, 1981

2. Obert, L., Duvall, W.I.; Rock Mechanics and The Design of Structures in Rock, John Wiley & Sons, 1967

3. Kovari, K., Tisa, A; Multiple Failure State and Strain Controlled Triaxial Tests, Rock Mech. 7, 17-33, 1975

4. Kovari, K., Tisa, A.,Attinger, R., The Concept of "Continuous Failure State" Triaxial Tests, Rock Mech. Rock Engineering 16(2), 117-131, 1983

5. Kovari, K., Tisa, A., Einstein, H.H., Franklin, J.A., Suggested Methods for Determining the Strength of Rock Materials in Triaxial Compression: Revised Version, Int. J. Rock. Mech. Min. Sci. Geomech. Abstr. Vol. 20, N.6, 283-290, 1983

TABLE 1

TESTING PROGRAM FOR PHASE 1

ASPECT TO BE STUDIED	SCOPE/SPECIAL FEATURE OF TESTING	REFERENCE/ TEST STANDARD	NO. OF TESTS
1. Conventional Triaxial Tests - strength characteristics of reference material and effect of various loading rate	• Series of conventional triaxial tests to establish strength characteristics of the reference material. • Scope of testing for each series includes: ° Brazilian Tensile test ° Uniaxial Compression test (σ_3=0) ° Triaxial test σ_3=5,10,20,30 MPa ° Rate of loading Series 1 ISRM Standard (Slow) Series 2 2 times faster (moderate) than ISRM Standard (2 MPa/sec) Series 3 43.7 MPa/sec ° Pore gas maintained at atmospheric pressure • Conventional triaxial tests to establish the strength characteristics of the failed samples	ISRM Standard method of rock testing Brazian test Uniaxial compression Triaxial test	 16 7 5 3
2. Calibration tests to study the feasibility of optimizing the number of samples	• Development of a multi-stage triaxial test to permit the optimization of the number of samples. • Include the determination of a relevant criterion for imminent failure • Monitoring of strains on specimen during triaxial tests (σ_3=0,10,20,30 MPa) • Pore gas maintained at atmospheric pressure	ISRM Standard method of rock testing (modified accordingly to the relevant criterion for imminent failure)	2 (preliminary) 4

continued....

Golder Associates

TABLE 1 (continued)

ASPECT TO BE STUDIED	SCOPE/SPECIAL FEATURE OF TESTING	REFERENCE/ TEST STANDARD	NO. OF TESTS
3. Calibration tests to establish a procedure for controlling the rate of loading and unloading	• Reproduce, under laboratory conditions, the stress changes around an opening being developed • Develop a procedure that simultaneously reduce σ_3 and increase σ_1 (at various rates) • Development of a servo-controlled loading/ unloading system • Pore gas maintained at atmospheric pressure	ISRM Standard of rock testing with modifications to suit the modelled phenomenon	2
4. Tests to simulate the stress changes and underground openings	• Samples subjected to various initial stress conditions are then brought to failure at various rates and under different stress paths • Study the effect of stress changes on the failure mode • Reproduce failure mode similar to the rock burst of No. 26 Colliery • Pore gas maintained at atmospheric pressure	As determined in Section 3	13
5. Investigation of the effect of gas pore pressure on the failure mode	• Testing of the specimen under gas pore pressure (uniaxial, triaxial) • Study the effect of stress changes on the failure mode • Reproduce failure mode similar to the rock burst of No. 26 Colliery • Pore gas pressure ranging between 3.1 and 5 MPa	ISRM as determined in Section 3	15
		TOTAL	64

Golder Associates

TABLE 2

PHYSICAL PROPERTIES OF PIER CAP SANDSTONE

AND DIMENSIONS OF TEST SPECIMENS

(a) Physical Properties

Bulk Density	2.19 Mg/m^3
Porosity	19%
Gas Permeability	5.22×10^{-6} cm/s at 5 MPa
	5.24×10^{-6} cm/s at 10 MPa

(b) Average Strength and Deformation Characteristics

Uniaxial Compressive Strength (1)	43.3 MPa
Tensile (Brazilian) Strength (1)	4.3 MPa
Elastic Modulus (1)	10.78 GPa (3)
Dynamic Modulus (2)	11.95 GPa

(c) Dimensions of Test Specimens

Type of Test	Dimensions of Specimens	ISRM Standard
Brazilian Tests	54 mm dia. x 27 mm	NX Sample L/D = 0.5
Uniaxial and Triaxial Tests (with no gas pressure)	54 mm dia. x 125 mm (L/D - 2.35)	NX Sample L/D = 2.0-3.0
Uniaxial and Triaxial Tests (with gas pressure)	54 mm dia. x 115 mm (L/D = 2.11)	NX Sample L/D = 2.0-3.0

Notes:

(1) Based on results obtained from phase one

(2) Determined from velocities of compressional waves through the sample

(3) Secant modulus at 50%.

TABLE 3

SUMMARY OF TEST RESULTS, INTACT SAMPLES
ASPECT NO. 1, SLOW STRESS RATE

SAMPLE NO.	TYPE OF TEST	ASPECT RATIO (L/D)	PORE GAS PRESSURE	INITIAL STRESS LEVEL (MPa)		STRESS LEVEL AT FAILURE (MPa)			APPLIED STRESS RATE	OBSERVED FAILURE MODE	REMARKS
			P(MPa)	σ_3	σ_1	σ_3	σ_1	σ_t			
1	BRAZILIAN	0.51	atm	-	-	-	-	4.58	ISRM	AS	
2	BRAZILIAN	0.48	atm	-	-	-	-	4.04	ISRM	AS	
3	UNIAXIAL	2.35	atm	-	-	-	40.6	-	300 sec. to failure	AS, CN, S	
4	UNIAXIAL	2.35	atm	-	-	-	43.6	-	300 sec. to failure	AS, CN, S	
5	UNIAXIAL	2.35	atm	-	-	-	43.8	-	300 sec. to failure	AS, CN, S	Instrumented for strain measurements
6	UNIAXIAL	2.35	atm	-	-	-	45.1	-	300 sec. to failure	AS, CN, S	
7	TRIAXIAL	2.35	atm	5.0	5.0	5.0	99.8	-	300 sec. to failure	S, AS,	Shear along diagonal
8	TRIAXIAL	2.35	atm	10.0	10.0	10.0	114.7	-	300 sec. to failure		
9	TRIAXIAL	2.35	atm	10.0	10.0	10.0	97.2	-	300 sec. to failure		
10	TRIAXIAL	2.35	atm	10.0	10.0	10.0	124.5	-	300 sec. to failure	S, C, H	Shear along diagonal
11	TRIAXIAL	2.35	atm	10.0	10.0	10.0	122.5	-	300 sec. to failure		
12	TRIAXIAL	2.35	atm	20.0	20.0	20.0	167.2	-	300 sec. to failure	S, C, H	Shear at 62°
13	TRIAXIAL	2.35	atm	20.0	20.0	20.0	169.2	-	300 sec. to failure		Instrumented for strain measurements

D = 54 mm

MODE OF FAILURE:

AC: AXIAL CRACKS
AS: AXIAL SPLITTING
C: CONJUGATE PLANES
CN: CONICAL
H: HORIZONTAL SPLITTING
PC: PERIPHERICAL CRACKS
S: SHEAR
SC: CURVED SHEAR PLANE

con't.....

Golder Associates

TABLE 3 (cont'd)

SLOW RATE TEST

SAMPLE NO.	TYPE OF TEST	ASPECT RATIO (L/D)	PORE GAS PRESSURE	INITIAL STRESS LEVEL (MPa)		STRESS LEVEL AT FAILURE (MPa)			APPLIED STRESS RATE	OBSERVED FAILURE MODE	REMARKS
			P(MPa)	σ_3	σ_1	σ_3	σ_1	σ_c			
14	TRIAXIAL	2.35	atm	30.0	30.0	30.0	204.2	-	300 sec. to failure	S	
15	TRIAXIAL	2.35	atm	30.0	30.0	30.0	188.6	-	300 sec. to failure	S	Shear at 62°
16	TRIAXIAL	2.35	atm	30.0	30.0	30.0	190.6	-	300 sec. to failure	S	Shear at 62°

Golder Associates

TABLE 4

SUMMARY OF TEST RESULTS, INTACT SAMPLES
ASPECT NO. 1, MODERATE STRESS RATE

SAMPLE NO.	TYPE OF TEST	ASPECT RATIO (L/D)	PORE GAS PRESSURE	INITIAL STRESS LEVEL (MPa)		STRESS LEVEL AT FAILURE (MPa)			APPLIED STRESS RATE	OBSERVED FAILURE MODE	REMARKS
			P(MPa)	σ_3	σ_1	σ_3	σ_1	σ_t			
17	BRAZILIAN	0.50	atm	-	-	-	-	3.52	0.5 MPa/s	AS	
18	UNIAXIAL	2.35	atm	-	-	-	48.6	-	1.5 MPa/s	S, C, AS	
19	TRIAXIAL	2.35	atm	2.5	2.5	2.5	80.0	-	2.0 MPa/s	S	Shear along diagonal
20	TRIAXIAL	2.35	atm	5.0	5.0	5.0	108.0	-	1.9 MPa/s	S	Shear along diagonal
21	TRIAXIAL	2.35	atm	10.0	10.0	10.0	136.1	-	1.9 MPa/s	S	Shear at 62°
22	TRIAXIAL	2.35	atm	20.0	20.0	20.0	180.8	-	1.95 MPa/s	S	Shear at 59°
23	TRIAXIAL	2.35	atm	30.0	30.0	30.0	218.8	-	1.75 MPa/s	S	Shear at 55°

Golder Associates

TABLE 5

SUMMARY OF TEST RESULTS, INTACT SAMPLES
ASPECT NO. 1, RAPID STRESS RATE

SAMPLE NO.	TYPE OF TEST	ASPECT RATIO (L/D)	PORE GAS PRESSURE	INITIAL STRESS LEVEL (MPa)		STRESS LEVEL AT FAILURE (MPa)			APPLIED STRESS RATE	OBSERVED FAILURE MODE	REMARKS
			P(MPa)	σ_3	σ_1	σ_3	σ_1	σ_t			
24	UNIAXIAL	2.35	atm	-	-	-	69.7	-	43.7 MPa/s	S, AS	Excessive crushing. Some cracking probable due to MTS pressure
25	TRIAXIAL	2.35	atm	5.0	5.0	5.0	148.6	-	43.7 MPa/s	S, H	Shear along diagonal
26	TRIAXIAL	2.35	atm	10.0	10.0	10.0	166.1	-	43.7 MPa/s	S, H	Shear along diagonal
27	TRIAXIAL	2.35	atm	20.0	20.0	20.0	215.0	-	43.7 MPa/s	SC, H	Shear along diagonal curved failure surface
28	TRIAXIAL	2.35	atm	30.0	30.0	30.0	248.2	-	43.7 MPa/s	S	Shear along diagonal

Golder Associates

TABLE 6

SUMMARY OF TEST RESULTS, FAILED SAMPLES
ASPECT NO. 1

SAMPLE NO.	TYPE OF TEST	ASPECT RATIO (L/D)	PORE GAS PRESSURE	INITIAL STRESS LEVEL (MPa)		STRESS LEVEL AT FAILURE (MPa)			APPLIED STRESS RATE	OBSERVED FAILURE MODE	REMARKS
			P(MPa)	σ_3	σ_1	σ_3	σ_1	σ_t			
9	TRIAXIAL	2.35	atm	20.0	20.0	20.0	112.8	-	ISRM		
9	TRIAXIAL	2.35	atm	30.0	30.0	30.0	157.5	-	ISRM		
10	TRIAXIAL	2.35	atm	10.0	10.0	10.0	62.2	-	ISRM		
10	TRIAXIAL	2.35	atm	20.0	20.0	20.0	106.9	-	ISRM		
10	TRIAXIAL	2.35	atm	30.0	30.0	30.0	149.7	-	ISRM		
12	TRIAXIAL	2.35	atm	20.0	20.0	20.0	105.0	-	ISRM		
12	TRIAXIAL	2.35	atm	10.0	10.0	10.0	56.4	-	ISRM		
12	TRIAXIAL	2.35	atm	20.0	20.0	20.0	101.1	-	ISRM		
12	TRIAXIAL	2.35	atm	30.0	30.0	30.0	140.0	-	ISRM		

Golder Associates

TABLE 7

SUMMARY OF TEST RESULTS, STRAIN MEASUREMENTS

SAMPLES 5 and 13 ASPECT NO. 2

a) Sample No. 5 Uniaxial Compression ($\sigma_3=0$)

AXIAL STRESS σ_1 (MPa)	DEVIATORIC STRESS $\sigma_1-\sigma_3$ (MPa)	AXIAL STRAIN $\bar{\varepsilon}_a$ (1) μ	LONGITUDINAL STRAIN $\bar{\varepsilon}_\ell$ (1) μ	VOLUMETRIC STRAIN $\varepsilon_v=\bar{\varepsilon}_a+2\bar{\varepsilon}_\ell$ μ
0	0	0	0	0
2	2	-333	+ 50	-233
4	4	-534	+ 93	-348
6	6	-713	+132	-449
8	8	-878	+172	-534
10	10	-1024	+209	-606
12	12	-1147	+245	-657
14	14	-1276	+283	-710
16	16	-1394	+324	-746
18	18	-1529	+376	-777
20	20	-1630	+423	-784
22	22	-1777	+485	-807
24	24	-1896	+545	-806
26	26	-2018	+610	-798
28	28	-2138	+694	-750
30	30	-2270	+787	-696
32	32	-2385	+870	-645
34	34	-2513	+978	-557
36	36	-2640	+1112	-416
38	38	-2755	+1227	-301
40	40	-2891	+1386	-119
42	42	-3071	+1659	+247

(1) Average of two gauges

TABLE 7 (continued)

b) Sample No. 13 Triaxial Compression, σ_3=20 MPa

AXIAL STRESS σ_1 (MPa)	DEVIATORIC STRESS $\sigma_1-\sigma_3$ (MPa)	AXIAL STRAIN $\bar{\varepsilon}_a$ (1) (μ)	LONGITUDINAL STRAIN $\bar{\varepsilon}_\ell$ (1) (μ)	VOLUMETRIC STRAIN $\varepsilon_v=\bar{\varepsilon}_a+2\bar{\varepsilon}_\ell$ (μ)
20	0	0	0	0
22	2	- 144	+ 14	- 116
24	4	- 280	+ 23	- 234
26	6	- 394	+ 34	- 326
28	8	- 544	+ 48	- 448
30	10	- 678	+ 73	- 532
35	15	- 970	+114	- 742
45	25	-1512	+205	-1102
80	60	-3210	+578	-2054
85	65	-3414	+638	-2138
90	70	-3650	+702	-2246
95	75	-3910	+783	-2344
105	85	-4444	+986	-2472
115	95	-4952	+1189	-2574
125	105	-5496	+1476	-2544
135	115	-6232	+1825	-2482
145	125	-6974	+2326	-2322
152	132	-7636	+2835	-1966
154	134	-7992	+3094	-1804
162	142	-8894	+3913	-1063
164	144	-9760	+4902	+ 40
166	146	-10714	+5948	+1182
168	148	-14354	+10920	+7486

(1) Average of two gauges

TABLE 8

SUMMARY OF TEST RESULTS

DETERMINATION OF FAILURE ENVELOPE (MST)

ASPECT NO. 2

Sample No. 29

CONFINING PRESSURE σ_3 (MPa)	AXIAL STRESS AT $\Delta v/v=0$ σ_1 (MPa)
0	33.4
10	117.0
20	164.0
30	208.0
σ_1 (failure)	214.0

Sample No. 30

0	34.0
10	112.0
20	164.0
30	Creep failure at 198 MPa

TABLE 9

SUMMARY OF TEST RESULTS, MULTISTAGE TESTS

SAMPLES 29 AND 30, ASPECT NO. 2

AXIAL STRESS σ_1 (MPa)	DEVIATORIC STRESS $\sigma_1-\sigma_3$ (MPa)	AXIAL STRAIN ε_a (avg) μ	LONGITUDINAL STRAIN ε_ℓ (avg) μ	VOLUMETRIC STRAIN ε_v μ
A) SAMPLE NO. 29				
Stage 1 σ_3 = 0				
0	0	0	0	0
2	2	-402	+99	-205
4	4	-635	+154	-328
6	6	-348	+214	-421
8	8	-1053	+279	-495
10	10	-1215	+334	-547
15	15	-1597	+493	-612
20	20	-1938	+672	-594
25	25	-2253	+884	-486
30	30	-2582	+1164	-254
32	32	-2719	+1307	-105
34	34	-2845	+1454	+63
Stage 2 σ_3 = 10 MPA				
10	0	0	0	0
15	5	-271	+13	-245
20	10	-561	+64	-433
25	15	-796	+125	-546
30	20	-1044	+170	-704
35	25	-1257	+219	-819
40	30	-1488	+281	-926
45	35	-1747	+375	-997
50	40	-1974	+435	-1104
60	50	-2430	+591	-1248
70	60	-2916	+770	-1376
80	70	-3425	+1012	-1401
90	80	-3918	+1269	-1380
100	90	-4608	+1782	-1044
105	95	-4955	+2043	-869
110	100	-5319	+2400	-519
115	105	-5765	+2730	-305
118.7	108.7	-5971	+3165	+359

TABLE 9 (cont'd)

SUMMARY OF TEST RESULTS, MULTISTAGE TESTS

SAMPLES 29 AND 30, ASPECT NO. 2

AXIAL STRESS σ_1 (MPa)	DEVIATORIC STRESS $\sigma_1-\sigma_3$ (MPa)	AXIAL STRAIN ε_a (avg) μ	LONGITUDINAL STRAIN ε_ℓ (avg) μ	VOLUMETRIC STRAIN ε_v μ
Stage 3 σ_3 = 20 MPa				
20	0	0	0	0
25	5	-175	+30	-115
30	10	-410	+50	-310
35	15	-624	+88	-448
40	20	-846	+128	-590
45	25	-1115	+189	-737
50	30	-1300	+231	-838
55	35	-1538	+303	-932
60	40	-1798	+366	-1066
70	50	-2260	+502	-1256
80	60	-2694	+623	-1448
90	70	-3135	+768	-1599
100	80	-3631	+980	-1671
110	90	-4149	+1210	-1739
120	100	-4663	+1417	-1829
130	110	-5204	+1725	-1754
135	115	-5527	+1924	-1679
140	120	-5825	+2123	-1579
145	125	-6245	+2435	-1375
150	130	-6514	+2598	-1318
155	135	-6825	+2845	-1085
160	140	-7195	+3330	-535
161.4	141.4	-7585	+3580	-425
163.3	143.3	-7888	+3840	-208
165	145	-8150	+4190	+230
Stage 4 σ_3 = 30 MPa				
30	0	0	0	0
35	5	-184	+19	-146
40	10	-399	+58	-283
45	15	-614	+81	-452
50	20	-881	+146	-589
55	25	-1008	+159	-690
60	30	-1175	+189	-797
70	40	-1738	+308	-1122
80	50	-2221	+441	-1399
90	60	-2633	+529	-1575
100	70	-3123	+644	-1835
110	80	-3587	+806	-1975
120	90	-4153	+1008	-2137
130	100	-4652	-1217	-2218
140	110	-5231	+1438	-2355
150	120	-5817	+1779	-2259

TABLE 9 (cont'd)

SUMMARY OF TEST RESULTS, MULTISTAGE TESTS

SAMPLES 29 AND 30, ASPECT NO. 2

AXIAL STRESS σ_1 (MPa)	DEVIATORIC STRESS $\sigma_1-\sigma_3$ (MPa)	AXIAL STRAIN ε_a (avg) μ	LONGITUDINAL STRAIN ε_ℓ (avg) μ	VOLUMETRIC STRAIN ε_v μ
Stage 4 (cont'd)				
160	130	-6406	+2030	-2346
170	140	-7065	+2449	-2167
175	145	-7486	+2658	-2170
180	150	-7772	+2894	-1984
185	155	-8068	+3094	-1880
190	160	-8416	+3361	-1694
195	165	-8850	+3667	-1516
200	170	-9238	+3981	-1276
204	174	-9838	+4592	-654
Ultimate = 214 MPa		-10716*	+7606*	+4496

* 1 gauge broken, probably crack through 1 side where gauges were located.

B) SAMPLE NO. 30

Stage 1 σ_3 = 0				
0	0	0	0	0
2	2	-659	+99	+461
4	4	-832	+137	-558
6	6	-978	+174	-631
8	8	-1123	+214	-695
10	10	-1261	+261	-739
15	15	-1671	+429	-814
20	20	-2071	+613	-791
25	25	-2366	+851	-664
30	30	-2737	+1169	-399
32	32	-2856	+1295	-266
34	34	-3020	+1497	-26
35	35	-3111	+1643	+175
Stage 2 σ_3 = 10 MPa				
10	0	0	0	0
15	5	-493	+69	-356
20	10	-761	+123	-515
25	15	-930	+156	-618
30	20	-1199	+223	-754
35	25	-1443	+287	-870
40	30	-1644	+336	-972

TABLE 9 (cont'd)

SUMMARY OF TEST RESULTS, MULTISTAGE TESTS

SAMPLES 29 AND 30, ASPECT NO. 2

AXIAL STRESS σ_1 (MPa)	DEVIATORIC STRESS $\sigma_1-\sigma_3$ (MPa)	AXIAL STRAIN ε_a (avg) μ	LONGITUDINAL STRAIN ε_ℓ (avg) μ	VOLUMETRIC STRAIN ε_v μ
Stage 2 (cont'd)				
50	40	-2136	+476	-1185
60	50	-2590	+637	-1317
70	60	-3127	+842	-1443
80	70	-3611	+1092	-1427
90	60	-4245	+1445	-1355
95	85	-4598	+1679	-1240
100	90	-4955	+1966	-1023
105	95	-5354	+2306	-742
110	100	-5759	+2703	-354
112	102	-6027	+3032	+37
112.78	102.78	-6227	+3240	+253
Stage 3 σ_3 = 20 MPa				
20	0	0	0	0
25	5	-111	+23	-65
30	10	-493	+59	-375
35	15	-932	+137	-658
40	20	-1169	+186	-797
45	25	-1422	+239	-944
50	30	-1674	+301	-1072
60	40	-2102	+412	-1278
70	50	-2545	+584	-1477
80	60	-3034	+678	-1778
90	70	-3551	+864	-1924
100	80	-4030	+1061	-1998
110	90	-4536	+1276	-2085
120	100	-5153	+1625	-2003
130	110	-5696	+1879	-1938
140	120	-1351	+2262	-1827
145	125	-6781	+2562	-1657
150	130	-7105	+2778	-1549
152	132	-7281	+2908	-1465
154	134	-7512	+3065	-1382
156	136	-7741	+3287	-1167
158	138	-804	+3510	-992
160	140	-8278	+3714	-850
162	142	-8556	+3972	-612
164	144	-9039	+4507	-25
165.48	145.48	-9584	+5115	+645

TABLE 9 (cont'd)

SUMMARY OF TEST RESULTS, MULTISTAGE TESTS

SAMPLES 29 AND 30, ASPECT NO. 2

AXIAL STRESS σ_1 (MPa)	DEVIATORIC STRESS $\sigma_1-\sigma_3$ (MPa)	AXIAL STRAIN ε_a (avg) μ	LONGITUDINAL STRAIN ε_ℓ (avg) μ	VOLUMETRIC STRAIN ε_v μ
Stage 4 σ_3 = 30 MPa				
30	0	0	0	0
35	5	-262	+36	-166
40	10	-476	+64	-317
45	15	-712	+90	-485
50	20	-947	+130	-640
55	25	-1174	+158	-804
60	30	-1388	+200	-924
80	50	-2341	+380	-1471
100	70	-3529	+680	-1999
120	90	-4643	+1020	-2345
140	110	-5824	+1456	-2546
160	130	-7053	+2000	-2553
180	150	-8365	+2710	-2291
185	155	-8876	+2970	-2236
190	160	-9228	+3212	-2076
192	162	-9542	+3390	-2022
198	168	-10138	+3820	-1798

Creep failure at σ_1 = 198 MPa

TABLE 10

SUMMARY OF TEST RESULTS, ASPECT NO. 3

SAMPLE NO.	TYPE OF TEST	ASPECT RATIO (L/D)	PORE GAS PRESSURE	INITIAL STRESS LEVEL (MPa)		STRESS LEVEL AT FAILURE (MPa)			APPLIED STRESS RATE	OBSERVED FAILURE MODE	REMARKS
			P(MPa)	σ_3	σ_1	σ_3	σ_1	σ_t	MPa/s		
31	Stress change simulation	2.35	atm	20.0	20.0	2.5	80.0	-	$R\sigma_1$ = 1.82 $R\sigma_3$ = 0.53	SC	Shear along diagonal curved shear plane
32	Rapid confining pressure reduction	2.35	atm	30.0	100.0	3.75	100.0	-	$R\sigma_3$ = 1.00	S	Shear crack only, sample did not fail

Golder Associates

TABLE 11

SUMMARY OF TEST RESULTS, STRESS CHANGE SIMULATION
ASPECT NO. 4

SAMPLE NO.	TYPE OF TEST	ASPECT RATIO (L/D)	PORE GAS PRESSURE	INITIAL STRESS LEVEL (MPa)		STRESS LEVEL AT FAILURE (MPa)			APPLIED STRESS RATE	OBSERVED FAILURE MODE	REMARKS
			P(MPa)	σ_3	σ_1	σ_3	σ_1	σ_t			
33	Stress change simulation	2.35	atm	30.0	30.0	4.0	100.1	-	$R\sigma_1$=1.84 MPa/s $R\sigma_3$=0.68 MPa/s	S,C	Shear along diagonal
34	Stress change simulation	2.35	atm	30.0	30.0	10.0	139.6	-	$R\sigma_1$=1.93 MPa/s $R\sigma_3$=0.33 MPa/s	S	Shear along diagonal
35	Stress change simulation	2.35	atm	30.0	30.0	16.0	158.5	-	$R\sigma_1$=1.84 MPa/s $R\sigma_3$=0.20 MPa/s	S	Shear along 62°
36	Stress change simulation	2.35	atm	30.0	30.0	23.0	192.5	-	$R\sigma_1$=1.85 MPa/s $R\sigma_3$=0.08 MPa/s	S	Shear along 59°
37	Stress change simulation	2.35	atm	30.0	30.0	6.0	103.1	-	300 sec. to failure	S	Shear along diagonal + cracks around the centre
38	Stress change simulation	2.35	atm	30.0	30.0	10.5	130.7	-	300 sec. to failure	S, AS	Shear along diagonal
39	Stress change simulation	2.35	atm	30.0	30.0	18.0	159.5	-	300 sec. to failure	S	Shear along diagonal
40	Stress change simulation	2.35	atm	30.0	30.0	23.5	191.5	-	300 sec. to failure	S	Shear along 62°

Golder Associates

TABLE 12

SUMMARY OF TEST RESULTS, RAPID CONFINING PRESSURE REDUCTION

ASPECT NO. 4

SAMPLE NO.	TYPE OF TEST	ASPECT RATIO (L/D)	PORE GAS PRESSURE	INITIAL STRESS LEVEL (MPa)		STRESS LEVEL AT FAILURE (MPa)			APPLIED STRESS RATE	OBSERVED FAILURE MODE	REMARKS
			P(MPa)	σ_3	σ_1	σ_3	σ_1	σ_t			
41	Rapid confining pressure reduction	2.35	atm	30.0	50.0	0.0	50.0	-	less than 1 sec.	PC	
42	Rapid confining pressure reduction	2.35	atm	30.0	55.0	0.0	55.0	-	less than 1 sec.	PC	
43	Rapid confining pressure reduction	2.35	atm	30.0	100.0	1.0 to 2.0	100.0	-	less than 1 sec.	S,H,AS	Shear at 65°
44	Rapid confining pressure reduction	2.35	atm	30.0	150.0	5.0 to 7.0	150.0	-	less than 1 sec.	SC	Shear and curved failure plan
45	Rapid confining pressure reduction	2.35	atm	30.0	200.0	14.0 to 16.0	200.0	-	less than 1 sec.	S	Shear at 65°

Golder Associates

TABLE 13

SUMMARY OF TEST RESULTS
STRENGTH CHARACTERISTICS OF SAMPLES WITH PORE GAS PRESSURE
ASPECT NO. 5

SAMPLE NO.	TYPE OF TEST	ASPECT RATIO (L/D)	PORE GAS PRESSURE	INITIAL STRESS LEVEL (MPa)		STRESS LEVEL AT FAILURE (MPa)			APPLIED STRESS RATE	OBSERVED FAILURE MODE	REMARKS
			P(MPa)	σ_3	σ_1	σ_3	σ_1	σ_t			
46	Triaixal	2.11	5	15.0	15.0	15.0	148.0	-	2 MPa/s	S, PC	Curved shear surface along diagonal
49	Uniaxial	2.11	3.1	0	0	0	28.8	-	43.7 MPa/s	AS, C	Excessive damages may have been caused by MTS
50	Triaxial	2.11	3.1	5.0	5.0	5.0	125.4	-	43.7 MPa/s	S, H	Shear along diagonal, curved shear surface, damages MTS
51	Triaxial	2.11	3.1	10.0	10.0	10.0	160.4	-	21.9 MPa/s	S,	Shear along diagonal
52	Triaxial	2.11	3.1	30.0	30.0	30.0	206.3	-	21.9 MPa/s	S, C	
53	Triaxial	2.11	3.1	13.0	13.0	13.0	161.8	-	43.7 MPa/s	S, AC, H	Shear along diagonal, axial & horizontal cracking observed
54	Triaxial	2.11	3.1	20.0	20.0	20.0	186.6	-	43.7 MPa/s	S, AC, C	2 wedges formed axial cracks observed
60	Triaxial	2.11	3.1	30.0	30.0	30.0	223.3	-	43.7 MPa/s	S, AC	Shear at 62° Axial cracks observed

Golder Associates

TABLE 14

SUMMARY OF TEST RESULTS
UNIAXIAL COMPRESSION TESTS, SAMPLES WITH PORE GAS PRESSURE

SAMPLE NO.	TYPE OF TEST	ASPECT RATIO (L/D)	PORE GAS PRESSURE	INITIAL STRESS LEVEL (MPa)		STRESS LEVEL AT FAILURE (MPa)			APPLIED STRESS RATE	OBSERVED FAILURE MODE	REMARKS
			P(MPa)	σ_3	σ_1	σ_3	σ_1	σ_t			
47	UNIAXIAL	2.11	1.86	0	0	0	7.8	1.86		AS	Vertical splitting around the sample surface
48	UNIAXIAL	2.11	2.6	0	0	0	20.0	2.6		BURSTING	Vertical splitting, sample pulverized
58	UNIAXIAL	2.11	1.4	0	0	0	55.0	1.4		AS, AC, S	Some gas leakage. A lot of vertical cracks observed on remaining pieces

Golder Associates

TABLE 15

SUMMARY OF TEST RESULTS
RAPID REDUCTION OF CONFINING PRESSURE, SAMPLES WITH PORE GAS PRESSURE
ASPECT NO. 5

SAMPLE NO.	TYPE OF TEST	ASPECT RATIO (L/D)	PORE GAS PRESSURE	INITIAL STRESS LEVEL (MPa)		STRESS LEVEL AT FAILURE (MPa)			APPLIED STRESS RATE	OBSERVED FAILURE MODE	REMARKS
			P(MPa)	σ_3	σ_1	σ_3	σ_1	σ_t			
55	Rapid confining pressure reduction	2.11	5.0	35.0	65.0	5.0	65.0	-	less than 1 sec.	S, AC, PC	Sample did not fail cracks only
56	Rapid confining pressure reduction	2.11	5.0	35.0	105.0	5.0 - 6.0	105.0	-	less than 1 sec.	S, AC, AS, C	Extensive vertical cracks through shear plane
57	Rapid confining pressure reduction	2.11	4.0	10.0	65.0	4.0	65.0	-	less than 1 sec.	AC, AS	Did not fail completely, outer perimeter failed in tension. Lots of vertical cracks in remaining pieces
59	Rapid confining pressure reduction	2.11	4.0	20.0	115.0	6.0	115.0	-	less than 1 sec.	S, AS, AC	tensile failure signs in remaining pieces

Golder Associates

TABLE 1

TESTING PROGRAM FOR PHASE 1

	ASPECT TO BE STUDIED	SCOPE/SPECIAL FEATURE OF TESTING	REFERENCE/ TEST STANDARD	NO. OF TESTS
1.	Conventional Triaxial Tests strength characteristics of reference material and effect of various loading rate	o Series of conventional triaxial tests to establish strength characteristics of the reference material. o Scope of testing for each series includes: -Brazilian Tensile test -Uniaxial Compression test (σ_3 = 0) -Triaxial test σ_3 = 5,10,20,30 MPa -Rate of loading Series 1 ISRM Standard (Slow) Series 2 2 times faster (moderate) than ISRM Standard (2 MPa/sec) Series 3 43.7 MPa/sec -Pore gas maintained at atmospheric pressure o Conventional triaxial tests to establish the strength characteristics of the failed samples	ISRM Standard method of rock testing Brazian test Uniaxial compression Triaxial test	 16 7 5 3
2.	Calibration tests to study the feasibility of optimizing the number of samples	o Development of a multi-stage triaxial test to permit the optimization of the number of samples. o Include the determination of a relevant criterion for imminent failure o Monitoring of strains on specimen during triaxial tests (σ_3 = 0,10,20,30 MPa) o Pore gas maintained at atmospheric pressure	ISRM Standard method of rock testing (modified accordingly to the relevant criterion for imminent failure)	2 (preliminary) 4

continued...

Golder Associates

TABLE 16 (continued)

ASPECTS TO BE STUDIED	TEST SCHEDULE AND SPECIAL FEATURES	NO OF TESTS
4. Simulation of stress changes with the introduction of pore gas pressure (on samples from No. 26 Colliery)	• The mode of failure under conditions of rapid stress changes and the effect of pore gas pressure are the prime factors to be studied in this aspect. The testing program includes sixteen tests in which the samples would initially be loaded hydrostatically and then brought to failure by increasing σ_1 and reducing σ_3 simultaneously. The main area of interest is the examination of the failure mode of the specimens in the vicinity of the tensile region of the strength envelope. Pore gas pressure of up to 7 MPa will be introduced in the specimens.	16
	TOTAL NO. OF TESTS	39

NOTE: In the event that enough samples from the No. 26 Colliery cannot be made available, the tests would be conducted on the sample from the Lingan Colliery.

Golder Associates

PROPOSED MTS σ_3 SERVO CONTROLLED SYSTEM

FIGURE 1

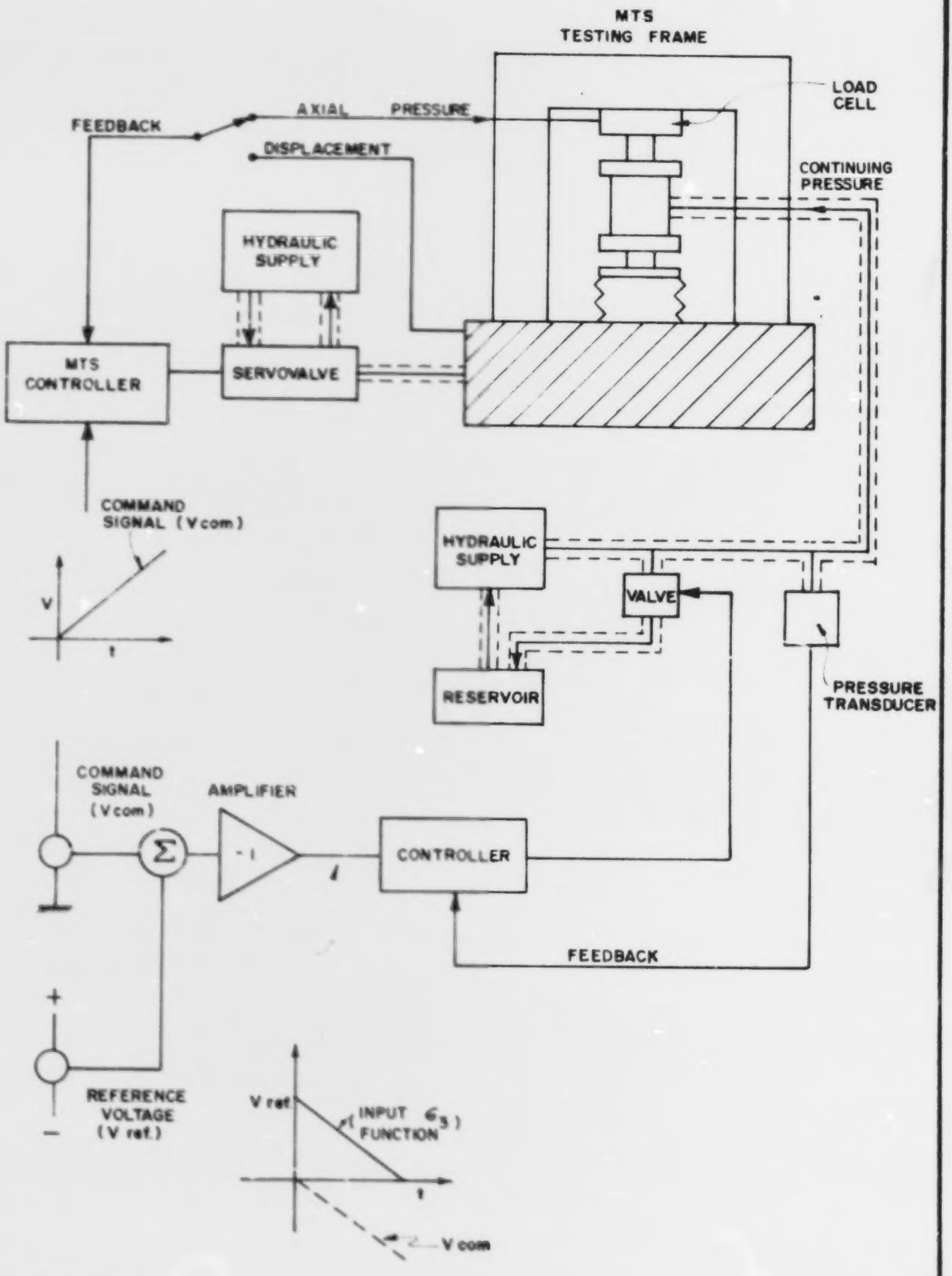

Date DEC. 12, 1984

Project 841-1207

Golder Associates

Drawn L.L.

Chkd

Form GA-C-4 (M)

STRENGTH ENVELOPES OF INTACT SPECIMENS OF PIER CAP SANDSTONE AT 3 STRESS RATES

FIGURE 2

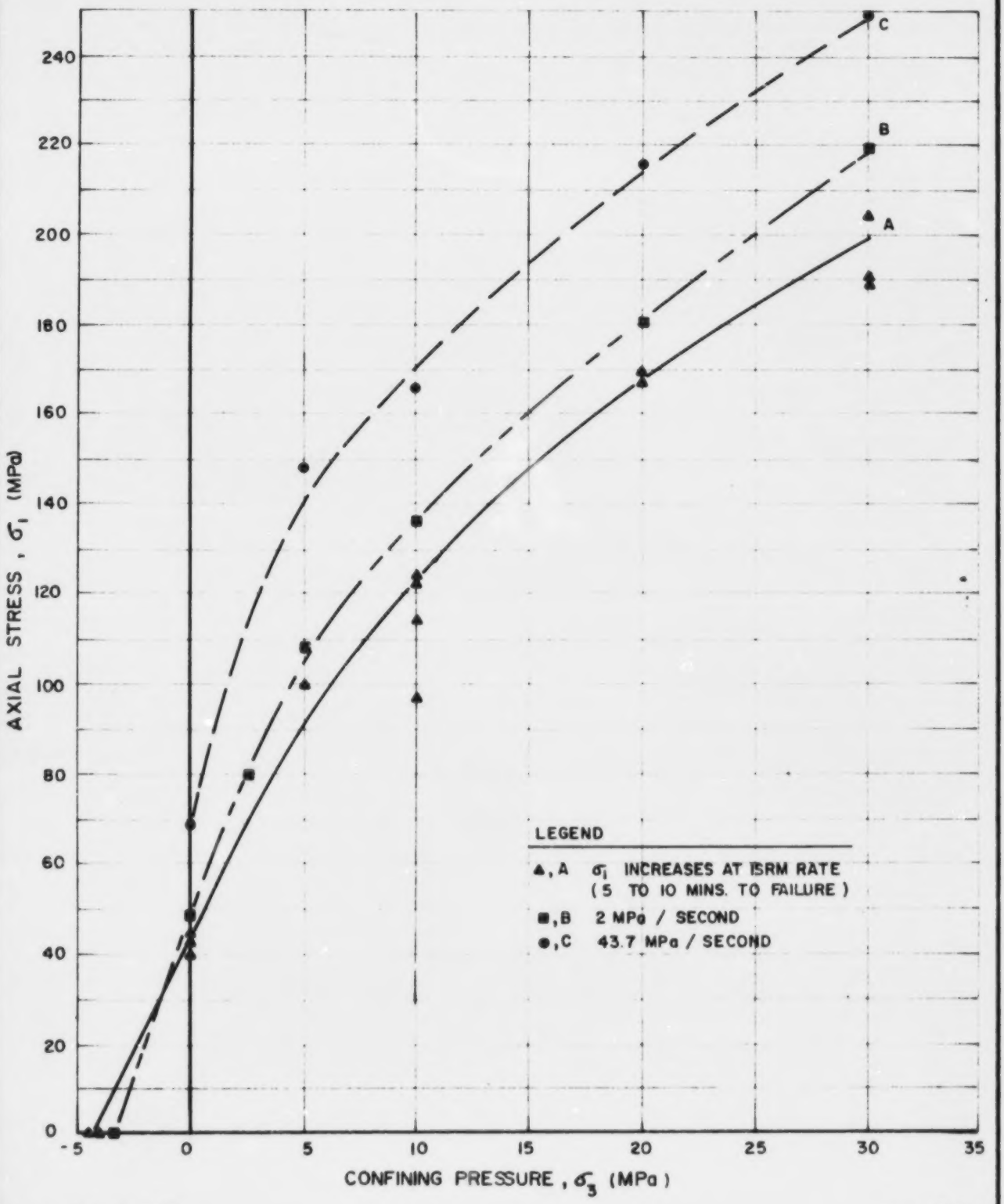

Date DEC. 6, 1984

Project 841-1287

Golder Associates

Drawn D.M.

Chkd

STRENGTH ENVELOPE OF FAILED SPECIMENS OF PIER CAP SANDSTONE

FIGURE 3

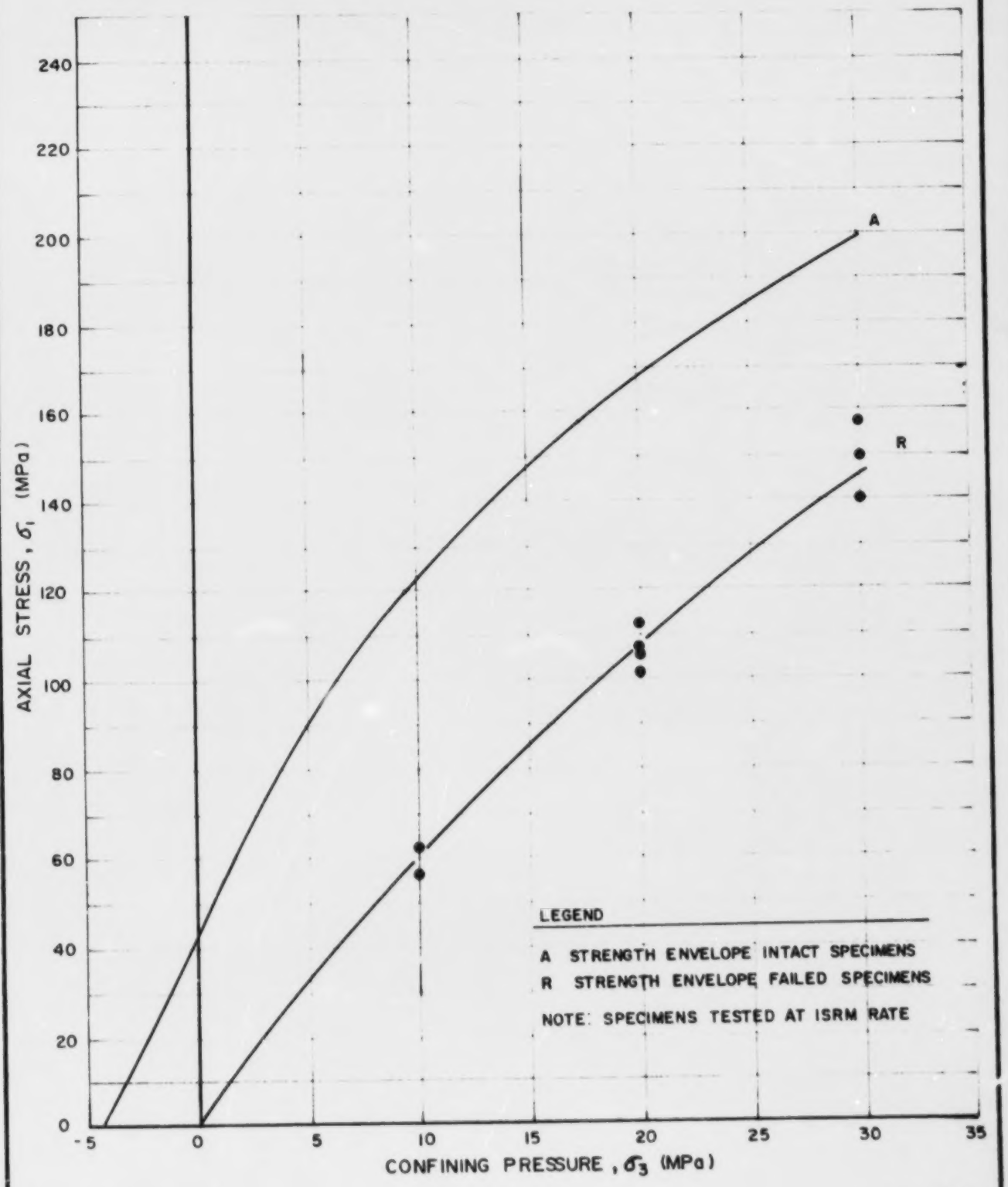

Date DEC. 6, 1984

Project 841-1287

Golder Associates

Drawn D.M.

Chkd

Form GA-D-4 (M)

STRESS PATHS OF ISRM AND PROPOSED MULTIPLE STAGE TRIAXIAL TESTS

FIGURE 4

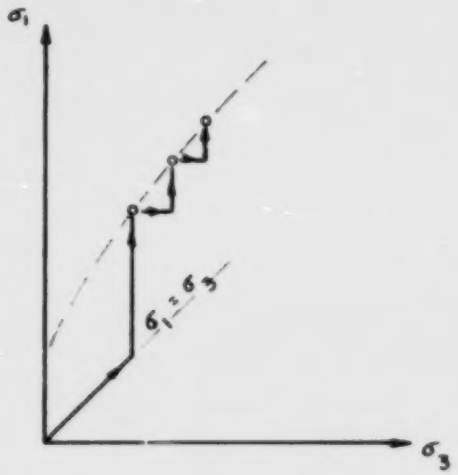

A) ISRM MULTIPLE FAILURE STATE TEST STRESS PATH (EDWARD, 1983)

1. HYDROSTATIC LOADING
2. AXIAL LOADING AT CONSTANT STRAIN RATE
3. END OF THE STAGE GIVEN BY THE PEAK ON THE σ_1 VS ε_1 CURVE
4. CONFINING PRESSURE IS MANUALLY INCREASED IN ONE STEP
5. STEP 2, 3 AND 4 REPEATED 4 TIMES
6. ON THE 5TH STAGE, AXIAL LOADING MAINTAINED UNTIL FAILURE

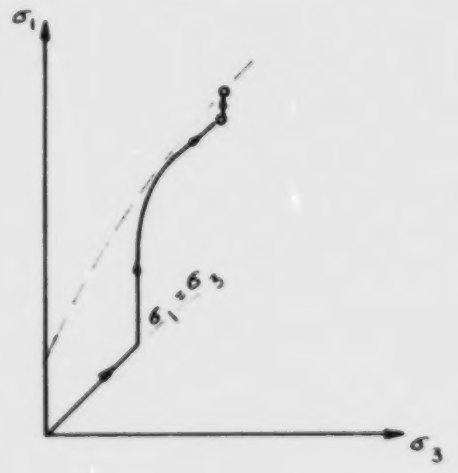

B) ISRM CONTINUOUS FAILURE STATE TEST STRESS PATH (EDWARD, 1983)

1. HYDROSTATIC LOADING
2. AXIAL LOADING AT CONSTANT STRAIN RATE UNTIL THE PEAK IS REACHED ON THE σ_1 VS ε_1 CURVE.
3. CONFINING PRESSURE IS THEN CONTINUOUSLY INCREASED AT A PREDETERMINED RATE AS A FUNCTION OF THE AXIAL LOADING RATE (SUCH THAT THE σ_1 VS ε_1 CURVE MAINTAINS THE SAME SLOPE AS IN STEP 2)
4. AT A CHOSEN POINT, CONFINING PRESSURE IS HELD CONSTANT AND AXIAL LOADING MAINTAINED UNTIL FAILURE

C) [illegible] TEST STRESS PATH

1. HYDROSTATIC CONSOLIDATION (DATA POINTS AT [illegible] AND OTHER DATA POINTS AT COMPLETION OF [illegible])
2. [illegible] TO INITIAL CONFINING [illegible]
3. [illegible]
4. AXIAL LOADING AT CONSTANT STRESS RATE UNTIL [illegible]
5. UNLOADING HYDROSTATIC CONDITIONS
6. STEPS 2, 3 AND 4 REPEATED 3 TIMES
7. ON THE 4TH STAGE, AXIAL LOADING MAINTAINED UNTIL FAILURE

Date DEC. 18, 1984
Project 841-1287

Golder Associates

Drawn G.P.
Chkd

Form G.A.-D-4 (M)

STRESS - STRAIN RELATIONSHIP
PIER CAP SANDSTONE

FIGURE 5

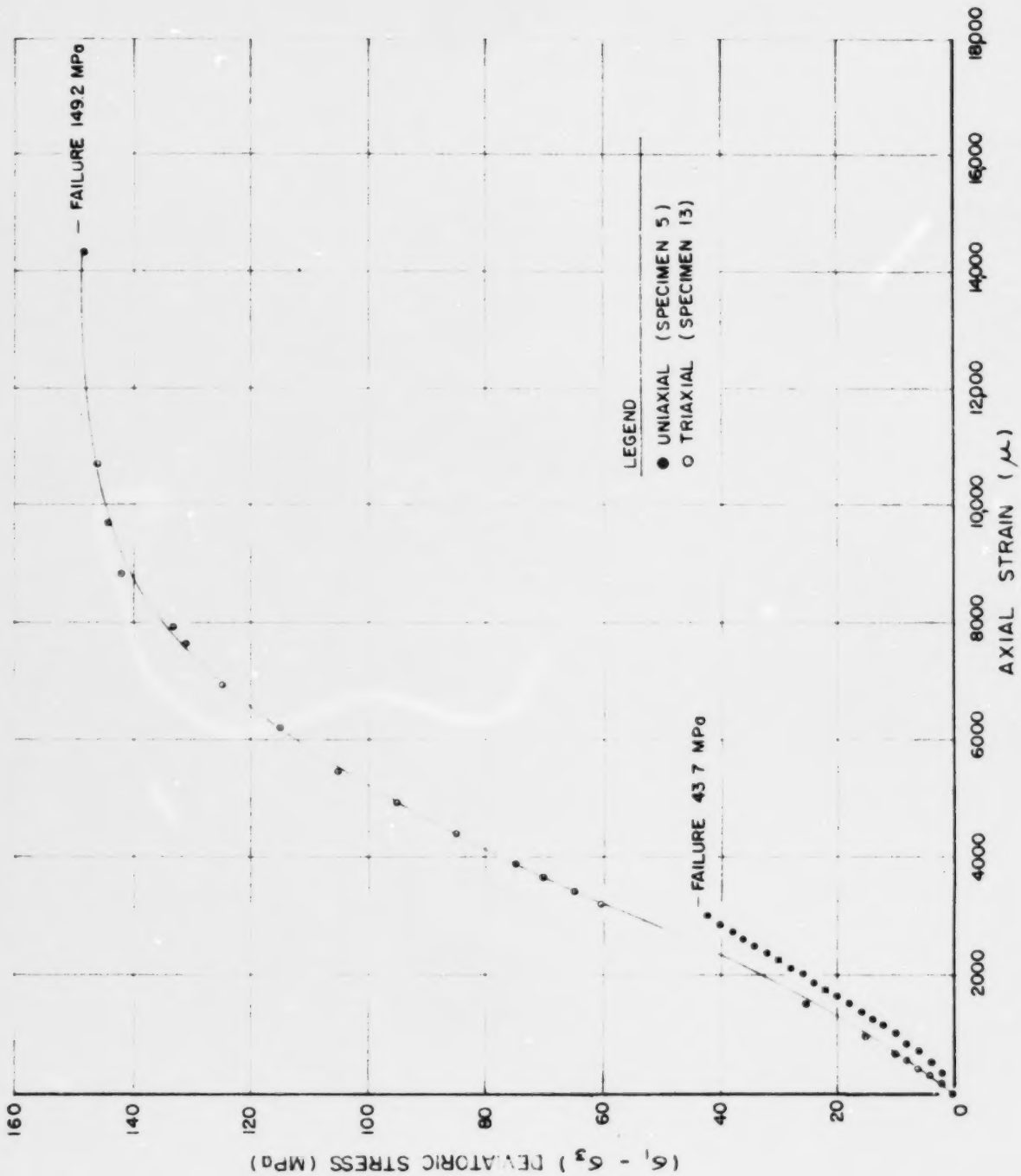

Date DEC 18,1984
Project 841-1287

Golder Associates

Drawn G.P.
Chkd

Form G.A.-D-4 (M)

EXAMINATION OF VARIOUS IMMINENT FAILURE CRITERIA – SPECIMEN 5

FIGURE 6

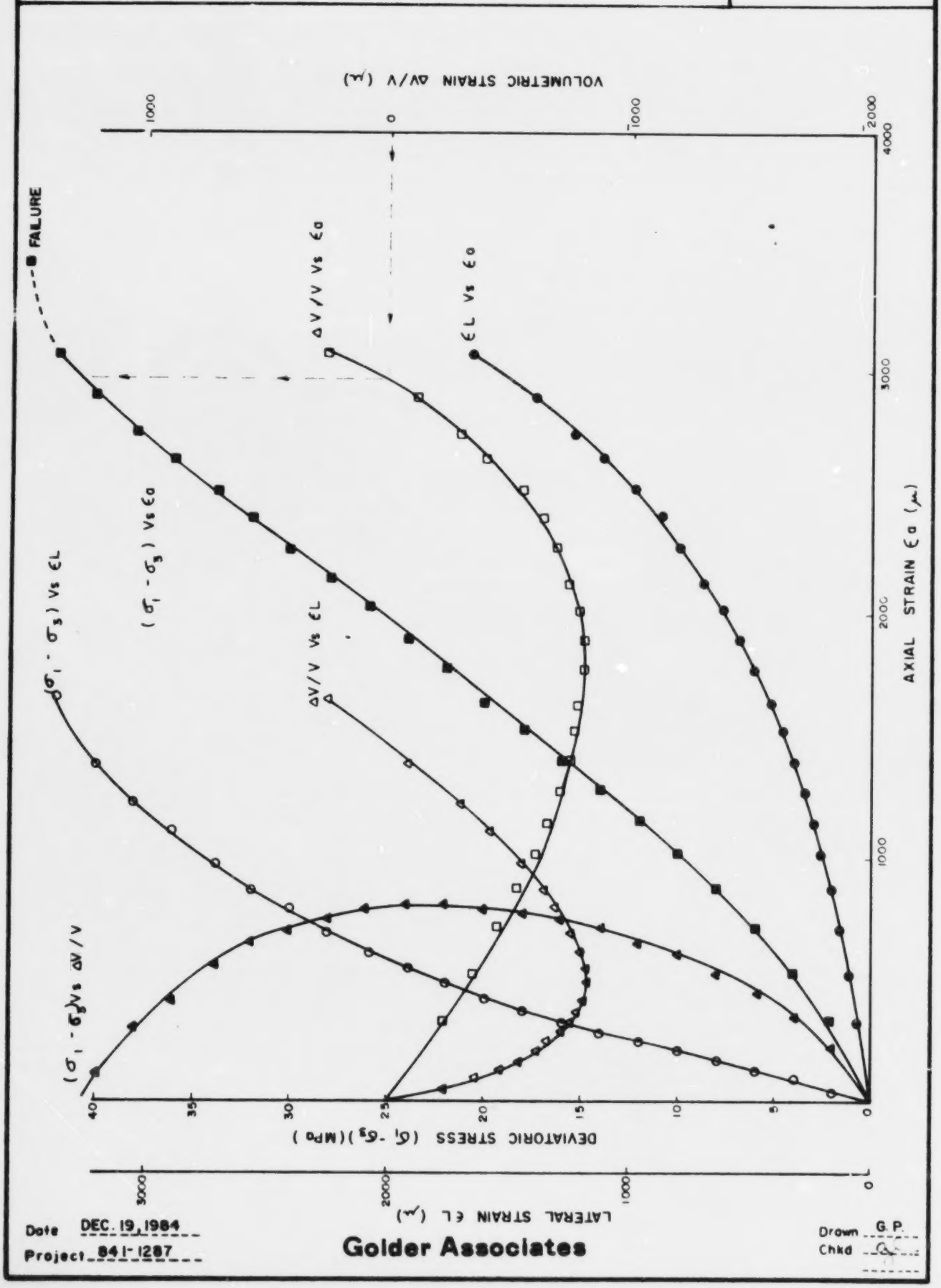

Date DEC. 19, 1984

Project 841-1287

Golder Associates

Drawn G.P.

Chkd

Form G.A.-D-4 (M)

EXAMINATION OF VARIOUS IMMINENT FAILURE CRITERIA – SPECIMEN 13

FIGURE 7

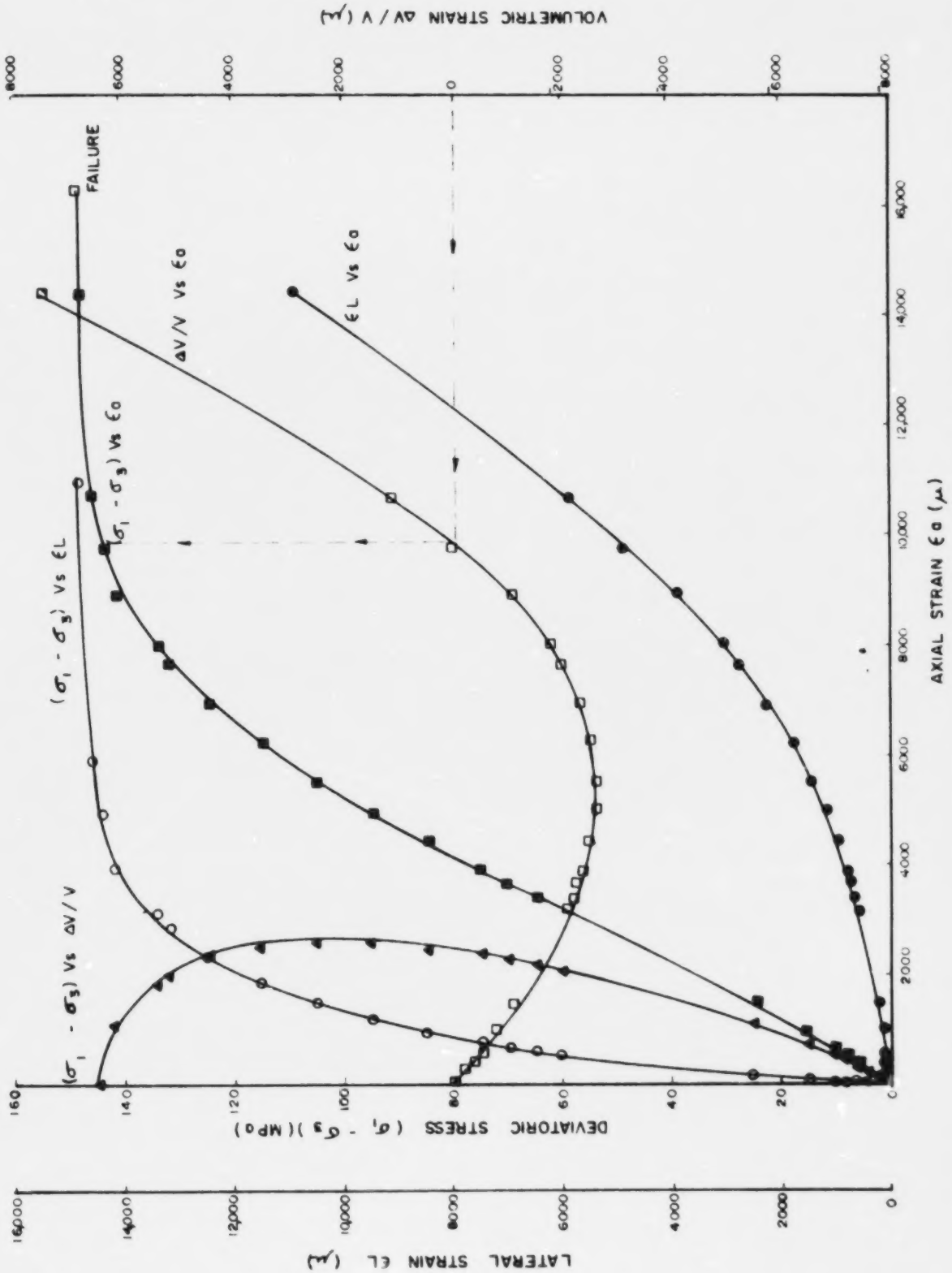

Date DEC. 19, 1984

Project 841-1287

Golder Associates

Drawn G.P.

Chkd.

Form G.A.-D.-4 (M)

STRENGTH ENVELOPES OF PIER CAP SANDSTONE
SINGLE STAGE AND MULTISTAGE TRIAXIAL TESTS

FIGURE 8

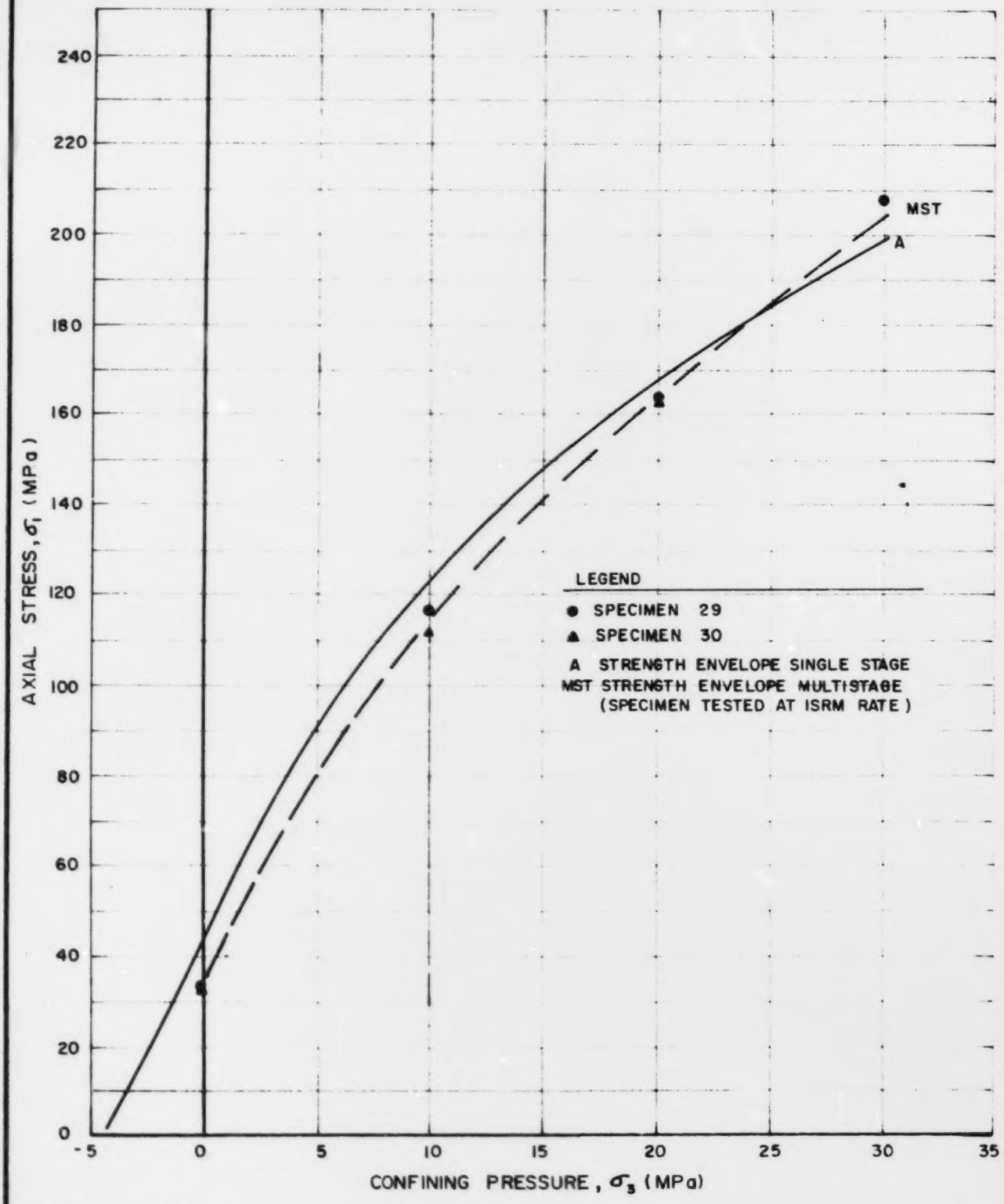

Date DEC. 6, 1984
Project 841-1287

Golder Associates

Drawn D.M.
Chkd

Form G.A.-D.-4 (M)

STRESS PATH OF CALIBRATION TESTS

FIGURE 9

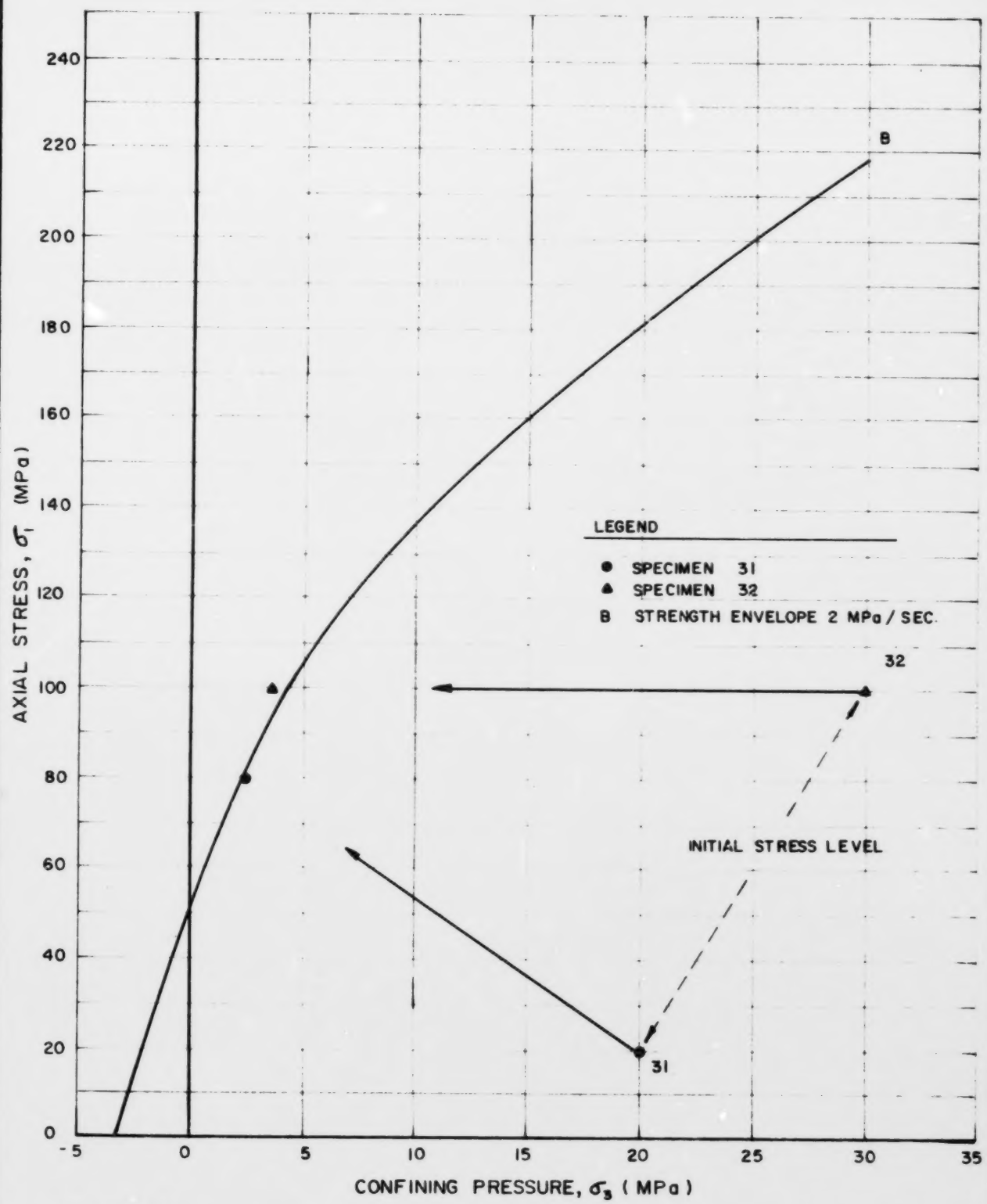

Date DEC. 6, 1984

Project 841-1287

Golder Associates

Drawn D.M.

Chkd

FORM GA-U-4 (M)

STRESS CHANGES SIMULATIONS

FIGURE 10

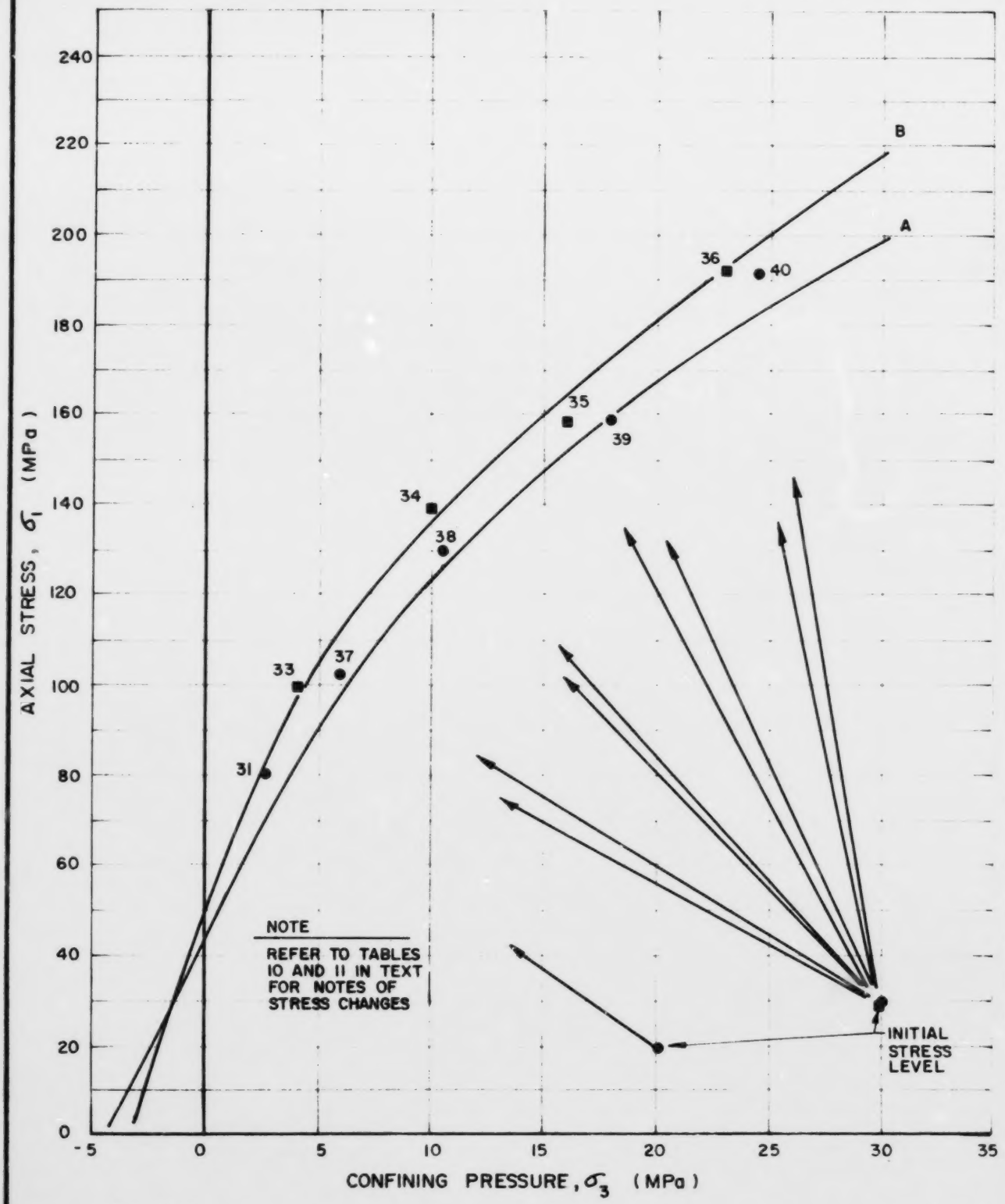

Date DEC. 6, 1984

Project 841-1287

Golder Associates

Drawn D.M

Chkd

Form G.A.-D.-4 (M)

RAPID REDUCTION OF CONFINING PRESSURE

FIGURE 11

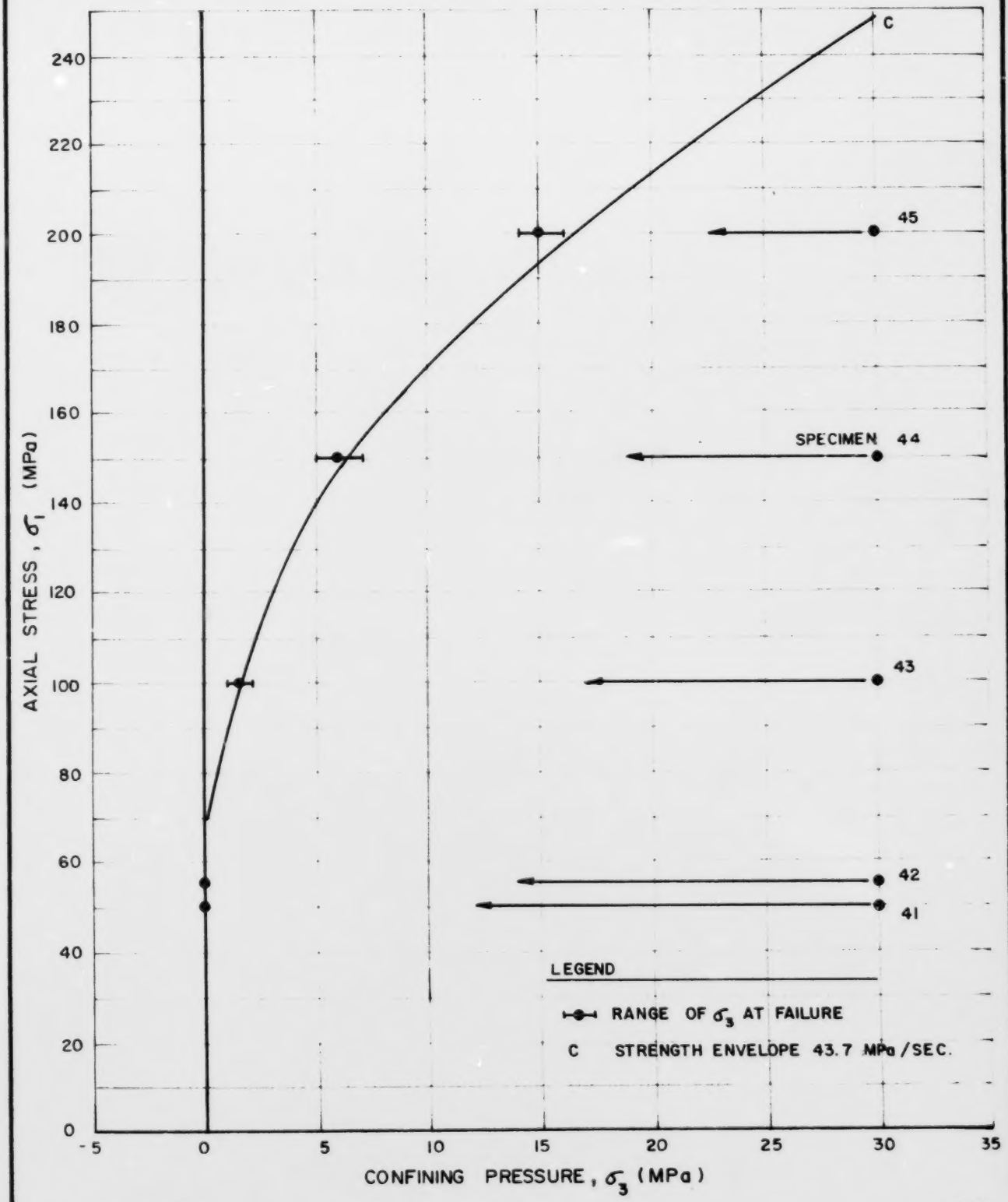

Date DEC. 6, 1984

Project 841-1287

Golder Associates

Drawn D.M.

Chkd

Form G.A.-D-4 (M)

STRENGTH OF SPECIMENS WITH PORE GAS PRESSURE | FIGURE 12

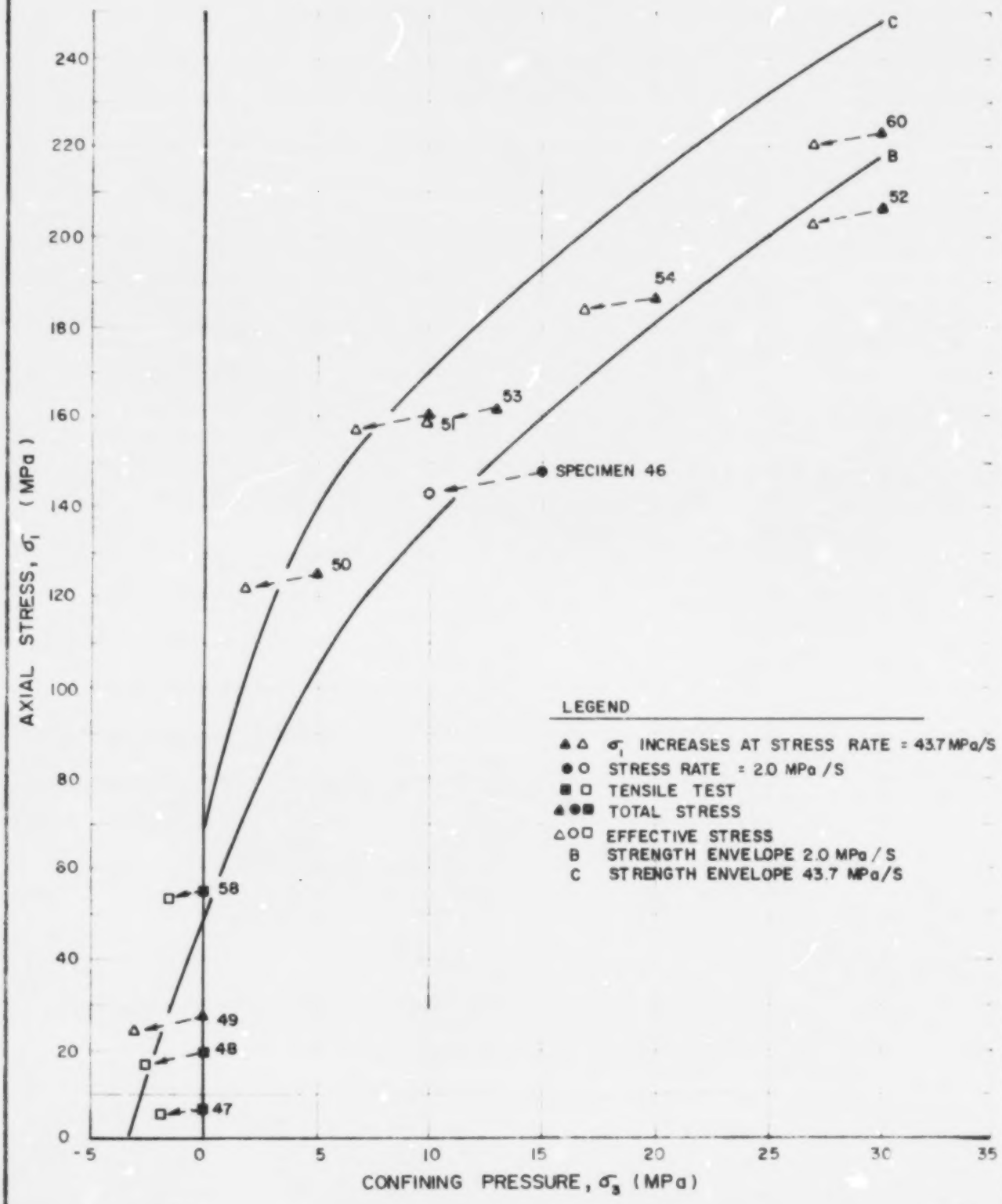

Date DEC 6, 1984

Project 841-1287

Golder Associates

Drawn D.M

Form GA-D-4 (M)

RAPID REDUCTION OF CONFINING PRESSURE SPECIMENS WITH PORE GAS PRESSURE

FIGURE 13

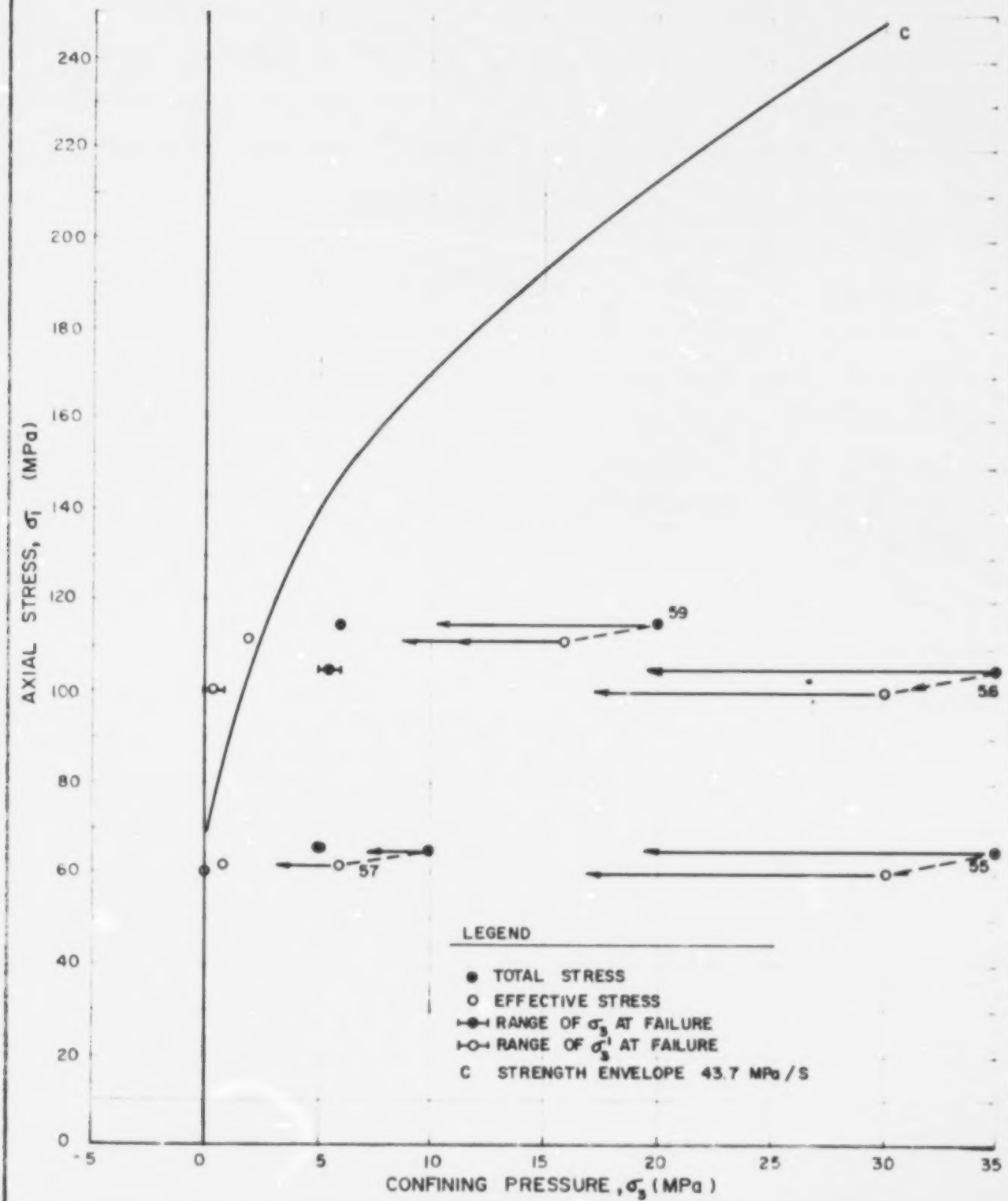

Date DEC 6, 1984

Project 841-1287

Golder Associates

Drawn D.M

Chkd

Form GA 0-4 (M)

CORRELATION BETWEEN FAILURE MODE AND STRESS CONDITIONS AT FAILURE, SPECIMENS WITH PORE GAS PRESSURE

FIGURE 14

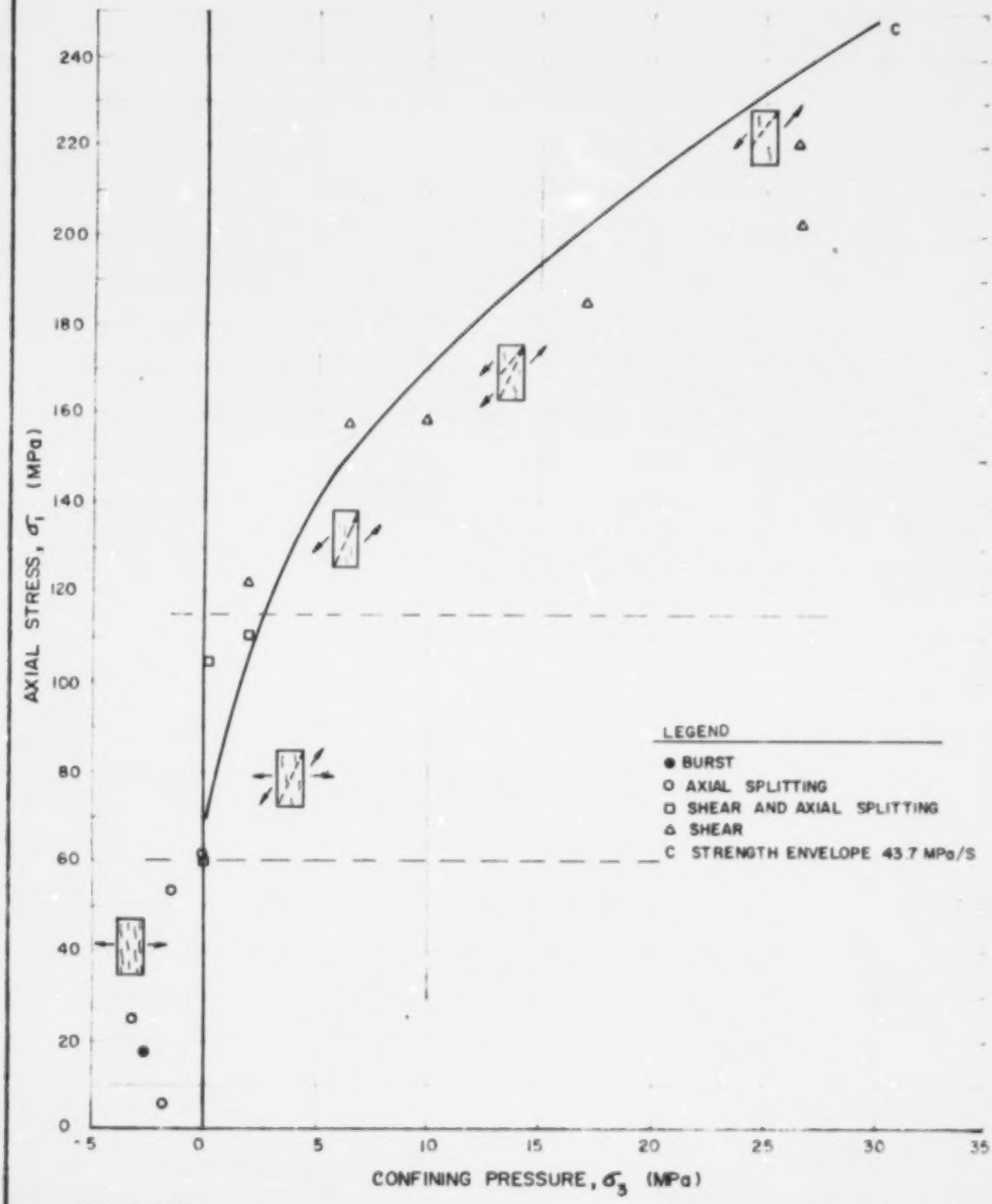

Date DEC 6, 1984

Project 841-1287

Golder Associates

Drawn D M

Chkd

Form G A-0-4 (M)

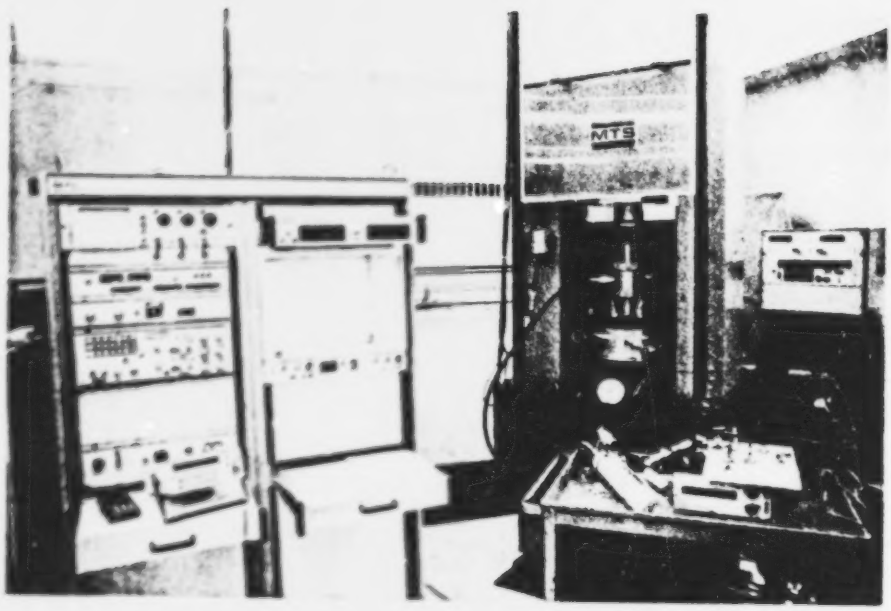

Plate 1 MTS Testing Equipment

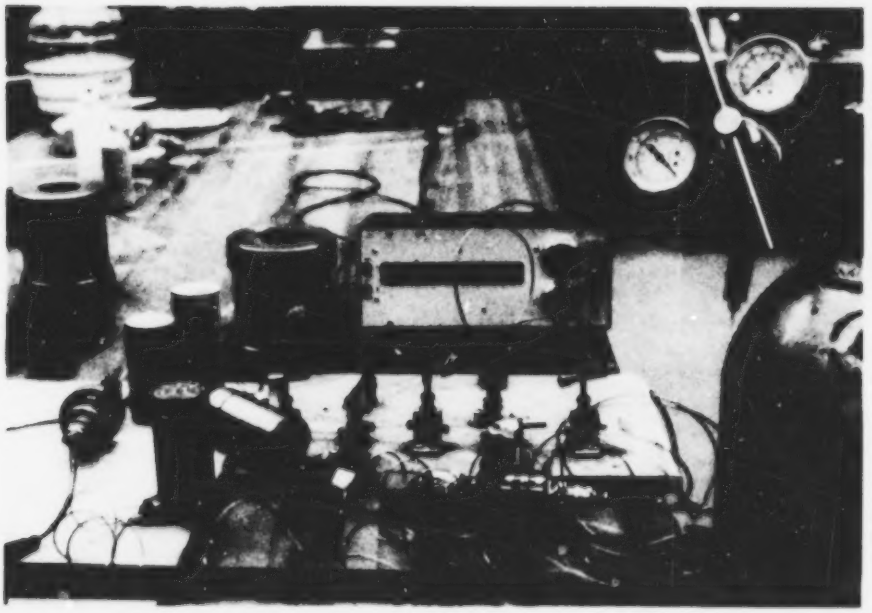

Plate 2 Special Platens for Testing Samples with Pore Gas Pressure

Plate 3 Strain Gauges on Specimen 29

Plate 4 Flaky Broken Pieces of Specimen 48 After Bursting. (Intact Specimen Shown for Comparison Purpose)

Plate 5 Specimen 14

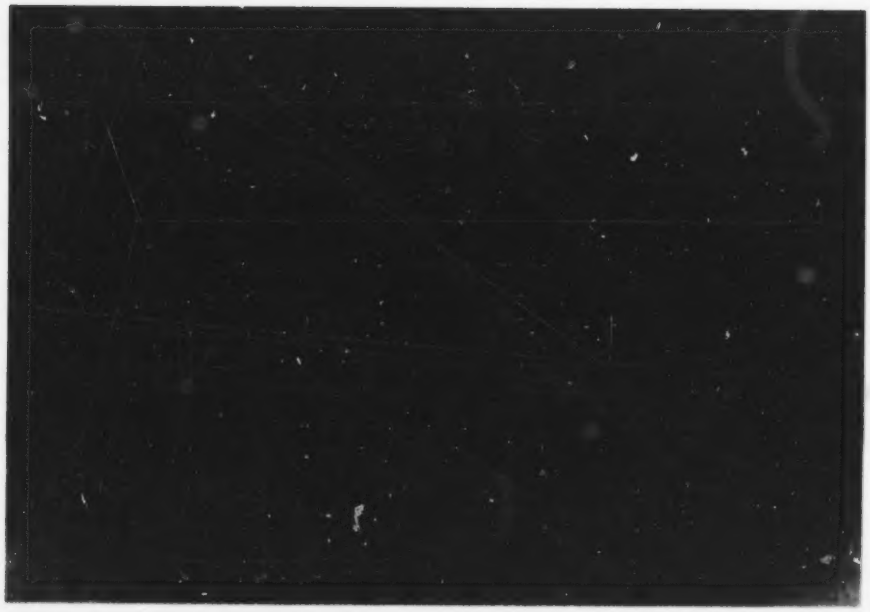

Plate 6 Specimen 18

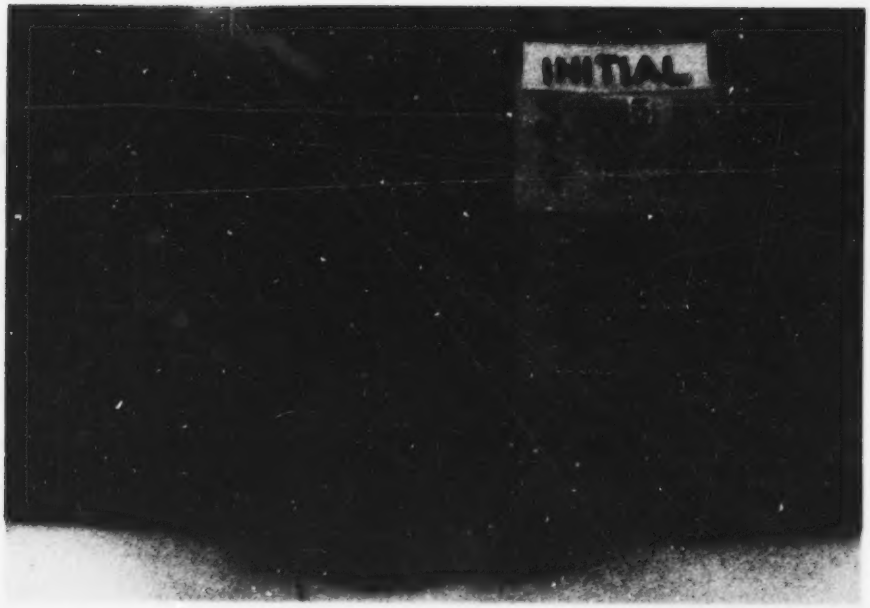

Plate 7 Specimen 56

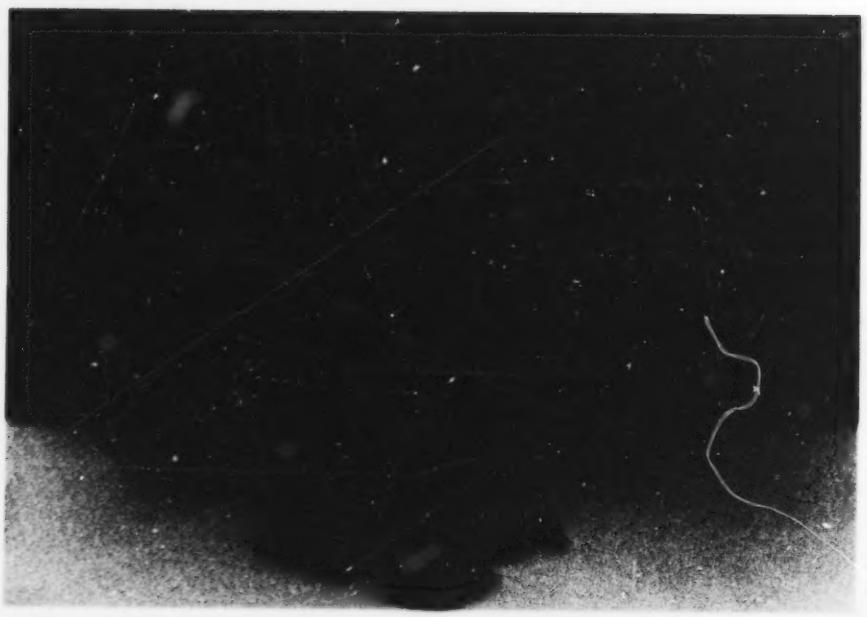

Plate 8 Specimen 49

APPENDIX I

ISRM SUGGESTED METHODS, BRAZILIAN, UNIAXIAL AND TRIAXIAL ROCK TESTING

December 1984

841-1287

Suggested Methods for Determining the Uniaxial Compressive Strength and Deformability of Rock Materials

PART 1. SUGGESTED METHOD FOR DETERMINATION OF THE UNIAXIAL COMPRESSIVE STRENGTH OF ROCK MATERIALS

1. SCOPE

This method of test is intended to measure the uniaxial compressive strength of a rock sample in the form of specimens of regular geometry. The test is mainly intended for strength classification and characterization of intact rock.

2. APPARATUS

(a) A suitable machine shall be used for applying and measuring axial load to the specimen. It shall be of sufficient capacity and capable of applying load at a rate conforming to the requirements set in Section 3. It shall be verified at suitable time intervals and shall comply with accepted national requirements such as prescribed in either ASTM Methods E4: Verification of Testing Machines or British Standard 1610, Grade A or Deutsche Normen DIN 51 220, DIN 51 223, Klasse 1 and DIN 51 300.

(b) A spherical seat, if any, of the testing machine, if not complying with specification 2(d) below, shall be removed or placed in a locked position, the two loading faces of the machine being parallel to each other.

(c) Steel platens in the form of discs and having a Rockwell hardness of not less than HRC58 shall be placed at the specimen ends. The diameter of the platens shall be between D and D + 2 mm where D is the diameter of the specimen. The thickness of the platens shall be at least 15 mm or D/3. Surfaces of the discs should be ground and their flatness should be better than 0.005 mm.

(d) One of the two platens shall incorporate a spherical seat. The spherical seat should be placed on the upper end of the specimen. It should be lightly lubricated with mineral oil so that it locks after the deadweight of the cross-head has been picked up. The specimen, the platens and spherical seat shall be accurately centred with respect to one another and to the loading machine. The curvature centre of the seat surface should coincide with the centre of the top end of the specimen.

3. PROCEDURE

(a) Test specimens shall be right circular cylinders having a height to diameter ratio of 2.5–3.0 and a diameter preferably of not less than NX core size, approximately 54 mm. The diameter of the specimen should be related to the size of the largest grain in the rock by the ratio of at least 10:1.

(b) The ends of the specimen shall be flat to 0.02 mm and shall not depart from perpendicularity to the axis of the specimen by more than 0.001 radian (about 3.5 min) or 0.05 mm in 50 mm.

(c) The sides of the specimen shall be smooth and free of abrupt irregularities and straight to within 0.3 mm over the full length of the specimen.

(d) The use of capping materials or end surface treatments other than machining is not permitted.

(e) The diameter of the test specimen shall be measured to the nearest 0.1 mm by averaging two diameters measured at right angles to each other at about the upper-height, the mid-height and the lower height of the specimen. The average diameter shall be used for calculating the cross-sectional area. The height of the specimen shall be determined to the nearest 1.0 mm.

(f) Samples shall be stored, for no longer than 30 days, in such a way as to preserve the natural water content, as far as possible, and tested in that condition.* This moisture condition shall be reported in accordance with "Suggested method for determination of the water content of a rock sample", Method 1, ISRM Committee on Laboratory Tests, Document No. 2, First Revision, December 1977 (this volume, p. 83).

(g) Load on the specimen shall be applied continuously at a constant stress rate such that failure will occur within 5–10 min of loading, alternatively the stress rate shall be within the limits of 0.5–1.0 MPa/s.

(h) The maximum load on the specimen shall be

* It is recognized that in some cases for some materials it may be desired to test specimens in other moisture conditions, for example, saturated or oven dry at 105 C. Such conditions shall be noted in the test report.

recorded in newtons (or kilonewtons and meganewtons where appropriate) to within 1%.

(j) The number of specimens tested should be determined from practical considerations but at least five are preferred.

4. CALCULATIONS

(a) The uniaxial compressive strength of the specimen shall be calculated by dividing the maximum load carried by the specimen during the test, by the original cross-sectional area.

5. REPORTING OF RESULTS

(a) Lithologic description of the rock.

(b) Orientation of the axis of loading with respect to specimen anisotropy, e.g. bedding planes, foliation, etc.

(c) Source of sample, including: geographic location, depth and orientations, dates and method of sampling and storage history and environment.

(d) Number of specimens tested.

(e) Specimen diameter and height.

(f) Water content and degree of saturation at time of test.

(g) Test duration and stress rate.

(h) Date of testing and type of testing machine.

(i) Mode of failure, e.g. shear, axial cleavage, etc.

(j) Any other observations or available physical data such as specific gravity, porosity and permeability citing the method of determination for each.

(k) Uniaxial compressive strength for each specimen in the sample, expressed to three significant figures, together with the average result for the sample. The pascal (Pa) or its multiples shall be used as the unit of stress and strength.

(l) Should it be necessary in some instances to test specimens that do not comply with specifications as stated above these facts shall be noted in the test report.

REFERENCES

1. Obert L., Windes S. L. & Duvall W. I. Standardized tests for determining the physical properties of mine rocks. *U.S. Bureau of Mines Report of Investigations*. No. 3891, 1946, 67 p.
2. International Bureau for Rock Mechanics. Richtlinien zur Durchführung von Druckversuchen an Gesteinen im Bergbau. *Bericht. 5. Ländertreffen des I.B.G.*, Akademie-Verlag, Berlin, 1964, pp. 21-25.
3. U.S. Corps of Engineers. Strength parameters of selected intermediate quality rocks—testing procedures. *Missouri River Division Laboratory Reports*. No. 64/493, July 1966, pp. 1A-6A; 1B-7B.
4. ASTM. Standard method of test for unconfined compressive strength of rock core specimens. *American Society for Testing and Materials*. ASTM Designation D-2938-71a.
5. Hawkes I. & Mellor M. Uniaxial testing in rock mechanics laboratories. *Engng. Geol.* 4, July 1970, pp. 177-285.

PART 2. SUGGESTED METHOD FOR DETERMINING DEFORMABILITY OF ROCK MATERIALS IN UNIAXIAL COMPRESSION

1. SCOPE

This method of test is intended to determine stress-strain curves and Young's modulus and Poisson's ratio in uniaxial compression of a rock specimen of regular geometry. The test is mainly intended for classification and characterization of intact rock.

2. APPARATUS

(a) to (d)—See Part 1.

(e) Electrical resistance strain gauges, linear variable differential transformers, compressometers, optical devices or other suitable measuring devices. Their design shall be such that the average of two circumferential and two axial strain measurements, equally spaced, can be determined for each increment of load. The devices should be robust and stable, with strain sensitivity of the order of 5×10^{-6}.

Both axial and circumferential strains shall be determined within an accuracy of 2% of the reading and a precision of 0.2 percent of full scale.

If electrical resistance strain gauges are used, the length of the gauges over which axial and circumferential strains are determined shall be at least ten grain diameters in magnitude and the gauges should not encroach within D/2 of the specimen ends, where D is the diameter of the specimen.

If dial micrometers of LVDT's are used for measuring axial deformation due to loading, these devices should be graduated to read in 0.002 mm units and accurate within 0.002 mm in any 0.02 mm range and within 0.005 mm in any 0.25 mm range. The dial micrometer or LVDT's should not encroach within D/2 of the specimen ends.

(f) An apparatus for recording the loads and deformations; preferably an X–Y recorder capable of direct plotting of load-deformation curves.

3. PROCEDURE

(a) to (e)—See Part 1.

(f) Moisture can have a significant effect on the deformability of the test specimen. When possible, *in situ* moisture conditions should be preserved until the time of the test. When the characteristic of the rock material under conditions varying from saturation to dry is required, proper note shall be made of moisture conditions so that correlation between deformability and moisture content can be made. Excess moisture can create a problem of adhesion of strain gauges which may require making a change in moisture content of the sample. The moisture condition shall be reported

in accordance with "Suggested method for determination of the water content of a rock sample", Method 1, ISRM Committee on Laboratory Tests, Document No. 2, December 1977 (this volume, p. 83).

(g) Load on the specimen shall be applied continuously at a constant stress rate such that failure will occur within 5–10 min of loading, alternatively the stress rate shall be within the limits of 0.5–1.0 MPa/s.

(h) Load and axial and circumferential strains or deformations shall be recorded at evenly spaced load intervals during the test, if not continually recorded. At least ten readings should be taken over the load range to define the axial and diametric stress-strain curves.

(i) It is sometimes advisable for a few cycles of loading and unloading to be performed.

(j) The number of specimens instrumented and tested under a specified set of conditions shall be governed by practical considerations but at least five are preferred.

4. CALCULATIONS

(a) Axial strain, ϵ_a, and diametric strain, ϵ_d, may be recorded directly from strain indicating equipment or may be calculated from deformation readings depending upon the type of instrumentation such as discussed in paragraph 2(e).

(b) Axial strain is calculated from the equation

$$\epsilon_a = \frac{\Delta l}{l_0}$$

where

l_0 = original measured axial length

Δl = change in measured axial length (defined to be positive for a decrease in length)

(c) Diametric strain may be determined either by measuring the changes in specimen diameter or by measuring the circumferential strain. In the case of measuring the changes in diameter, the diametric strain is calculated from the equation

$$\epsilon_d = \frac{\Delta d}{d_0}$$

where

d_0 = original undeformed diameter of the specimen

Δd = change in diameter (defined to be negative for an increase in diameter)

In the case of measuring the circumferential strain ϵ_c, the circumference is $C = \pi d$, thus the change in circumference is $\Delta C = \pi \Delta d$. Consequently, the circumferential strain, ϵ_c, is related to diametric strain, ϵ_d, by

$$\epsilon_c = \frac{\Delta C}{C_0} = \frac{\Delta d}{d_0},$$

so that

$$\epsilon_c = \epsilon_d$$

where C_0 and d_0 are original specimen circumference and diameter, respectively.

(d) The compressive stress in the test specimen, σ, is calculated by dividing the compressive load P on the specimen by the initial cross-sectional area, A_0. Thus

$$\sigma = \frac{P}{A_0}$$

where in this test procedure, compressive stresses and strains are considered positive.

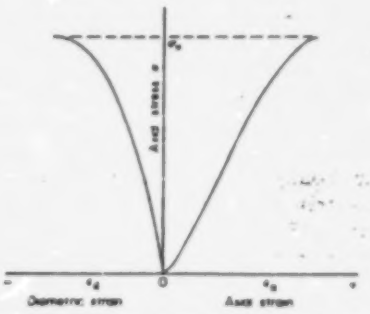

Fig. 1. Format for graphical presentation of axial and diametric stress-strain curves.

(e) Fig. 1 illustrates typical plot of axial stress versus axial and diametric strains. These curves show typical behaviour of rock materials from zero stress up to ultimate strength, σ_u. The complete curves give the best description of the deformation behaviour of rocks having non-linear stress-strain behaviour at low and high stress levels.

(f) Axial Young's modulus, E (defined as the ratio of the axial stress change to axial strain produced by the stress change) of the specimen may be calculated using any one of several methods employed in accepted engineering practice. The most common methods, listed in Fig. 2, are as follows:

(1) Tangent Young's modulus, E_t, is measured at a stress level which is some fixed percentage of the ulti-

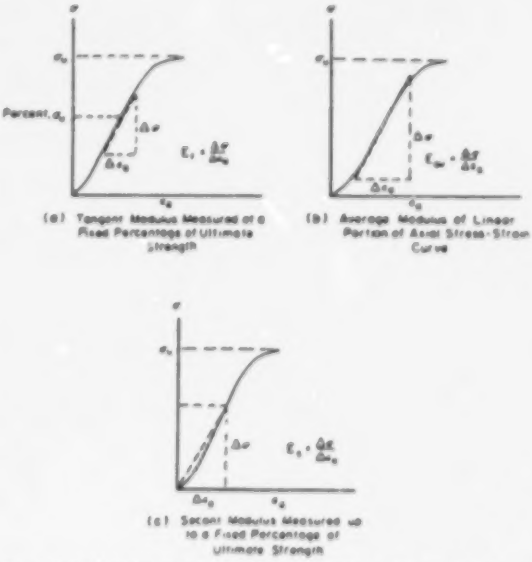
(a) Tangent Modulus Measured at a Fixed Percentage of Ultimate Strength
(b) Average Modulus of Linear Portion of Axial Stress-Strain Curve
(c) Secant Modulus Measured up to a Fixed Percentage of Ultimate Strength

Fig. 2. Methods for calculating Young's modulus from axial stress-strain curve.

mate strength (Fig. 2a). It is generally taken at a stress level equal to 50% of the ultimate uniaxial compressive strength.

(2) Average Young's modulus, E_{av}, is determined from the average slopes of the more-or-less straight line portion of the axial stress-axial strain curve (Fig. 2b).

(3) Secant Young's modulus, E_s, is usually measured from zero stress to some fixed percentage of the ultimate strength (Fig. 2c), generally at 50%.

Axial Young's modulus E is expressed in units of stress i.e. pascal (Pa) but the most appropriate multiple is the gigapascal (GPa = 10^9 Pa).

(g) Poisson's ratio, ν, may be calculated from the equation

$$\nu = -\frac{\text{slope of axial stress–strain curve}}{\text{slope of diametric stress–strain curve}}$$

$$= -\frac{E}{\text{slope of diametric curve}},$$

where the slope of the diametric curve is calculated in the same manner for either of the three ways discussed for Young's modulus in paragraph 4(f). Note that Poisson's ratio in this equation has a positive value, since the slope of the diametric curve is negative by the conventions used in this procedure.

(h) The volumetric strain, ϵ_v, for a given stress level is calculated from the equation

$$\epsilon_v = \epsilon_a + 2\epsilon_d.$$

5. REPORTING OF RESULTS

The report should include the following:

(a) to (j)—See Part 1.

(k) Values of applied load, stress and strain as tabulated results or as recorded on a chart.

(l) Young's modulus and Poisson's ratio for each specimen in the sample, expressed to three significant figures, together with the average result for the sample.

(m) Method of determination of Young's modulus and at what axial stress level or levels determined.

(n) Sould it be necessary in some instances to test specimens that do not comply with the above specifications, these facts shall be noted in the test report.

REFERENCE

Standard method of test for elastic moduli of rock core specimens in uniaxial compression. *American Society for Testing and Materials*, ASTM Designation D 3148-72.

Published in

Suggested Methods for Determining Tensile Strength of Rock Materials

PART 1: SUGGESTED METHOD FOR DETERMINING DIRECT TENSILE STRENGTH

1. SCOPE

This method of test is intended to measure directly the uniaxial tensile strength of a rock specimen of regular geometry. The test is mainly intended for classification and characterization of intact rock.

2. APPARATUS

(a) A suitable machine shall be used for applying and measuring the axial load to the specimen. It shall be of sufficient capacity and capable of applying load at a rate conforming to the requirements set in section 3. It shall be verified at suitable time intervals and shall comply with accepted national requirements such as prescribed in either ASTM Methods E4, Verification of Testing Machines or British Standard 1610, Grade A or Deutsche Normen DIN 51 220 and DIN 51 223, Klasse 1.

(b) Cylindrical metal caps shall be cemented to the specimen ends, providing a means through which the direct uniaxial tensile load can be applied. The diameter of the metal caps shall not be less than that of the test specimen nor shall it exceed the test specimen diameter by more than 2 mm. Caps shall have a thickness of at least 15 mm. Caps shall be provided with a suitable linkage system for load transfer from the loading device to the test specimen. The linkage system shall be so designed that the load will be transmitted through the axis of the test specimen without the application of bending or torsional stresses. The length of the linkages at each end shall be at least twice the diameter of the metal caps.*

3. PROCEDURE

(a) The test specimens shall be right circular cylinders having a height to diameter ratio of 2.5:3.0 and a diameter preferably of not less than NX core size, approximately 54 mm. The diameter of the specimen should be related to the size of the largest grain in rock by the ratio of at least 10:1.

(b) The ends of the specimen shall be generally smooth and flat.† The ends shall not depart from perpendicularity to the axis of the specimen by more than 0.001 radian (about 3.5 min) or 0.05 in 50 mm.

(c) The sides of the specimen shall be smooth and free of abrupt irregularities and straight to within 0.1 mm over the full length of the specimen.

(d) The diameter of the test specimen shall be measured to the nearest 0.1 mm by averaging two diameters measured at right angles to each other at about the mid-height of the specimen. The average diameter shall be used for calculating the cross-sectional area. The height of the specimen shall be determined to the nearest 1.0 mm.

(e) Samples shall be stored, for no longer than 30 days, in such a way as to preserve the natural water content, as far as possible, until the time of specimen preparation. Following their preparation, the specimens shall be stored prior to testing for 5–6 days in an environment of 20°C ± 2°C and 50% ± 5% humidity.‡ This moisture condition shall be reported in accordance with "Suggested method for determination of the water content of a rock sample", Method 1, Committee on Laboratory Tests, Document No. 2, First Revision, Dec. 1977 (this volume p. 83).

(f) The metal caps should be cemented to the specimen in such a manner as to ensure alignment of the cap axes with the longitudinal axis of the specimen. The thickness of the cement layer should not exceed 1.5 mm at each end. After the cement has hardened sufficiently to exceed the tensile strength of the rock, the test speciment shall be placed in the testing machine in such a way that the load transfer system is properly aligned.

(g) The tensile load on the specimen shall be applied continuously at a constant stress rate such that failure will occur within 5 min of loading; alternatively the stress rate shall be within the limits of 0.5 MPa/s to 1.0 MPa/s.

(h) The maximum load on the specimen shall be recorded to within 1%.

(i) The number of specimens per sample tested should be determined from practical considerations but at least five are preferred.

4. CALCULATIONS

The tensile strength of the specimen shall be calcu-

---

* According to the *Annual Book of ASTM Standards*, Test D2936-71, a roller or link chain of suitable capacity has been found to perform quite well in this application. Because roller chain flexes in one plane only, the upper and lower segments are positioned at right angles to each other to reduce bending in the specimen. Ball-and-socket, cable or similar arrangements have been found to be generally unsuitable because their tendency for bending and twisting makes the assembly unable to transmit a purely direct tensile stress to the test specimen.

‡ In direct tension tests, the condition of the specimen ends with regard to the degree of flatness and smoothness is not as critical as in compression tests. End surfaces such as result from sawing with a diamond cut-off wheel are entirely adequate.

† It is recognized that in some cases for some materials (e.g. shale), it may be desired to test specimens in other moisture conditions, for example, saturated or oven dry at 105°C. Such conditions shall be noted in the test report.

lated by dividing the maximum load applied to the specimen by the original cross-sectional area.

5. REPORTING OF RESULTS

(a) Lithologic description of the rock.

(b) Orientation of the axis of loading with respect to specimen anisotropy, e.g. bedding planes, foliation, etc.

(c) Source of sample, including: geographic location, depth and orientation, dates of sampling and storage history and environment.

(d) Number of specimens tested.

(e) Specimen diameter and height.

(f) Water content and degree of saturation at time of test.

(g) Test duration and/or stress rate.

(h) Date of testing and type of testing machine.

(i) Mode of failure, e.g. location and orientation of failure surface.

(j) Any other observations or available physical data, such as specific gravity, porosity and permeability, citing the method of determination of each.

(k) The tensile strength for each specimen in the sample, expressed to three significant figures, together with the average result for the sample. The pascal (Pa) or kilopascal (kPa) or mega-pascal (MPa) shall be used as the unit of stress and strength.

(l) Should it be necessary in some instances to test specimens that do not comply with the above specifications, these facts shall be noted in the test report.

PART 2: SUGGESTED METHOD FOR DETERMINING INDIRECT TENSILE STRENGTH BY THE BRAZIL TEST

1. SCOPE

This test is intended to measure the uniaxial tensile strength of prepared rock specimens indirectly by the Brazil test. The justification for the test is based on the experimental fact that most rocks in biaxial stress fields fail in tension at their uniaxial tensile strength when one principal stress is tensile and the other finite principal stress is compressive with a magnitude not exceeding three times that of the tensile principal stress.

2. APPARATUS

(a) Two steel loading jaws designed so as to contact a disc-shaped rock sample at diametrically-opposed surfaces over an arc of contact of approx 10° at failure. The suggested apparatus to achieve this is illustrated in Fig. 1. The critical dimensions of the apparatus are the radius of curvature of the jaws, the clearance and length of the guide pins coupling the two curved jaws

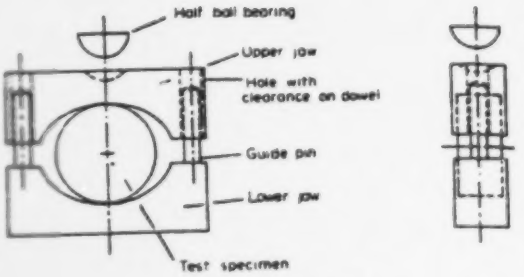

Fig. 1. Apparatus for Brazil test.

and the width of the jaws. These are as follows: Radius of jaws—1.5 × specimen radius; guide pin clearance—permit rotation of one jaw relative to the other by 4×10^{-3} rad out of plane of the apparatus (25 mm penetration of guide pin with 0.1 mm clearance); width of jaws—1.1 × specimen thickness. The remaining dimensions can be scaled from Fig. 1. The upper jaw contains a spherical seating conveniently formed by a 25-mm diameter half-ball bearing.

(b) Double thickness (0.2–0.4 mm) adhesive paper strip (masking tape) with a width equal to or slightly greater than the specimen thickness.

(c) A suitable machine for applying and measuring compressive loads to the specimen. It shall be of sufficient capacity and be capable of applying load at a rate conforming to the requirements set out in section 3. It shall be verified at suitable time intervals and shall comply with accepted national requirements such as prescribed in either ASTM Methods E4, Verification of Testing Machines or British Standard 1610, Grade A or Deutsche Normen DIN 51 220 and DIN 51 223, Klasse 1.

(d) A spherical seat, if any, of the testing machine crosshead shall be placed in a locked position, the two loading surfaces of the machine being parallel to each other.

(e) It is preferable but not obligatory that the testing machine be fitted with a chart recorder to record load against displacement to aid in the measurement of the failure load.

3. PROCEDURE

(a) The test specimens should be cut and prepared using clean water. The cylindrical surfaces should be free from obvious tool marks and any irregularities across the thickness of the specimen should not exceed 0.025 mm. End faces shall be flat to within 0.25 mm and square and parallel to within 0.25°.

(b) Specimen orientation shall be known and the water content controlled or measured and reported in accordance with the "Suggested method for determination of water content of a rock sample", Method 1, ISRM Committee on Laboratory Tests, Document No. 2, First Revision, Dec. 1977 (this volume p. 83).

(c) The specimen diameter shall not be less than NX

core size, approximately 54 mm, and the thickness should be approximately equal to the specimen radius.

(d) The test specimen shall be wrapped around its periphery with one layer of the masking tape and mounted squarely in the test apparatus such that the curved platens load the specimen diametrally with the axes of rotation for specimen and apparatus coincident.

(e) Load on the specimen shall be applied continuously at a constant rate such that failure in the weakest rocks occurs within 15–30 s. A loading rate of 200 N/s is recommended.

(f) Where the testing machine is fitted with a force/displacement recorder, a record should be taken during testing—so that the load for primary fracture can be precisely determined (in some cases load continues to increase after primary failure as the split specimen is still bearing load). If a load/displacement recorder is not available on the testing machine, then care must be taken by the operator to detect the load at primary failure. At primary failure there will be a brief pause in the motion of the indicator needle. However, the difference between the load at primary failure and ultimate load bearing capacity is at most only about 5%.

(g) The number of specimens per sample tested should be determined from practical considerations, but normally ten are recommended.

4. CALCULATIONS

The tensile strength of the specimen σ_t, shall be calculated by the following formula:

$$\sigma_t = 0.636\, P/Dt \text{ (MPa)}$$

where P is the load at failure (N), D is the diameter of the test specimen (mm), t is the thickness of the test specimen measured at the center (mm).

5. REPORTING OF RESULTS

(a) Lithologic description of the rock.

(b) Orientation of the axis of loading with respect to specimen anisotropy, e.g. bedding planes, foliation, etc.

(c) Source of sample, including: geographic location, depth and orientation, dates and method of sampling and storage history and environment.

(d) Number of specimens tested.

(e) Specimen diameter and height.

(f) Water content and degree of saturation at time of test.

(g) Test duration and stress rate.

(h) Date of testing and type of testing machine.

(i) Mode of failure.

(j) Any other observations or available physical data such as specific gravity, porosity and permeability, citing the method of determination for each.

(k) The tensile strength for each specimen in the sample, expressed to three significant figures, together with the average result for the sample.

REFERENCES

Mellor M. & Hawkes I. Measurement of tensile strength by diametral compression of discs and annuli. *Engng Geol.* **5**, 173–225 (1971).

Suggested Methods for Determining the Strength of Rock Materials in Triaxial Compression

1. SCOPE

This test is intended to measure the strength of cylindrical rock specimens subjected to triaxial compression. This provides the values necessary to determine the strength envelope and from this the value of the internal friction angle ϕ and the "apparent" cohesion C may be calculated.*

2. APPARATUS

The apparatus consists essentially of three parts (See Fig. 1): a triaxial cell, a loading device and a device for generating confining pressure.

2.1. *A triaxial cell*

This comprises:

(a) A triaxial cell body, into which the specimen may be placed in order to apply the confining pressure. The body of the cell should have an air bleeder hole and a connection for a hydraulic line.

(b) A flexible jacket of suitable material to prevent the hydraulic fluid from entering the specimen, and which shall not significantly extrude into abrupt surface pores.

(c) Steel platens having Rockwell hardness of not less than C30 shall be placed at both specimen ends. The diameter of the platens shall be between D and $D + 2$ mm, where D is the diameter of the specimen. The thickness of the platens shall be at least 15 mm or $D/3$. Surfaces of platens should be ground and their flatness should be 0.005 mm.

(d) Spherical seats which are incorporated in each of the platens.† The curvature centre of the seat surfaces should coincide with the centre of the specimen ends.

2.2. *A loading device for applying and controlling axial load*

(a) A suitable machine shall be used for applying, controlling and measuring the axial load on the rock specimen. It shall be of sufficient capacity and capable of applying the load at a rate conforming to the requirements as set out in section 4(e). It shall be verified at certain time intervals‡ and shall comply with the accepted national requirements such as prescribed in either ASTM Methods E 4, Verification of Testing Machines; British Standard 1610, 1964, Grade A or Deutsche Normen DIN 51 220 and DIN 51 223, Klasse 1 and DIN 51 300.

(b) The spherical seat of the loading machine, if any, and if it is not complying with specification 2.1 (d) above, shall be removed or placed in a locked position, the two loading faces of the machine being parallel to each other.

2.3. *Equipment for generating and measuring the confining pressure*

This includes:

(a) A hydraulic pump or pressure intensifier or other system of sufficient capacity and capable of maintaining constant confining pressure within 2% of the desired value.

(b) A pressure indicating devices (pressure gauges or pressure transducers) which shall be accurate enough to allow the above to be observed or recorded.

3. PREPARATION OF THE TEST SPECIMENS

(a) Test specimens shall be right circular cylinders having a height to diameter ratio of 2.0-3.0 and a diameter preferably of not less than NX core size (approximately 54 mm). The diameter of the specimen should be related to the size of the largest grain in the rock by the ratio of at least 10:1.

(b) The ends of the specimen shall be flat to 0.02 mm and shall not depart from perpendicularity to the longi-

* No provision has been made for drainage of the pore water, nor for the measurement of its pressure. In certain rock types (e.g. shales) and under certain conditions the pore water pressure may influence the results. In such cases it is advisable to conduct tests on specimens with different degrees of saturation, e.g. saturated, oven dried at 105°C or any other. A comparison of the results allows an estimation of the influence of the pore water.

Such conditions shall be reported in accordance with "Suggested method for determination of the water content of a rock sample", Method 1, ISRM Committee on Laboratory Tests, Document 2, First Revision, Dec. 1977 (this volume p. 83).

† The concave halves of the spherical seats in triaxial machines usually have no freedom of movement in the direction perpendicular to the specimen axis. In order to align itself, the specimen must have two spherical seats. This is contrary to the uniaxial compression test where the top concave seat half has freedom in the lateral direction and where only one spherical seat is thus required.

‡ The procedure for, and time intervals between verifications are usually given in the National Standard specifications, e.g. ASTM E4, DIN 51300 and B.S. 1610.

§ In order to fulfil the requirements of section 2.3. (b) for the accuracy of the pressure indicating device, it may be necessary to use two or more interchangeable pressure indicating devices having different ranges. Their accuracy will generally have to be 4–5 times better than that of the pressure to be maintained.

tudinal axis of the specimen by more than 0.001 radian (about 3.5 minutes) or 0.05 mm in 50 mm.

(c) The sides of the specimen shall be smooth and free of abrupt irregularities and straight to within 0.3 mm over the full length of the specimen.

(d) The use of capping materials or end surface treatments other than machining is not permitted.

(e) The diameter of the test specimen shall be measured to the nearest 0.1 mm by averaging two diameters measured at right angles to each other at about the upper-height, the mid-height and the lower-height of the specimen. The average diameter shall be used for calculating the cross-sectional area. The height of the specimen shall be determined to the nearest 1.0 mm.

(f) Samples shall be stored for no longer than 30 days, in such a way as to preserve the natural water content, as far as possible, until the time of specimen preparation. Following their preparation, the specimens shall be stored prior to testing for 5–6 days in an environment of 20°C ± 2°C and 50% ± 5% humidity.* This moisture condition shall be reported in accordance with "Suggested method for determination of the water content of a rock sample", Method 1, ISRM Committee on Laboratory Tests, Document No. 2, Final Draft, November 1972.

(g) The number of specimens to be tested as well as the number of different confining pressure values should be determined from practical considerations, but at least five specimens per rock sample are preferred in addition to the uniaxial compressive strength tests conducted according to the relevant specifications.†

4. PROCEDURE

(a) The cell shall be assembled with the specimen aligned between steel platens and surrounded by the jacket.‡ The specimen, the platens and the spherical seats shall be accurately aligned so that each is coaxial with the others.

(b) The spherical seats should be lightly lubricated with mineral oil.

(c) The triaxial cell shall be filled with hydraulic fluid, allowing the air to escape through an air bleeder hole. Close air bleeder hole.

(d) The cell shall be placed into the axial loading device (Fig. 1).

(e) The axial load and the confining pressure must be increased simultaneously and in such a way that axial stress and confining pressure be approximately equal, until the predetermined test level for the confining pressure is reached. Subsequently, the confining pressure shall be maintained to within 2% of the prescribed value.

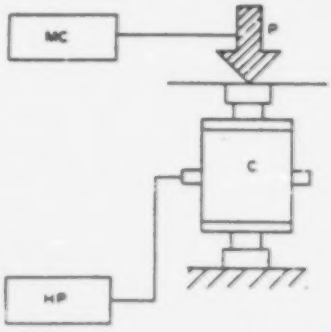

P Testing machine with: [for applying and controlling axial load]
MC Control unit

C Triaxial cell

HP Equipment for generating and controlling confining pressure

Fig. 1. Block diagram showing test arrangement for determining the triaxial compressive strength.

(f) The axial load on the specimen shall then be increased continuously at a constant stress rate such that failure will occur within 5–15 min of loading. Alternatively the stress rate shall be within the limits of 0.5 to 1.0 MPa/s.

(g) The maximum axial load and the corresponding confining pressure on the specimen shall be recorded.

5. CALCULATIONS

(a) The compressive strength of the specimen shall be calculated by dividing the maximum axial load, applied to the specimen during the test, by the original cross-sectional area.

(b) The confining pressures and the corresponding strength values for the different specimens are plotted with the confining pressures as abscissae and strengths as ordinates (Fig. 2).

(c) A strength envelope is obtained by fitting a mean curve to the above points. From practical considerations it may be advisable to fit a straight line to only the most relevant part of the curve, or to fit several straight lines to different parts of the curve. Each straight line is characterized by calculating its gradient (tangent of the inclination) m and its Y intercept, b. In each case the range in which the respective straight line is valid must be shown on the abscissa.

(d) Using parameters m and b, the internal friction angle ϕ and a value for the "apparent" cohesion C (in the sense of Coulomb's failure theory) may be calculated using the formulae:

$$\phi = \arcsin \frac{m-1}{m+1}; \quad C = b \frac{1-\sin\phi}{2\cos\phi}.$$

6. REPORTING OF RESULTS

The report should include the following:
(a) Lithologic description of the rock.

* See footnote * on p. 125.

† The test programme, i.e. the choice of the confining pressure values, depends on practical considerations regarding the purpose of the tests.

‡ The acceptable triaxial cells in use differ widely. No exact guidelines as how to install the rock specimen or how to assemble the cell can therefore be given.

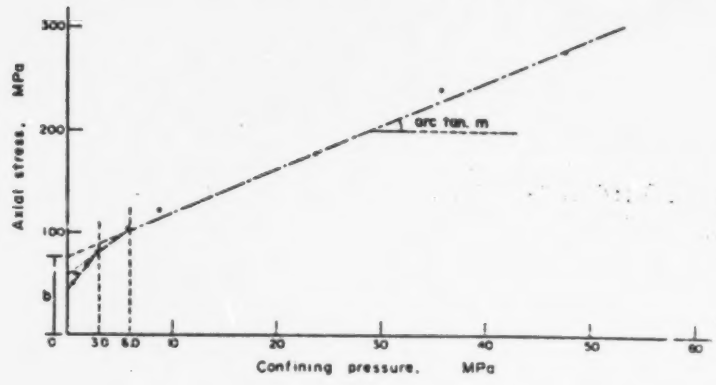

Fig. 2. Strength envelope.

(b) Orientation of the axis of loading of specimen with respect to anisotropy, bedding planes, foliation, etc.

(c) Source of sample including: geographic location, depth and orientation, data and method of sampling and storage history and environment.

(d) Water content and degree of saturation at time of test.

(e) Test duration and/or stress rate.

(f) Date of testing and description of testing machine, triaxial cell and equipment for creating and measuring of confining pressure.

(g) Number of specimens tested.

(h) Any other observations, e.g. mode of failure or available physical data, e.g. specific gravity, porosity, etc., citing the method of determination of each.

(i) A table giving specimen number, specimen height, specimen diameter, confining pressure and the corresponding axial strength to 3 significant figures.

(j) The plot of axial strength vs confining pressure as discussed in section 5(b) (Fig. 2).

(k) A table giving the values of C and ϕ together with the range of confining pressures in which they are valid.

(l) Should it be necessary in some instances to test specimens that do not comply with the above specifications, these facts shall be noted in the test report.

REFERENCES

1. International Society for Rock Mechanics. Committee on Laboratory Tests. Suggested method for determining the uniaxial compressive strength and deformability of rock materials. This volume pp. 111–116.
2. ASTM. Standard method of test for triaxial compressive strength of undrained rock core specimens without pore pressure measurements. ASTM Designation D 2664–67.
3. Kovari K. & Tisa A. *Höchstfestigkeit und Restfestigkeit von Gesteinen im Triaxialversuch*. Institut für Strassen- und Untertagbau an der ETH Zürich. Mitteilung Nr. 26.

REPORT TO
CANMET

DEVELOPMENT AND USE OF TRIAXIAL ROCK TESTING PROCEDURES FOR SAMPLES OF THE SYDNEY COALFIELD

PHASE TWO

SYDNEY NOVA SCOTIA

DSS CONTRACT NO. OSQ84-00214

March 1985

841-1287

ABSTRACT

In connection with the study of the rock-gas burst problem in the Sydney Coalfield in Nova Scotia, a program of laboratory tests was undertaken to investigate the strength characteristics of the burst prone strata and the effect of pore gas pressure on the failure behaviour of the rock in Phase 2 of the study.

Simulation of rock-gas burst was successfully demonstrated using laboratory specimens. Burst only occurred when the effective confining stress became negative. Under laboratory conditions, the intensity of the burst is generally dependent on whether gas can effectively be introduced into the specimen. For a porous material such as Pier Cap Sandstone (porosity 19%), violent bursting occurred at failure. On the other hand, for samples from the Lingan and No. 26 Collieries which have a very low gas permeability, (porosity ranging from 2 to 6%), the failure was very much subdued.

The strength characteristics of the samples from the Lingan Colliery are marginally higher than those from No. 26 Colliery. In the case of the samples from No. 26 Colliery, there is no clear distinction between the strength of the samples from the horizon where core discing has occurred and the strength of the samples from other horizons intersected by the same borehole.

The multistage triaxial testing procedure established for the homogeneous Pier Cap Sandstone was not applicable to the samples from the Sydney Coalfield. It led to underestimation of the strength of the rock unless correction factors were used.

It was noted that under the condition of rapidly and simultaneously increasing σ_1 and decreasing σ_3 to simulate field stress changes, the strength of the samples was lower than that obtained either by monotonically increasing σ_1 or reducing σ_3. It appears that the progressive decrease in confinement of the specimen during axial loading tends to allow accelerated dilation of the specimen when it starts to yield, thereby bringing forward the failure of the sample.

It is possible to increase the gas permeability of the samples from the Sydney Coalfield by inducing some microcracks through axial loading. However, the gas distribution within the sample is limited to the extent of the microcracking. Under actual field condition, gas was intrinsically trapped in the pores of the sandstone during formation of the sedimentary deposit. This naturally occurring condition apparently cannot be fully simulated with the current laboratory set-up.

Further research efforts directed toward the study of rock-gas burst problems should include the study of effect of pore gas pressure in a closed system and a comprehensive review and analyses of existing data on rock-gas bursting in the Sydney Coalfield.

RESUMÉ

En rapport avec l'étude du problème des dégagements instantanés sur tir dans les houillères de Sydney, en Nouvelle-Ecosse, un programme d'essais de laboratoire fut entrepris pour déterminer les caractéristiques de résistance du lit sujet aux dégagements et pour déterminer l'effet de la pression gaseuse intersticielle sur le comportement en rupture de la roche.

La simulation de dégagements instantanés fut reproduite avec succès sur des échantillons de laboratoire. Un dégagement ne se produit que lorsque la pression effective de confinement (σ_3) devient négative. En laboratoire, l'intensité du dégagement est généralement une fonction de la facilité avec laquelle le gas a pu être introduit dans l'échantillon. Pour un matériau poreux tel que le grès, (Pier Cap Sandstone) ayant une porosité de 19%, des dégagements instantanés violents se sont produits. Par contre, avec les échantillons des houillères Lingan et No. 26, qui ont une faible perméabilité gaseuse, (porosité variant entre 2 et 6%), la rupture fut beaucoup plus subjuguée.

Les caractéristiques de résistance des échantillons provenants des opérations de Lingan sont marginalement supérieures à celles des échantillons provenants de la houillère No. 26. Pour ce qui est des échantillons provenants de la No. 26, il n'y a aucune distinction dans la résistance des échantillons provenants de l'horizon où le disquage des carottes fut observé ou de d'autres horizons intersectés par le même trou de forage.

La procédure d'essais triaxiaux multistages établie (Phase 1) pour le grès homogène Pier Cap ne fut pas appliquable aux échantillons provenants des houillères de Sydney. Cette procédure conduit à une sous-estimation de la résistance de la roche à moins que des facteurs de correction soient utilisés.

Il fut remarqué que dans le cas où l'on augmentait σ_1 et réduisait σ_3 d'une façon rapide et simultanée, pour simuler le changement des contraintes lors de l'avancement d'une galerie, la résistance des échantillons était plus faible que celle obtenue quand seulement σ_1 était augmenté ou seulement σ_3 était réduit. Il semble que la réduction progressive du confinement, durant le chargement axial, permet la dilatation accélérée de l'échantillon lorsqu'il commence à céder, rapprochant ainsi le point de rupture de l'échantillon.

Il est possible d'augmenter la perméabilité gaseuse des échantillons provenants des houillères de Sydney en provoquant quelques micro-craques par chargement axial. Cependant, la distribution du gas à travers l'échantillon est limitée aux zones de micro-craquements. Dans les conditions actuelles de terrain, le gas fut intrinsèquement trappé dans les pores

du grès lors de la formation du dépot sédimentaire. Cette condition naturelle ne peut pas être totalement simulée avec l'équipement de laboratoire actuel.

De futures études du phénomène des dégagements instantanés sur tir devraient inclure l'étude de l'effet de la pression gaseuse intersticielle dans un système clos et une revision et des analyses compréhensives des données existantes sur les dégagements instantanés dans les houillères de Sydney.

TABLE OF CONTENTS

	Page No.
ABSTRACT	i
1. INTRODUCTION	1
2. SUMMARY OF PHASE 1 STUDY	2
3. PHASE 2 TEST PROGRAM	4
4. LABORATORY EQUIPMENT AND TESTING MATERIALS	5
4.1 Materials Tested and Sample Preparation	5
4.2 Laboratory Equipment and Instrumentation	8
5. Test Procedures and Results	10
5.1 Aspect No. 1 - Calibration of the Servo-Controlled Loading/Unloading System	10
5.2 Aspect No. 2 - Strength Characterization of Lingan Samples and Verification of the Multistage Triaxial Test Procedure	11
5.3 Aspect No. 3 - Strength Characterization of Samples from No. 26 Colliery	14
5.4 Aspect No. 4 - Simulation of Stress Changes on Samples from Lingan & No. 26 Collieries	16
6. DISCUSSION OF TEST RESULTS	19
6.1 Effect of Rapid Stress Changes on Pier Cap Sandstone	19
6.2 Strength Characteristics of Sandstone From Sydney Coalfield and Rate Effect	20
6.3 The Multistage Testing Procedure	20
6.4 Permeability of Sandstone from Sydney Coalfield	21
6.5 Effect of Rapid Stress Changes on Sandstone from Sydney Coalfield	22
7. REVIEW OF ROCK-GAS BURST PHENOMENON	25
7.1 General	25
7.2 The Material	26
7.3 The Gas	27
7.4 Stress Conditions	28
7.5 Detection and Prevention	29

TABLE OF CONTENTS (cont'd)

		Page No.
8.	CONCLUSIONS AND SUGGESTED FURTHER RESEARCH	33
9.	ACKOWLEDGEMENTS	38
10.	REFERENCES	39

APPENDIX A - σ_3 Servo Controlled Device

LIST OF TABLES

TABLE 1 - TESTING PROGRAM FOR PHASE 1

TABLE 2 - TESTING PROGRAM FOR PHASE 2

TABLE 3 - PHYSICAL PROPERTIES OF PIER CAP SANDSTONE AND DIMENSIONS OF TEST SPECIMENS

TABLE 4 - CLASSIFICATION OF LINGAN COLLIERY SAMPLES

TABLE 5 - CLASSIFICATION OF NO. 26 COLLIERY SAMPLES

TABLE 6 - PHYSICAL PROPERTIES OF LINGAN COLLIERY SAMPLES AND DIMENSIONS OF TEST SPECIMENS

TABLE 7 - PHYSICAL PROPERTIES OF NO. 26 COLLIERY SAMPLES AND DIMENSION OF TEST SPECIMENS

TABLE 8 - SUMMARY OF TEST RESULTS, ASPECT NO. 1 CALIBRATION OF σ_3 SERVO-CONTROLLED DEVICE

TABLE 9 - SUMMARY OF TEST RESULTS, LINGAN SAMPLES, ASPECT NO. 2, CHARACTERIZATION OF LINGAN SAMPLES AND VERIFICATION OF MULTISTAGE TRIAXIAL TEST PROCEDURE

TABLE 10 - SUMMARY OF TEST RESULTS, STRAIN MEASUREMENTS SAMPLES C-129-1 AND C-129-9, ASPECT NO. 2

TABLE 11 - SUMMARY OF TEST RESULTS, MULTISTAGE TESTS SAMPLE C-129-11

TABLE 12 - SUMMARY OF TEST RESULTS, MULTISTAGE TESTS SAMPLE C-129-12

TABLE 13 - GAS PERMEABILITY TEST, SAMPLE C-104-4 LINGAN SANDSTONE

TABLE 14 - SUMMARY OF TEST RESULTS, ASPECT NO. 3 STRENGTH CHARACTERIZATION OF NO. 26 COLLIERY

TABLE 15 - SUMMARY OF TEST RESULTS, MULTISTAGE TESTS SAMPLE D165-11

TABLE 16 - GAS PERMEABILITY TEST, SAMPLE D-165-17 COLLIERY NO. 26 SANDSTONE

TABLE 17 - GAS PERMEABILITY TEST, SAMPLE D-165-18 COLLIERY NO. 26 SANDSTONE

TABLE 18 - SUMMARY OF TEST RESULTS, STRESS CHANGE SIMULATIONS, ASPECT NO. 4, NO. 26 COLLIERY SAMPLES

LIST OF TABLES (cont'd)

TABLE 19 - UNIAXIAL LOADING UNDER PORE GAS PRESSURE ASPECT NO. 4, LINGAN COLLIERY SAMPLES

TABLE 20 - UNIAXIAL LOADING UNDER PORE GAS PRESSURE SAMPLE NO. C-104-5 LINGAN COLLIERY

TABLE 21 - RISK ASSESSMENT FOR EJECTION-PRONE SANDSTONES IN RUSSIA

LIST OF FIGURES

1. STRESS CHANGES SIMULATIONS, PIER CAP SANDSTONE

2. STRENGTH CHARACTERISTICS OF SANDSTONE FROM LINGAN COLLIERY

3. DEVIATOR STRESS VS. AXIAL STRAIN, SAMPLES C-129-1, C-129-9, LINGAN COLLIERY

4. VOLUMETRIC STRAIN VS. AXIAL STRAIN, SAMPLES C-129-1, C-129-9, LINGAN COLLIERY

5. MULTISTAGE TRIAXIAL TESTING, SANDSTONE FROM LINGAN COLLIERY

6. STRESS-PERMEABILITY TEST ARRANGEMENT, SAMPLES FROM LINGAN AND NO. 26 COLLIERIES

7. STRENGTH CHARACTERISTICS OF SANDSTONE FROM NO. 26 COLLIERY

8. MULTISTAGE TRIAXIAL TESTING, SANDSTONE FROM NO. 26 COLLIERY

9. SIMULATION OF STRESS CHANGES ON NO. 26 COLLIERY SANDSTONE

10. UNIAXIAL LOADING UNDER PORE GAS PRESSURE, TEST ARRANGEMENT, SAMPLES FROM LINGAN COLLIERY

A1. MTS σ_3 SERVO-CONTROLLED SYSTEM

LIST OF PLATES

1. SILICON RUBBER SPACER JACKET

2. SAMPLE C-104-1 (ADD-1)

3. SAMPLE C-104-2 (ADD-2)

4. SAMPLE C-104-3 (ADD-3)

5. SAMPLE C-104-5 (ADD-5)

1. INTRODUCTION

Golder Associates was awarded a research contract from the Department of Supply and Services (DSS Contract No. OSQ84-00215) to develop a triaxial rock testing procedure for testing samples from the Sydney Coalfield which has experienced difficulties in the development of access roadways due to rock-gas burst phenomena.

The specific factors required to be addressed in the research program include:

(a) the behaviour of the rock strata under the dynamic stress regime (stress changes) around the underground opening,

(b) the effect of gas pressure within the pores of the rock material, and

(c) the rate effects of (a) and (b).

The project is divided in two phases. Phase 1 entails the development of the triaxial testing equipment and techniques based on samples from a "reference material" and Phase 2 consists of testing samples from No. 26 or other Colliery using the procedures developed in Phase 1.

Phase 1 was completed in January 1985 (Golder Associates Report No. 841-1287 Phase 1) and Phase 2 was commenced in February 1985. This report summarizes the results of the Phase 2 study including the experimental procedure, and the problems encountered while testing samples from No. 26 Colliery and the Lingan Colliery. A review of the literature on rock-gas burst phenomena was also undertaken. This, combined with the findings of the present research project will help to define future research objectives. References to the Phase 1 report will be made throughout this report to avoid repetition.[1]

2. SUMMARY OF PHASE 1 STUDY

In connection with the study of the rock-gas burst problem in the Sydney Coalfield in Nova Scotia, a program of laboratory tests was undertaken to investigate the strength characteristics of the burst prone strata and the effect of pore gas pressure. Phase 1 of the program was directed towards the testing of a reference material (Pier Cap Sandstone) to establish the testing procedures and calibrate the equipment required to undertake the Phase 2 testing program. The scope of the Phase 1 program and the findings are summarized below.

(a) The effect of the rate of uniaxial and triaxial loading on the strength characteristic of the reference material was investigated. It was found that the strength of the reference material was rate dependent, the faster the loading rate, the higher the failure strength.

(b) A multistage triaxial testing procedure was developed in order to minimize the number of samples required to determine the failure envelope of brittle material. A criterion of imminent failure was established for the reference material tested. The sample was considered to be in the state of imminent failure when the volumetric strain ($\Delta v/v$) returned to zero on the $\Delta v/v$ vs. ε_a (axial strain) curve. By using this imminent failure criterion, the complete failure envelope was derived from a single sample.

(c) The effect of stress path on the strength characteristics was also investigated. Stress path testing procedures at low to moderate loading rates have been established to simulate stress changes in the field by predetermining the stress paths along which the samples have to follow. The reference material was used to calibrate the test

procedure developed and it was noted that the strength of this material was independent of the stress paths to failure. The design of a servo-controlled unit was developed to refine the test procedure and permit simultaneous changes in the axial (σ_1) and confining (σ_3) pressures on the sample at controlled rates.

(d) Finally, the effect of gas pressure on the strength and the mode of failure of Pier Cap Sandstone was studied under various uniaxial and triaxial testing conditions. The procedure and equipment for testing rock samples with the introduction of pore gas pressure have been established. Pore gas pressures of up to 5 MPa could be introduced into the specimen under various loading conditions. It was possible to cause bursting of the sample by inducing tensile failure which was manifested in violent expulsion and intense fragmentation of the test material at failure.

Over 60 tests were performed on the Pier Cap Sandstone during Phase 1. The details of the tests are given in Table 1.

3. PHASE 2 TEST PROGRAM

The central purpose of the project is to study the strength characteristic of the rock burst prone strata at the No. 26 Colliery and other mines in the Sydney Coalfield. In this phase of the research project, the reference material used for the Phase 1 study was initially tested at high simultaneous loading/unloading rates to calibrate the σ_3 servo-control unit built specifically for this study. Then, the sandstones from the Sydney Coalfield were tested according to the procedures developed in Phase 1 with appropriate modifications in the light of the results obtained as the study progressed. The aspects studied in the Phase 2 test program are outlined below.

(a) Investigation of the failure behaviour of the Pier Cap Sandstone and sandstone from the Sydney Coalfield under very fast changes in the stress conditions,

(b) Investigation of the effect of pore gas pressure on the mode of failure of the sandstone from Sydney Coalfield under various stress conditions, and

(c) Verification of the multistage testing procedure derived in Phase 1.

Table 2 presents the details of the testing features of this phase of the research project.

All the laboratory tests were carried out at the rock mechanics laboratory of the University of Toronto by Mr. D. Lau under the overall direction of Dr. A. Crawford.

4. LABORATORY EQUIPMENT AND MATERIALS TESTED

This section describes the materials tested and the equipment used for the second phase of the testing program.

4.1 Materials Tested and Sample Preparation

The materials tested in this phase of the research program include samples of Pier Cap Sandstone (reference material in Phase 1) and sandstones from the Sydney Coalfield which were provided by the Cape Breton Coal Research Laboratory.

The samples from the Sydney Coalfield were reported to be obtained from rock-gas burst prone strata (from No. 26 Colliery or material from similar sandstone channel).

Pier Cap Sandstone

The Pier Cap Sandstone is a light grey, homogenecus, medium grained sandstone obtained from a local supplier. The samples tested were cored from the same block. The preparation procedure has been described in the Phase 1 report. The geological name for this material is Elmhurst Sandstone. However, to remain consistent with the previous report, the name of Pier Cap Sandstone will be used throughout this report. Table 3 summarizes the physical properties and dimensions of the specimens tested.

Sandstones from the Sydney Coalfield

Sandstones from the Sydney Coalfield were obtained from three sources including:

- samples from Lingan Colliery (hole C-128, C-129)
- samples from Lingan Colliery (hole C-104)
- samples from No. 26 Colliery (hole D-165)

Borehole logs were available only for holes C-129, C-104 and D-165. However, the samples from hole C-129 were identified only in relation to the borehole number, no depth information was included. The available rock description for the samples are summarized below.

Source of Sample	Reference Borehole No.	Rock Description
Lingan Colliery	C-104	(57.22 m to 63.27 m) light grey-brown, generally massive, dense sandstone, cross bedding abundant.
No. 26 Colliery	D-165	Horizon 1) 2.84 m to 5.89 m: Light grey sandstone; fine to medium grained; thickly bedded with finely laminated dark grey siltstone layers along bedding ranging from 1/2" (12.7 mm) thick to 1-1/4" (31.8 mm) thick. Micaceous. Plant fossils and silty pods. Uneven contact with overlying sandstone. 4.305 m to 4.57 m: Discing - 105 discs/meter 4.57 to 4.87 m : Core missing 4.87 to 4.89 m : Discing - 113 discs/meter Horizon 2) 12.09 m to 14.65 m: Laminite-interbedded sandstone/ siltstone (65% sand/35% silt grading up to 55% sand/45% silt) fine grained, thinly bedded, finely laminated. Micaceous. Gradational contact with overlying siltstone. Horizon 3) 17.07 m to 18.39 m: Medium dark grey siltstone, well bedded and finely laminated, sandy film along lamination. Sandy lenses prevalent throughout. Gradational contact with overlying siltstone. Pyritic. Irregular beds, diagentic plastic deformation.

Even though the samples were obtained from similar sandstone channel in the Sydney Coalfield, there were natural variations with respect to the grain size, the amount of

interlayering and orientation of the bedding among the samples. For the purpose of this study, the samples were grouped into seven categories as described below.

Lingan Colliery

Class A - Light grey, homogeneous, fine to medium grained sandstone

Class B - Grey, homogeneous, medium grained sandstone with sparsely laminated siltstone with no well defined bedding planes

Class C - Grey, homogeneous, medium to coarse grained sandstone with well defined siltstone beddings less than 1 mm in thickness

No. 26 Colliery

Class D - Grey, homogeneous, medium grained sandstone

Class E - Grey, homogeneous, medium grained sandstone with isolated pockets of siltstone and mudstone

Class F - Alternate beddings of sandstone and siltstone/mudstone. The beddings are inclined with respect to the core axis at an angle of approximately 10°. The width of the sandstone bands varies between 1.0 to 3.0 mm whereas it is between 0.1 to 1.0 mm for the siltstone/mudstone bands. In some samples, the sandstone band was up to 20 mm in thickness.

Class G - Alternate beddings of sandstone and siltstone/mudstone. The beddings are nearly parallel to the core axis. The width of the sandstone and siltstone/mudstone bands are similar to the one described in (F).

Tables 4 and 5 summarize respectively the classification of the test specimens from the Lingan Colliery and the No. 26 Colliery in accordance with the above grouping. The physical properties and dimensions of the samples are presented in Tables 6 and 7 for test specimens from the Lingan Colliery and No. 26 Colliery respectively.

The samples obtained from both Lingan and No. 26 Colleries were too small for the NX size (54 mm) Hoek triaxial cell and too large for the BX size one (42 mm). Therefore, special spacer jackets were prepared to accommodate the samples into the NX size cell. These jackets were made of silicon rubber poured into the annular space between an NX size triaxial membrane and a rock sample. Curing time was 24 hours, then the rock sample was extruded and the jacket was oven dried (at 100°C) for another 24 hours (Plate 1).

In addition to the preparation of the rubber jackets, the samples, because of their diameter, caused considerable difficulties throughout the testing program. In particular, problems were severe when attempting to seal the interface between the sample and the platen arrangement for internal gas pressure tests and also with the strain-gauging of the samples. Since the sample was smaller than the platens, there were sharp bends in the lead wires of the strain gauges. The lead wires were subjected to shear, as a result of increased confining stress, and were under tension when the sample deformed under axial load. In several occasions, the wires were damaged causing malfunctioning of the strain gauges and premature termination of the tests.

4.2 Laboratory Equipment and Instrumentation

Five types of tests were conducted for Phase 2 of the research program. These are:

- Strength Characterization at standard testing rate (ISRM Standard, 300 sec. to failure)
- Strength Characterization at fast testing rate (43.7 MPa/sec. axially)
- Stress Change Simulation
  - (a) σ_1 constant, σ_3 reduced, without pore gas pressure
  - (b) σ_1 increased and σ_3 reduced simultaneously with and without pore gas pressure
  - (c) uniaxial loading with pore gas pressure

- Dynamic Modulus
- Gas Permeability tests under different stress conditions

The ISRM standard strength characterization, the stress change simulation types (a) and (c), and the gas permeability tests were performed using the Louis Small compression rig. The fast rate strength characterization and the stress change simulation type (b) tests were conducted using the MTS machine. For the stress change simulation (type a, b) tests, the new σ_3 servo-controlled device developed at the University of Toronto was used. Special platens were used in the gas permeability tests. The dynamic modulus was obtained by sonic velocity tests using the Pundit meter. All these equipment were used during the Phase 1 of the research project and described in the previous report.

A description of the working principle of the σ_3 servo-controlled device has been given in the Phase 1 report, and is reproduced in Appendix A. Based on the experience in Phase 2, supplementary description of the σ_3 servo-controlled system is given below:

An air operated hydraulic pump with a capacity of 70 MPa is used to charge an accumulator of 25 MPa capacity. In a σ_3 stress reduction test, the pump is shut off when the selected maximum confining pressure is attained. The pressure reading is obtained through a strain-gauged bourdon tube. During the test, the accumulator serves as a supply of pressure to the triaxial cell. In order that the confining stress be reduced according to a pre-determined linear ramp function, (MPa/sec), the bleeding valve is adjusted with the servomotor according to a command signal from the electronic controller. Prior to the commencement of the testing program, linearity of the ramp function was checked under different unloading conditions to ensure adequate σ_3 control during subsequent testing.

All the instrumentaion and measurement procedures were identical to those used in Phase 1.

5. TEST PROCEDURES AND RESULTS

This section describes the procedures adopted and the results obtained for each aspect of the test program as outlined in Table 2. In general, the procedures were as defined in the Phase 1 program. However, minor modifications have been necessary when special problems were encountered in order to meet the objectives of the test program.

5.1 Aspect No. 1 - Calibration of the Servo-controlled Loading/Unloading System

The first series of tests was directed toward the calibration of the σ_3 servo-controlled system that permits simultaneous changes in axial and confining stresses. The material used was the Pier Cap Sandstone, on which extensive testing was performed in Phase 1.

Of the five tests performed in this series, two were fast σ_3 reduction test in which an initial axial stress, higher than the confining pressure, was maintained constant as σ_3 was reduced to cause failure of the sample. The other three tests comprised simultaneous changes in both σ_1 and σ_3 along predetermined stress path until failure occurred.

In the first two tests the Louis Small Compression Rig was used to provide the axial stress whereas the reduction in confining pressure was controlled by the servo-system. Then, three fast rate stress path tests were conducted using the MTS machine and the σ_3 servo-controlled device.

The results of this series of tests are summarized in Table 8. Figure 1 presents the strength envelopes of the Pier Cap Sandstone (determined in Phase 1) with the axial stress (σ_1) plotted against the confining stress (σ_3) for three loading

rates, together with present test results (samples no. 71 to 75). An overlay shows the individual stress paths test results from Phase 1.

It is noticed that the failure conditions for the rapid σ_3 reduction test correlate well with the results obtained in Phase 1. However, the results of simultaneous stress changes indicated that the strength of the material tested under these conditions was lower than that tested under the conditions (defined by strength envelopes A, B & C) where the axial stresses were increased at different rates to cause failure while σ_3 was maintained constant.

5.2 Aspect No. 2 - Strength Characterization of Lingan Samples and Verification of the Multistage Triaxial Test Procedure

One of the main aspects of the study in Phase 1 was the development of a multistage triaxial testing procedure which allows an approximate strength envelope to be derived by testing a single specimen. The intent was to apply the procedure to the samples from No. 26 Colliery such that preliminary strength characterization could be achieved with a minimum number of specimens. However, it was considered that the procedure, which was established on a homogeneous rock material, should be checked again, using specimens from the Sydney Coalfield.

The material used was from the Lingan Colliery (holes #C-128, C-129, C-104). The strength characteristic of the material was determined through uniaxial, triaxial, direct tensile and Brazilian tensile tests. The uniaxial and most of the triaxial specimens were strain-gaged. Two multistage triaxial tests were then performed according to the results obtained by the strain-monitored tests. A complementary series of 3 fast rate triaxial tests (σ_1 increased at 43.7 MPa/s) was also conducted.

Tensile Testing

Two direct tensile tests, using samples from each of the holes C-129 and C-128, were performed. Although sample C-129-7 indicated a tensile strength of 3.90 MPa, sample C-128-9 split horizontally, during sample preparation, along a weakness plane.

Two Brazilian tensile tests (sample C-128-9A and 9B) were also performed to obtain more information on the tensile strength of this material. The results, as presented in Table 9 indicate that the tensile strength obtained from the two methods differs substantially. This was due to the fact that in the direct tensile tests, the tensile strength was strongly influenced by the bedding planes as evidenced from the failure mode.

Uniaxial and Triaxial Testing

The strength characterization comprised three uniaxial and four triaxial tests, all strain monitored. These samples were taken from the C-128 and C-129 holes. In addition, two samples from C-104 were tested triaxially (strain not monitored). The test samples were categorized according to the grouping described in Section 4.1 Figure 2 presents the failure strength of the materials from Lingan Colliery for two different axial loading rates. The test results are summarized in Table 9.

Multistage Triaxial Testing

The multistage triaxial testing (MST) procedure developed during Phase 1 was based on the relationship between the volumetric straing ($\Delta v/v$) and the axial strain (ε_a). The results of the tests on Pier Cap Sandstone indicated that amongst the various stress-strain relationships, the point

at which the volumetric strain ($\Delta v/v$) returned to zero, on the $\Delta v/v$ vs ε_a plot, appeared to be an appropriate criterion for imminent failure for this material. The term "imminent failure" was defined as the particular state in the specimen in which the growth and propagation of micro-cracks have been initiated, but the specimen remained stable and exhibited very little permanent deformation.

However, upon examining the various stress-strain plots obtained while testing the samples from Lingan Colliery (see Figures 3, 4 and Table 10 for example) it was observed that the use of the criterion established through the Pier Cap Sandstone was not appropriate for this inhomogeneous and bedded material. Consequently, the use of $\Delta v/v$ = (maximum) as a failure criterion was investigated. Based on the individual triaxial tests, the ratio between the axial stress at $\Delta v/v$ = (maximum) and the failure stress, σ_c, ranges from 66 to 93%. The ratio increases with increasing confining stress.

Using $\Delta v/v$ = (maximum) as the imminent failure criterion, two multistage triaxial tests were performed. The procedure followed was described in the Phase 1 Report. Results of these tests are given in Tables 11 and 12 for samples C-129-11 and C-129-12 respectively. Figure 5 compares the results of these two tests with all the single stage ones. After the multistage cycle at σ_3 = 30 MPa, the samples were loaded until failure. The failure strength corresponds with the ones recorded for single stage samples of the same class.

A permeability test was performed on sample C-104-4. Time was allowed for the sample to reach equilibrium. Figure 6 presents the test arrangement. For the permeability measurement, the pressure transducer on the downstream end was replaced by a soap bubble flow meter. The results are given in Table 13.

5.3 Aspect No. 3 - Strength Characterization of Samples From No. 26 Colliery

The strength characteristic of the sandstone from No. 26 Colliery was determined in this aspect of the research program. In addition, the relationship between permeability and applied stress was also investigated.

Strength Characterization

The strength characterization was obtained through one uniaxial and three triaxial tests, together with one multi-stage triaxial test based on the ($\Delta v/v$ = maximum) criterion. The results are presented in Tables 14 and 15 and Figures 7 and 8 respectively.

It was observed that the failure modes of the specimens were very dependent on the direction of the bedding planes. As an example, a sample having the bedding parallel to the core axis will split axially during uniaxial testing as generally expected. However, a specimen having the bedding oriented at 10 degree angle with the direction of the maximum stress will show axial cracks at both ends followed by shear along bedding planes. In triaxial tests, all the specimens failed along single shear planes which coincided with the bedding planes. In addition, it was observed that some samples failed prematurely due to the spalling of a wedge at the sample ends.

Gas Permeability Tests

A series of gas permeability tests were performed under different confining pressures. In the first test, an attempt was made to determine the peremeability of the No. 26 Colliery sandstone, using the arrangement shown on Figure 6. In this test, the specimen was subjected to the following conditions:

σ_1 = 4.0 MPa, σ_3 = 7.0 MPa, Pg = 7.0 MPa

It took 30 minutes to read a gas pressure of 0.07 MPa at the downstream pressure transducer. Forty-eight hours later, the pressure reading was still the same, indicating that the No. 26 Colliery sandstone has a very low gas permeability. This is consistent with the low porosity of the material.

A second test was undertaken to investigate whether the formation of microcracks could increase the permeability of the rock; and if so, to what extent. The following procedure was followed:

1) The sample was loaded axially to a percentage of its ultimate strength (40 to 88%).

2) The confining pressure was increased to a predetermined level, whereas the axial stress was reduced (σ_3 = 10,5,4 MPa).

3) Gas was introduced at one end and the pressure monitored at the downstream end.

4) The test was repeated on the same sample for a new axial stress condition.

Table 16 presents the results of this test.

In a third test, the pressure transducer was replaced by a soap bubble flowmeter for volumetric measurements. Table 17 presents the results. The permeability measurements in the last two tests are the measurement of the permeability of the cracks. In all tests, nitrogen gas was used.

5.4 Aspect No. 4 - Simulation of Stress Changes On Samples From Lingan & No. 26 Collieries

Samples From No. 26 Colliery

In this part of the research project, the strength and failure characteristics of the sandstone, from No. 26 Colliery, were investigated under the condition of rapid stress changes to simulate the field conditions. The samples were initially loaded under a hydrostatic stress of 20.7 MPa. They were then brought to failure by simultaneously increasing σ_1 and reducing σ_3 along predetermined stress paths as shown on Figure 9.

The rate of increase of σ_1 was 43.7 MPa/s whereas the reduction rate of σ_3 ranged from 0.4 to 32 MPa/s, depending upon the stress path followed. The MTS testing machine was used in conjunction with the σ_3 servo-controlled system to facilitate control of the stress changes. Gas pressure between 7.0 to 9.0 MPa was applied from the top of the specimen. However, at failure, only five out of the ten samples indicated a gas pressure at the bottom end and only two had a downstream pressure higher than 1.0 MPa. The results are presented in Table 18 and shown on Figure 9.

The results from these tests indicate that there appears to be correlation between the structure of the material and its failure mode. Furthermore, similar to the results obtained from stress change simulation test on Pier Cap sandstone, the results from the No. 26 Colliery samples indicate a lower strength under simultaneous rapid changes in σ_1 and σ_3.

Samples From Lingan Colliery

Four samples from the Lingan Colliery (hole #C-104) were tested under uniaxial stresses. In the first two tests (sample C-104-1, C-104-2), epoxy coated specimens were loaded uniaxially until failure with a constant gas pressure being applied at the top end (Sketch A on Figure 10). Negligible gas pressure was recorded at the bottom end. The samples failed by vertical splitting around the perimeter at the top end (where gas pressure was applied) to the middle height of the sample. Numerous vertical cracks were observed. (Plate 2, 3)

The third sample (C-104-3) was tested slightly differently. Constant gas pressure was applied at both ends and the sample was allowed to reach equilibrium prior to testing. The sample failed by vertical splitting, this time being more intensive than in the first two tests. The perimeter of the sample spalled substantially, although the sample did not disintegrate. Results are presented in Table 19. (Plate 4)

Because of the low gas permeability of the samples, an attempt was made to induce higher internal gas pressure in the next specimen (C-104-5). Based on the experience gained in the above tests, the following test procedure was established:

- The sample was loaded to predetermined axial stress (50% of σ_c).
- The sample was then coated with epoxy.
- Gas pressure was introduced at the top end of the specimen and pressure at the bottom end was recorded using a pressure transducer (Figure 10A).
- The downstream pressure reading was allowed to stabilize.
- The gas pressure was then increased and allowed to stabilize.

- If the downstream pressure was low, σ_1 was increased to enhance the permeation of gas through the sample.

The results of the test, including the different loading stages, are presented in Table 20. It was observed that even when the applied gas pressure was approximately 7.0 MPa, with an axial pressure of 19.0 MPa (≈30% of the ultimate strength) the downstream pressure monitored was only 1.1 MPa. The sample was then loaded to failure, which was in the form of vertical splitting through the centre of the specimen. (Plate 5)

6. DISCUSSION OF TEST RESULTS

6.1 Effect of Rapid Stress Changes on Pier Cap Sandstone

The Pier Cap Sandstone is a homogeneous material that has been extensively tested in Phase 1 of the present research project. The stress change simulations and the rapid reduction in confining pressure tests performed during Phase 1 yielded consistent and reproducible results.

In aspect No. 1 of this phase, the calibration tests of the σ_3 servo-controlled system provided additional data to the previous test results. In the first two tests, the reduction of the confining pressure using the servo-controlled unit at a rate slightly over 5.0 MPa/s produced the same results as that obtained from the test on sample Nos. 41, 42, 43, 44 and 45 (Phase 1) in which the confining pressure was reduced at 15 to 25 MPa/s simply by flipping the valve controlling the confining pressure system.

However, under the condition of simultaneously changing the axial and confining stresses, the specimens consistently failed (as shown on Figure 1) at a lower stress level than that obtained from both the standard and fast rate tests. In Phase 1, a rate effect was observed when loading the specimen axially with σ_3 kept constant. During the present tests, although σ_1 was increased at comparable rates which ranged from 24.0 to 43.6 MPa/s, the material behaved much differently when the confining pressure was decreased simultaneously at rates ranging between 1.0 and 5.6 MPa/s. The progressive decrease in confinement of the specimen during axial loading appears to allow accelerated dilation of the specimen when it starts to yield, thereby bringing forward the failure of the sample. This aspect can be examined in greater detail by monitoring the strains in the specimen during the process of stress changes.

6.2 Strength Characteristics of Sandstone from Sydney Coalfield and Rate Effect

The sandstones from Lingan Colliery and No. 26 Colliery were tested to determine their strength characteristic. It was found that the strength of the specimen tested under conventional triaxial conditions was influenced to different degrees by the structure within the sample (as defined by the various classes). No significant rate effect was observed in the single stage triaxial tests performed on the Lingan sandstone.

Samples from Lingan Colliery failed in a mixed mode when tested in uniaxial compression with no pore gas pressure. The samples failed by loosing a wedge at one of the ends or splitting axially. In triaxial testing, shear failure was developed. The samples from Colliery No. 26 always failed along beddings when they were present within the samples. Very little shear across the layers of rocks was observed. There was no significant difference in the strength and failure behaviour of the samples, from No. 26 Colliery, obtained from the various horizons in hole D-165.

6.3 The Multistage Testing Procedure

A multistage testing procedure was established during Phase 1 of this research project on the Pier Cap Sandstone. With this homogeneous material, the $\Delta v/v=0$ was a good criterion of imminent failure. However, while testing samples from the Sydney Coalfield, it was soon observed that the $\Delta v/v=0$ criterion was not applicable to these materials. Samples failed before the volumetric strain returned to zero (Figure 4). From the data gathered during the strength characterization tests, it was observed that the point at which $\Delta v/v$=maximum might be a good indicator of imminent failure. However, the determination of this unique value of $\Delta v/v$ would require precise instrumentation and feedback

control system. This is especially true when the rock is brittle and/or the rock is subjected to fast testing rates.

The two multistage tests performed on Lingan sandstone yielded very consistent results (see Figure 5), but the failure envelope derived from these tests is considerably lower than the one obtained for samples of the same class tested in single stage procedure. During the final loading of samples C-129-11 and C-129-12 at σ_3=30 MPa, the strength of these samples agreed closely with previous failure data (see Figure 2). Similar discrepancy between the multistage and single stage strength envelope results were also observed while testing the sandstone from No. 26 Colliery.

These results indicated that the $\Delta v/v$=maximum criterion underestimated the intrinsic strength of the specimen. Hence, it has to be used in conjunction with correction factors and more tests on various classes of the material would be required to ascertain the appropriate correction factors. It is believed that at this stage the best method of determining the strength characteristic of the material is by individual uniaxial and triaxial tests.

6.4 Permeability of Sandstone from Sydney Coal Field

It is recognized that the bursting phenomenon in the Sydney Coalfield is accompanied by ejection of gas. One of the basic objectives of this research program is to observe the failure mechanism when the specimens are subjected to various stresses and internal pore pressure conditions. It has been demonstrated in Phase 1 (using the Pier Cap Sandstone) that when the sample failed with an internal gas pressure, the failure was violent and even explosive. The failed material resembles the material collected at No. 26 Colliery in the area where bursts occurred. However, in Phase 2 of this project, this type of failure was not observed because it was difficult to introduce gas through

the samples from the Sydney Coal Field. As discussed earlier, some of the problems were due to the relative smaller size of the sample compared with the size of the platens and the associated sealing difficulties. However, the major problem was that the permeability of these materials was very low, as reflected by the low porosity measurements.

Attempts were made to increase the permeability of the samples by initiating microcracks through preloading. Nevertheless, the permeability was still low and the gas flow was only restricted to these cracks. Unless the network of cracks is extensive and the cracks are interconnected, the macroscopic permeability of the sample remained very low. In addition, an increase in the confining pressure results in a decrease in permeability.

In the cases where gas was successfully introduced into the specimen, the pore pressure distribution remained unknown along the length of the specimen. For example, C-104-5 a gas pressure of approximately 7.0 MPa was applied at one end, whereas only 1.1 MPa was measured at the other end.

Under actual field condition, gas was intrinsically trapped in the pores of the sandstone and in the cleats and fractures of coal seams during formation of the sedimentary deposit. This naturally occurring condition apparently cannot be fully simulated with the current laboratory set up with low permeability samples.

6.5 Effect of Rapid Stress Changes on Sandstone From Sydney Coalfield

The testing of the Colliery No. 26 sandstone at high rate of changes of axial and confining stresses was performed. The failure planes generally coincided with the pre-existing bedding plane(s) within the samples. It was also noted that

the more homogeneous the sample, the higher the strength at failure.

As with the Pier Cap Sandstone, failure generally occurred at lower stress level than that in which the sample was failed by monotonically increasing σ_1 with σ_3 kept constant. In connection with the results of this series of tests, it was also noted that rate effect was negligible when testing the Lingan samples at high loading rate (σ_1 increase and σ_3 constant).

Even though pore gas pressure was applied at one end of the sample, very little is known about the actual pressure distribution within the samples. Therefore, the total stress conditions were plotted on Figure 9.

Results of the triaxial tests indicated that none of the samples failed close to the tensile region despite the fact that 7.0 to 9.0 MPa of gas pressure was applied at the top end of the sample. While the results of the gas permeability tests showed that the permeability of the sample could be increased upon the formation of microcracks within the specimen, the results of this series of tests illustrated that the gas pressure within the sample was insufficient to cause tensile fracture of the specimen. It is believed that gross failure of the sample took place even before the formation of a system of induced microcracks that were sufficiently extensive to allow increased gas permeation. The high loading rate used obviously did not enhance the flow of gas through the sample.

In order to complement these tests, four samples from Lingan Colliery were tested uniaxially under gas pressure. Failure occurred in the tensile region for all of the samples tested. However, as gas was not permeating uniformly through the samples, the effective stress within the samples was unknown.

It was noticed that the specimen failed close to the end where the gas pressure was applied. When the gas pressure was applied at both ends, failure was more uniform and extensive with numerous cracks being present at the centre of the failed specimen. The fragments produced also showed signs of tensile failure as obtained during Phase 1 of this project, even though they are not as "flaky" as those from the Pier Cap Sandstone. A significant implication of these test results is that violent explosion of material can only occur when the sample is brought into tensile failure with a sufficiently uniform gas pressure.

As for sample C-104-5, which was pre-loaded to induce microcracking, this specimen failed by axial splitting along one major crack at the centre of the specimen. No spalling of the material at the perimeter of the sample was noticed. It is believed that the gas permeates preferrentially through the network of cracks rather than into the rock material, thus not achieving uniform gas distribution within the specimen.

7. REVIEW OF ROCK-GAS BURST PHENOMENON

7.1 General

The results presented in previous sections represent the first series of experimental data on the strength characterization of the burst prone strata in the Sydney Coalfied. In order to provide some background data for further research objectives to be developed, a review of the rock-gas burst phenomena experienced in other countries is presented below.

Pressurized gas has been encountered in coal, salt and associated rocks all over the world. Mining in such seams have generated sudden catastrophic outbursts of rock and gas (hereinafter referred to as rock-gas bursts). The rock-gas bursts are the result of a violent release of a large amount of energy. It can only occur when an accumulation of energy is rapidly released by strata deformation and/or gas contained in the strata[3]. These dynamic events occur almost without any precursors. However, in some cases certain warning signs have been observed such as:[4]

- an increase in the gas concentration after shotfiring, often too slight to be noticed unless methane levels were recorded
- minor flaking of the roadway sides or heading face
- increased comminution of broken material

In the destroyed rock mass, fragments of flake-like shapes are always encountered. The onion skin appearance of walls in the bursted area is sometimes referred to as pressure relief exfoliation. The same failure mode was observed in the outburst area in No. 26 Colliery.

Although the rock-gas burst mechanism has not been fully understood, two following statements underline the basic causes for such events.

- rock-gas bursts are initiated by dynamic loading
- rock fracturing during bursting is a self-sustaining process

In outburst prone seams, rock-gas bursts can be induced by very low disturbances. Tests have shown that there is a threshold value for the triggering impulse; if the impulse is too small, no reaction; if the impulse is large enough, the event occurs at full strength. Rock-gas bursts are the result of an interaction between the material, the gas and the stress field.

7.2 The Material

The material involved in most of the rock-gas bursts reported is sandstone. In all cases, the sandstone has been described as strong and rigid. The uniaxial compressive strength ranges from 60 to 80 MPa in France and Germany to 90 to 120 MPa in Russia. The reported porosity is generally over 6%. The permeability was not always measured, but since there is general agreement that the rock cannot be drained of its gas, the permeability is probably very low.

In Russia, over 150 burst prone strata have been identified. The rock most frequently found to have an outburst hazard are alluvial sandstones, sandstone from underwater river drifts and offshore sandstones.[5] However, geological methods alone cannot predict which sandstone will be prone to bursting. In Germany, the burst prone sandstone have a porosity of 10 - 14% whereas the non-burst prone ones have a porosity ranging from 2.7 to 6.9%. It was found that the porosity increases with an increase in the quartz-feldspar

content and/or a decrease in the phyllosilicates-carbonates content. In addition, it is believed that when less cementing materials are present, there is a higher grain-to-grain quartz binding therefore reducing the tensile strength. It was also noticed that the quartz grain size was twice as large in the burst prone strata than in the non-burst prone ones.[6] Finally, a lighter sandstone colour would be of higher risk than a darker coloured sandstone.

It was also observed[4] that the cavity developing in sandstone during an event stops when it reaches a bed of shale. This would indicate that the rock-gas burst is indeed characteristic of a certain rock type. The considerable rigidity of the sandstone layer favours a build-up of energy and its rapid release.

7.3 The Gas

The gas plays two different roles; it contributes towards the origin of the phenomenon and it helps to maintain the propagation of the failure zone.[3] It is generally agreed that the gas pressure facilitates rupture by displacing the effective stress toward the tensile region, although according to Josien[7], the gas pressure to consider is the one being established at the fracture wave front. There, due to a rapid dynamic stress relief, the total gas pressure differential concentrates in a very narrow near-face layer of rock. It causes layer-by-layer breaking away.[8] The pressure gradient is a function of the insitu gas pressure and the permeability under the stresses in the strata. It is also a function of the rate of advance and the width of the opening. The self-sustaining process of rock breakage is believed to be due to the gas expansion energy. The propagation of the crush wave being the most significant part of the complicated mechanism governing a rock-gas burst.

In the field, the strata are subjected to an all around compressive stress; the gas became isolated in pores. In zones of uniaxial stress relief during the creation of an underground opening, the gas can expand only by rupturing the rock and thus forming a system of cracks which gradually obtain a penny-shape form and grow in planes orthogonal to the direction of minor compression. The oriented cracks are filled with compressed gas, whose pressure, though less than initial, acts over a considerably larger area.[8]

In addition, the modulus of elasticity will sharply be reduced by the creation of the system of parallel cracks, therefore contributing in moving the stress away from the periphery of the opening.

In areas where there is an increase in the stress level, the pore sizes are reduced thereby compressing and trapping the gas more tightly. The internal gas pressure could be high enough to overcome the tensile strength of the material. The increase in stress level could be caused, for example, by the shock wave (induced by blasting) travelling through the material.

7.4 Stress Conditions

The underground rock strata are subjected to different stress conditions which include (a) virgin state of insitu stress in unmined areas remote from areas of active development, (b) concentration or relief of the insitu stress in the vicinity of the underground workings which is a function of the size of the openings, their geometric relationships and the insitu state of stress; and (c) the dynamic stresses caused by mining activities such as drilling and blasting. The stress conditions in most rock-gas burst areas were unknown because very few stress measurements were obtained in those areas. It was generally agreed that high stress concentration are present in the

abutment zone of a longwall face.[9] In addition, tectonic structures have been found to affect the lateral stresses.

The dynamic stresses are known to trigger the event. Blasting within or in the vicinity of the strata can start the event. In Germany, a rock-gas burst occurred when drilling through a burst prone sandstone.[6] Similar incident was experienced in Russia when drilling a 1.0 m borehole at a rate of 2.7 m/hr., whereas the strata remained stable when the penetration rate was reduced to less than 0.5 m/hr.[5] The dynamic compressive wave caused by blasting is accompanied by a tangential tensile stress which, when superimposed on the stress conditions and the pore gas pressure, can be sufficient to induce failure of the rock. At present, very little is known on this aspect due to the lack of experimental data.

7.5 Detection and Prevention

In Russia, an elaborate method of detection is based on the various properties of the material and the depth. Table 21 shows the risk-assessment table used in USSR. The Index is obtained by arithmetic means and a value between 0.8 and 1.0 indicates very high possibilities of dynamic behaviour. The method is complex but could be modified and improved as research in this field is persued. For example, the depth could be replaced by some indicator of the horizontal stress.

In Western Europe, the most reliable method of prediction is core discing, which was first observed by Karagodin et. al.[5]. The discs are of convex-concave shape with the convexity always on the side facing towards the origin of the drillhole. But core discing is a necessary but not a sufficient condition for predicting rock-gas burst.[4]

In Germany, all core drilling with hole diameter ranging between 48 and 200 mm produced clear pressure relief exfoliation of the cores in the area of burst-prone sandstone. Compact and sound cores were obtained only when the sandstone was stress-relieved, ie. in mined out areas and in the immediate vicinity of burst cavities.

Paul[6] states that pressure relief exfoliation is independent of stratification and direction of drilling and clearly correlate with the risk of burst. Belin[4], however, affirms that physical laboratory models have shown that discing was related to the stress conditions of the rock and in particular, that the stress perpendicular to the direction of the borehole had to be much greater than the stress parallel to the borehole axis.

Josien[7] has developed a laboratory testing apparatus and procedure that permits the reproduction of the conditions leading to dynamic behaviour during drilling. The specimen is loaded under triaxial stresses to simulate field conditions. The set-up permits the drilling of the specimens (mini-coring) in controlled conditions and therefore the understanding of the mechanism that provokes this behaviour by studying the effect of stress levels, grain size, drilling conditions, rock properties, etc.

No relationship was found between the discs thickness and the intensity of ejection.

The prevention methods published in the literature fall within the following categories:

- Modification of blasting procedure,
- Degassing of the burst prone strata,
- Destressing the burst prone strata,
- Modification of the planning and design.

Modification of the Blasting Procedures

Many attempts were made in order to decrease the influence of blasting in triggering the dynamic events. The amount of explosive were reduced, pre-splitting and line drilling of unloaded holes around the perimeter were tried. Such procedure was not successful in eliminating the occurrence of rock-gas burst. However, many of these experiments were undertaken directly within the burst-prone strata and therefore, are not exactly representative of the conditions encountered in Nova Scotia.

The experience in Russia indicated that the quantity of material ejected and the number of occurrences could be reduced by changing from high velocity explosive to low-shattering explosive in some smaller quantities.

Degassing of the Burst Prone Strata

Degassing of the strata was not successful where attempted. The low permeability that generally characterize the burst-prone strata really handicapped this solution. The use of hydrofracturing techniques for degassing has not been reported.

Destressing the Burst Prone Strata

Various degrees of success were encountered by mining a protective seam prior to excavating close or through a burst prone strata. However, the method is too costly in the case where no valuable seam can be extracted. Drilling of a pilot hole ahead of the face when excavating through the burst prone sandstone has had very limited success in Germany, because the destressed area around the pilot heading was not large enough to protect the full roadway.

(4) Modification of Planning and Design

In Germany, dropping the gate road to increase the thickness of shale between roadway and burst prone sandstone was successful in conjunction with driving the gate road 30 m ahead of the face line, in a zone that lies outside of the stress concentration due to the longwall face.

Therefore, the most suitable preventive measures to be used for a particular mine have to be developed on the basis of site specific parameters together with field trials to demonstrate the validity of the proposed method.

8. CONCLUSIONS AND SUGGESTED FURTHER RESEARCH

In connection with the study of the rock-gas burst problem in the Sydney Coalfied in Nova Scotia, a program of laboratory tests was undertaken to investigate the strength characteristics of the burst prone strata and the effect of pore gas pressure on the failure behaviour of the rock.

Phase 1 of the program was directed towards the testing of a reference material to establish the testing procedures and the equipment required to undertake the Phase 2 testing program. In Phase 2, samples from the Sydney Coalfield were tested and the following conclusions are derived from the results of all the tests performed in this research project.

1. Simulation of rock-gas burst was successfully demonstrated using laboratory specimens. Burst only occurred when the effective confining stress became negative. That is, failure took place in the tensile region in the σ_1 vs σ_3 plot.

   Under laboratory conditions, the intensity of the burst is generally dependent on whether gas can effectively be introduced into the specimen. For a porous material such as Pier Cap Sandstone (porosity 19%), violent bursting occurred at failure. On the other hand, for samples from the Lingan Colliery and No. 26 Colliery which have a very low gas permeability, (porosity ranging from 2 to 6%) the failure was very much subdued.

2. Sandstone samples from the Sydney Coalfield were categorized in accordance with the natural variability of the material. Such variability accounts for the apparent inconsistencies of the test results. In the overall

context, the strength of the samples from the Lingan Colliery is marginally higher than those from No. 26 Colliery.

In the case of the samples from No. 26 Colliery, there is no clear distinction between the strength of the samples from the horizon where core discing has occurred and the strength of the samples from other horizons intersected by the same borehole.

3. A multistage triaxial testing procedure and an imminent failure criterion were established for the homogeneous Pier Cap Sandstone. However, the same failure criterion was not applicable to the samples from the Sydney Coalfield. With samples showing high natural variability, strength characterization based on multistage testing procedure can lead to under-estimation of the strength of the rock unless correction factors are established by means of an extensive testing program.

   It is considered therefore that single stage triaxial tests will yield more reliable results.

4. The procedures for stress path testing at low to fast loading rates have been established to simulate stress changes in the field by predetermining the stress paths along which the samples were to follow.

   It was noted that under the condition of rapidly and simultaneously increasing σ_1 and decreasing σ_3 to simulate field stress changes, the strength of the Pier Cap Sandstone is lower than that obtained either by monotonically increasing σ_1 or reducing σ_3. Similar results were obtained from the tests on samples from No. 26 Colliery. It appears that the progressive decrease in confinement of the specimen during axial loading tends to allow accelerated dilation of the specimen when it starts to yield thereby bringing forward the failure of the sample.

5. It is possible to increase the gas permeability of the samples from the Sydney Coalfied by inducing some micro-cracks through axial loading. However, due to the random nature of the induced cracks, the gas distribution within the sample remains unknown and the effective gas permeability is limited by the extent of the micro-cracking. Under actual field condition, gas was intrinsically trapped in the pores of the sandstone during formation of the sedimentary deposit. This naturally occurring condition apparently cannot be fully simulated with the current laboratory set-up.

Suggested Further Research

The results obtained from the two phases of the triaxial testing program has provided a valuable data base for the understanding of the conditions governing the rock-gas bursting. The emphasis of the current program was to develop the triaxial testing procedure and to characterize the strength of the burst prone strata under different loading/unloading conditions. Some fundamental problems were not particularly addressed. The following is a list of the items which, in our opinion, are required to be examined should further research efforts be directed toward the study of rock-gas burst problems.

1. Effect of Pore Gas Pressure in a Closed System.

One of the hypothesis put forward in the literature[7,10] is that pore gas pressure increases as the rock deforms under stress. The high pore pressure could overcome the tensile strength of the rock and lead to failure. In order to examine this hypotheis, the testing of a porous material, such as Pier Cap Sandstone, within a closed system could be undertaken. Full strain monitoring for a range of confining pressure would yield a valuable data base that would

be compared with data obtained while testing the same material as an open system.

In the present program, all the tests were conducted in an open system. Under actual field condition, the gas is already trapped in the pores, and changes in the externally applied stress system would cause pore gas pressure changes initially under a closed system until overstressing of the strata or induced fracturing have provided access for the release of the pressurized gas. This aspect is fundamental to a better understanding of the bursting phenomena observed in the field.

2. Review and Analysis of Existing Data Base on Rock-Gas Bursting in Sydney Coalfied.

The ultimate goal of the rock-gas burst study is to develop a method of detecting or preventing the occurrence of out-bursting in the operating coal mines. The first step in achieving this is to review the existing data base from the burst sites with particular emphasis on the following aspects.

- gas volume and pressure data if any at the bursting sites.
- geological and geomechanical (rock mass) characterization of the bursting and non-bursting sites.
- sequence of mining development and support at problem areas and in areas where stability of the strata have been maintained.
- blasting data including the blasting pattern, charge weight and firing sequence etc. This may include dynamic stress analysis of the blast effects by numerical modelling.

- Induced stress conditions at the burst sites prior and subsequent to the development of the roadway to assess the potential for the benefit of implementing alternative development schemes. This should include an assessment of the overall stress distribution in the present mining layout as well as the stress conditions in the immediate vicinity of the development roadway. Some form of two-dimensional and three-dimensional numerical analyses would be appropriate to examine the stress condition.

- The rock failure conditions could also be assessed on the basis of the strength characterization obtained through the present program.

In conjunction with the review, it would also be desirable to carry out some preliminary laboratory index tests which were used by other countries (such as France and USSR) as indicators for burst prone area. These could include thin section work and laboratory discing tests. The results of these tests can be calibrated with the actual occurrences of bursts to assess the usefulness of such predictive methods.

3. Based on the results of the review and the preliminary laboratory works, a more comprehensive program can then be developed. This may include the following:

   - development of laboratory index tests suitable for the identification of potential problem areas in the Sydney Coalfield.

   - examination of alternative mining developme sequence to prevent or control the occurrence of bursting. Further insitu stress and laboratory data may be required to provide the necessary input parameter.

9. ACKNOWLEDGEMENTS

Golder Associates wishes to thank Dr. A. Crawford and Mr. D. Lau of the University of Toronto for their contributions and assistance in the preparation of the Phase 2 report. Helpful discussion of Dr. Peter Cain of the Cape Breton Coal Research Laboratory during the course of the study was also gratefully acknowledged.

GOLDER ASSOCIATES

Clement M. K. Yuen, P. Eng.

REGISTERED PROFESSIONAL ENGINEER C.M.-k. Yuen PROVINCE OF ONTARIO

for Guy LeBel

10. REFERENCES

1. Development and Use of Triaxial Rock Testing Procedures for Samples of the Sydney Coalfield, Nova Scotia, Phase 1, Golder Associates Report No. 841-1287 Phase 1.

2. Aston, T., Cain, P., Gas and Rock Outburst at No. 26 Colliery, Sydney Coalfield, Nova Scotia - A Case History Paper for presentation and publication in: Proceedings of the 21st In. Conf. of Safety in Mine Research Institute, Sydney, Australia, October 1985.

3. Josien, J.P., and al; The Dynamic Effects of Strata-Pressure-Rock Bursts; 7th International Strata Control Conference, Liège, Sept. 1982.

4. Belin, J., Prevention of Instantaneous Outbursts of Methane and Coal or Rock, Working party on ventilation, firedamp and other mine gases, Safety and Health Commission for the Mining and Other Extractive Industries, Commission of the European Communities, Doc. 6093/81EN., Nov. 1981.

5. Karagodin, L., Kolesov, O., Bol' Shinskii, M., Method of Forecasting and Suppression of Rock and Gas Outbursts in Dombass, 20th International Conference of Safety in Mines Research Institutes, Sheffield, U.K, Oct. 1983.

6. Paul, K., Methane Bursts Involving the Ejection of Rock Material, Symposium on Methane Bursts Involving the Ejection of Coal or Rock, Luxembourg, July 1983.

7. Josien, J.P., personal Communication, March 1985.

8. Khristianovich, S.A., Salganik, R.L., Several Basic Aspects of the Forming of Sudden Outbursts of Coal (Rock) and Gas, 5th Congress of the ISRM, Melbourne, Australia, 1983.

9. Shepherd, R., Kellet, W.H., Strata Behaviour, Colliery Guardian, V. 221, No. 3, March 1973.

10. Hargraves, A.M., Failure of Porous Rocks with Contained Gas, Symposium on Stress and Failure Around Underground Openings, University of Sydney, Australia, March 1967.

REFERENCES (cont'd)

11. Revalor, R., and al., In Situ Rock Stress Measurements in French Coal Mines. Relation Between Virgin Stresses and Rock Bursts, Unpublished paper, 1985.

12. Barron, K., An Analytical Approach to the Study of Outbursts, Dept. Energy, Mines and Resources, Mine Branch, Internal Report 72/29-ID.

13. Gray, W.M., Towes, N.A., Notes on the Theory of Flow of Gas in Coal, Dept. Energy, Mines and Resources, Mine Branch, Internal Report 70/96-ID.

14. Gale, J.E., The Effects of Fracture Type (Induced vs Natural) on the Stress-Fracture Closure-Fracture Permeability Relationships, 23rd U.S. Symposium on Rock Mechanics, 1982.

15. Kozlowski, B., Kalisz, E., Results of Research Into the Background of the Gas and Outburst Hazard in Crosscuts Driven Under Very Difficult Mining Conditions, 19th Int. Conf. on Mine Safety Research, Poland, 1981.

16. Zonin, F.N., Prusova, A.A., Kolesnikov, V.V., Driving Near Burst-Prone Rocks, Ugol'Ukrainy (Ukrainian Coal), 1981.

17. Kozlowski, B., Opening-up and Development of Seams Prone to Sudden Outbursts, 20th Int. Conf. on Mine Safety Research, U.K. 1983.

18. Stewart, I. McC., Diffusional Analysis of Seam Gas Emission in Coal Mines, CIM. April, 1971.

19. Noack, K., Paul, K., Portge, F., Present Stage in the Prevention of Outbursts of Gas and Coal in the West German Bituminous Coal Mines, 20th Int. Conf. on Mine Safety Research, U.K. 1983.

20. Kusznir, N.J., Farmer, I.W., Rockburst Phenomena in British Coal Mines, Rockburst Symposium,IMM, October, 1983.

21. Whittaker, B.N., Longwall Planning with Reference to Rockbursts, Rockburst Symposium, IMM, October, 1983.

TABLE 1

TESTING PROGRAM FOR PHASE 1

ASPECT TO BE STUDIED	SCOPE/SPECIAL FEATURE OF TESTING	REFERENCE/ TEST STANDARD	NO. OF TESTS
1. Conventional Triaxial Tests - strength characteristics of reference material and effect of various loading rate	• Series of conventional triaxial tests to establish strength characteristics of the reference material. • Scope of testing for each series includes: ° Brazilian Tensile test ° Uniaxial Compression test (σ_3=0) ° Triaxial test σ_3=5,10,20,30 MPa ° Rate of loading Series 1 ISRM Standard (Slow) Series 2 2 times faster (moderate) than ISRM Standard (2 MPa/sec) Series 3 43.7 MPa/sec ° Pore gas maintained at atmospheric pressure • Conventional triaxial tests to establish the strength characteristics of the failed samples	ISRM Standard method of rock testing Brazian test Uniaxial compression Triaxial test	 16 7 5 3
2. Calibration tests to study the feasibility of optimizing the number of samples	• Development of a multi-stage triaxial test to permit the optimization of the number of samples. • Include the determination of a relevant criterion for imminent failure • Monitoring of strains on specimen during triaxial tests (σ_3=0,10,20,30 MPa) • Pore gas maintained at atmospheric pressure	ISRM Standard method of rock testing (modified accordingly to the relevant criterion for imminent failure)	2 (preliminary) 4

continued....

Golder Associates

TABLE 1 (continued)

ASPECT TO BE STUDIED	SCOPE/SPECIAL FEATURE OF TESTING	REFERENCE/ TEST STANDARD	NO. OF TESTS
3. Calibration tests to establish a procedure for controlling the rate of loading and unloading	• Reproduce, under laboratory conditions, the stress changes around an opening being developed • Develop a procedure that simultaneously reduce σ_3 and increase σ_1 (at various rates) • Development of a servo-controlled loading/ unloading system • Pore gas maintained at atmospheric pressure	ISRM Standard of rock testing with modifications to suit the modelled phenomenon	2
4. Tests to simulate the stress changes and underground openings	• Samples subjected to various initial stress conditions are then brought to failure at various rates and under different stress paths • Study the effect of stress changes on the failure mode • Reproduce failure mode similar to the rock burst of No. 26 Colliery • Pore gas maintained at atmospheric pressure	As determined in Section 3	13
5. Investigation of the effect of gas pore pressure on the failure mode	• Testing of the specimen under gas pore pressure (uniaxial, triaxial) • Study the effect of stress changes on the failure mode • Reproduce failure mode similar to the rock burst of No. 26 Colliery • Pore gas pressure ranging between 3.1 and 5 MPa	ISRM as determined in Section 3	15
		TOTAL	64

Golder Associates

TABLE 2

TESTING PROGRAM FOR PHASE 2

ASPECTS TO BE STUDIED	TEST SCHEDULE AND SPECIAL FEATURES	NO. OF TESTS
1. Calibration of the servo-controlled loading/unloading system (using reference material, Pier Cap Sandstone)	• Five tests along different predetermined stress paths. Emphasis on fast loading/unloading rates. Pore gas pressure maintained at atmospheric pressure.	5
2. Verification of the multistage triaxial test procedure (sample from Lingan Colliery	• Three uniaxial compression and four triaxial tests with strain monitoring to establish the data base for multistage triaxial tests (at ISRM rate). • Two (2) multistage tests based on the imminent failure criterion established in phase 1 (at ISRM rate). • Two (2) direct tensile tests to determine the tensile strength (at ISRM rate), two Brazilian tensile tests. • Three (3) triaxial tests with loading rate at 43.7 MPa/s at confining pressure ranging from 5 to 30 MPa. • One gas-permeability test	17
3. Determination of Strength Characteristics of samples from No. 26 Colliery	• One uniaxial and three triaxial tests with strain monitoring to define the failure envelope and provide data base for MST. • One multistage test • Three gas-permeability tests to determine the variation in permeability under different conditions.	8

Golder Associates

TABLE 2 (continued)

ASPECTS TO BE STUDIED	TEST SCHEDULE AND SPECIAL FEATURES	NO. OF TESTS
4. Simulation of stress changes with the introduction of pore gas pressure (on samples from No. 26 Colliery and Lingan Colliery	• The mode of failure under conditions of rapid stress changes and the effect of pore gas pressure are the prime factors to be studied in this aspect. The testing program includes fourteen tests in which the samples would initially be loaded hydrostatically and thenbrought to failure by increasing σ_1 and reducing σ_3 simultaneously. Pore gas pressure of up to 9 MPa will be introduced in the specimens.	14
	TOTAL NO. OF TESTS	44

Golder Associates

TABLE 3

PHYSICAL PROPERTIES OF PIER CAP SANDSTONE

AND DIMENSIONS OF TEST SPECIMENS

(a) Physical Properties

Bulk Density	2.19 Mg/m^3
Porosity	19%
Gas Permeability	5.22×10^{-6} cm/s at 5 MPa
	5.24×10^{-6} cm/s at 10 MPa

(b) Average Strength and Deformation Characteristics

Uniaxial Compressive Strength (1)	43.3 MPa
Tensile (Brazilian) Strength (1)	4.3 MPa
Elastic Modulus (1)	10.78 GPa (3)
Dynamic Modulus (2)	11.95 GPa

(c) Dimensions of Test Specimens

Type of Test	Dimensions of Specimens	ISRM Standard
Brazilian Tests	54 mm dia. x 27 mm	NX Sample L/D = 0.5
Uniaxial and Triaxial Tests (with no gas pressure)	54 mm dia. x 125 mm (L/D - 2.35)	NX Sample L/D = 2.0-3.0
Uniaxial and Triaxial Tests (with gas pressure)	54 mm dia. x 115 mm (L/D = 2.11)	NX Sample L/D = 2.0-3.0

Notes:

(1) Based on results obtained from phase one

(2) Determined from velocities of compressional waves through the sample

(3) Secant modulus at 50%.

TABLE 4

CLASSIFICATION OF LINGAN COLLIERY SAMPLES

SAMPLE NO.	CLASS
C-128-1	B
C-128-2	A
C-128-3	C
C-128-4	A
C-128-8	B
C-128-9(A,B)	B
C-129-1	C
C-129-2	C
C-129-4	C
C-129-5	A
C-129-7	C
C-129-8	B
C-129-9	B
C-129-11	B
C-129-12	B
C-104-1	A
C-104-2	A
C-104-3	A
C-104-4	B
C-104-5	B
C-104-7	B
C-104-8	B

NOTE: Refer to Section 4 for descriptions of classifications

TABLE 5

CLASSIFICATION OF NO. 26 COLLIERY SAMPLES

ORIGIN: COLLIERY NO. 26

BOREHOLE: DRILL HOLE D-165

SAMPLE DESIGNATION	DEPTH	L/D	DESCRIPTION RESEARCH PROJECT	DESCRIPTION BOREHOLE LOG
D165-1	10'-5.5" to 10'-9"		D	Horizon 1
D165-2	18'-0" to 18'-3.5"		F	" "
D165-3	19'-2.5" to 19'-6"		E	" "
D165-4	20'-0" to 20'-3.5"		F	" "
D165-5	40'-6" to 40'-9.5"		F	Horizon 2
D165-6	41'-3.5" to 41'-7"		F	" "
D165-7	41'7" to 41'-10.5"		G	" "
D165-8	41'-10.5" to 42'-2"	≈1.90 TO	F	" "
D165-9	42'-3.5" to 42'-7"	≈1.95	F	" "
D165-10	42'-7" to 42'-10.5"		F	" "
D165-11	42'-10.5" to 43'-2"		F	" "
D165-12	43'-2" to 43'-5.5"		F	" "
D165-13	43'-9" to 44'-0.5"		F	" "
D165-14	44'-0.5" to 44'-4"		G	" "
D165-15	44'-7.5" to 44'-11"		F	" "
D165-16	44'-11" to 45'-2.5"		G	" "
D165-17	45'-2.5" to 45'-6"		F	" "
D165-18	56'-9" to 57'-2.5"	3.0	F	Horizon 3

NOTE: Refer to Section 4 for descriptions of classifications

TABLE 6

PHYSICAL PROPERTIES OF LINGAN COLLIERY SAMPLES

AND DIMENSIONS OF TEST SPECIMENS

(a) Physical Properties

Bulk density	2.46 Mg/m^3
Porosity	6%
Gas Permeability	2.93×10^{-6} cm/s at 7.1 MPa

(b) Average Strength and Deformation Characteristics

Uniaxial Compressive Strength[1]	73.4 MPa
Tensile Strength[1]	3.9 - 9.2 MPa
Elastic Modulus[1]	11.57 GPa[3]
Dynamic Modulus[2]	19.4 GPa

(c) Dimensions of Test Specimens

Type of Test	Dimensions of Specimens	ISRM Standard
Brazilian Tests	45 mm dia. x 23 m	NX Samples L/D = 0.5
Uniaxial and Triaxial Tests (with no gas pressure)	45 mm dia x 90 mm	NX Samples L/D = 2.0-3.0
Direct Tensile Test	45 mm dia. x 135 mm	NX Samples L/D = 2.5-3.0
Stress Permeability Tests	47.5 m dia. x 109 mm	NX Samples L/D = 2.5-3.0

NOTES:

(1) Based on results obtained from phase two.

(2) Determined from velocities of compressional waves through the sample.

(3) Secant modulus at 50%.

March 1985

841-1287

TABLE 7

PHYSICAL PROPERTIES OF NO. 26 COLLIERY SAMPLES

AND DIMENSION OF TEST SPECIMENS

(a) Physical Properties

Bulk density	2.59 Mg/m^3
Porosity	2%
Gas Permeability	Very Low

(b) Average Strength and Deformation Characteristics

Uniaxial Compressive Strength[1]	49.0 MPa	60-100 MPa[3]
Tensile Strength	-	2.6-8.0 MPa[3]
Elastic Modulus[1]	17.53 GPa[2]	12-20 GPa[3]
Dynamic Modulus	34.96 GPa[4]	

(c) Dimensions of Test Specimens

Type of Test	Dimensions of Specimens	ISRM Standard
Uniaxial and Triaxial Tests (with and without gas)	47.5 mm dia. x 95 m	NX Samples L/D = 2.0-3.0
Stress permeability tests	47.5 mm dia. x 142.5 m	NX Samples L/D = 2.0-3.0

NOTES:

(1) Based on results obtained from Phase two.

(2) Secant modulus at 50%

(3) From Reference 2

(4) Determined from velocities of compressional waves through the sample.

TABLE 8

SUMMARY OF TEST RESULTS, ASPECT NO. 1

CALIBRATION OF σ_3 SERVO-CONTROLLED DEVICE

SAMPLE NO.	TYPE OF TEST	ASPECT RATIO (L/D)	PORE GAS PRESSURE	INITIAL STRESS LEVEL (MPa)		STRESS LEVEL AT FAILURE (MPa)			APPLIED STRESS RATE	OBSERVED FAILURE MODE	REMARKS
			P(MPa)	σ_3	σ_1	σ_3	σ_1	σ_t			
71	RAPID CONFINING PRESSURE REDUCTION	2.5	ATM	22.0	157.5	8.6	157.5	-	$R\sigma_1$=0 $R\sigma_3$=5.19 MPa/s	S	Shear along diagonal
72	"	2.5	"	21.8	155.6	5.6	155.6	-	$R\sigma_1$=0 $R\sigma_3$=5.27 MPa/s	S	"
73	STRESS CHANGE SIMULATION	2.5	"	20.7	20.7	17.4	143.8	-	$R\sigma_1$=38.0 MPa/s $R\sigma_3$=1.04 MPa/s	S	"
74	"	2.5	"	20.7	20.7	9.9	106.7	-	$R\sigma_1$=43.6 MPa/s $R\sigma_3$=5.56 MPa/s	S	"
75	"	2.0	"	20.7	20.7	5.3	93.2	-	$R\sigma_1$=24.0 MPa/s $R\sigma_3$=5.17 MPa/s	S	"

D = 54 mm

MODE OF FAILURE:
AC: Axial Cracks
AS: Axial Splitting
C: Conjugates Planes
CN: Conical
H: Horizontal Splitting
PC: Peripheral Cracks
S: Shear
SAB: Shear Along Bedding
SC: Curved Shear Plane
MS: Multiple Shear

Golder Associates

TABLE 9

SUMMARY OF TEST RESULTS, LINGAN SAMPLES, ASPECT NO. 2

CHARACTERIZATION OF LINGAN SAMPLES AND VERIFICATION OF MULTISTAGE TRIAXIAL TEST PROCEDURE

SAMPLE NO.	TYPE OF TEST	ASPECT RATIO (L/D)	PORE GAS PRESSURE	INITIAL STRESS LEVEL (MPa)		STRESS LEVEL AT FAILURE (MPa)			APPLIED STRESS RATE	OBSERVED FAILURE MODE	REMARKS
			P(MPa)	σ_3	σ_1	σ_3	σ_1	σ_t			
C-128-9	Direct Tensile	3.0	ATM	-	-	-	-	0.04	-	H	Sample failed during preparation of test
C-128-9A	Brazilian Tensile	0.5	ATM	-	-	-	-	9.2	117 N/S	AS	Possible plane of weakness
C-128-9B	Brazilian Tensile	0.5	ATM	-	-	-	-	8.8	103 N/S	AS	Class B
											19 lbs
C-129-7	Direct Tensile	2.0	ATM	-	-	-	-	3.9	ISRM	Horizontal and inclined splitting	Sample broken during preparation, ends trimmed to a 2:1 ratio Class C
C-128-1	Uniaxial	2.0	ATM	-	-	-	58.7	-	ISRM	AS, S	Class B
C-128-3	Uniaxial	2.0	ATM	-	-	-	85.9	-	ISRM	S, CN, AS, AC	Class C
C-129-1	Uniaxial	2.0	ATM	-	-	-	75.5	-	ISRM	AS, S, CN	Class C
C-129-2	Triaxial	2.0	ATM	5.0	5.0	5.0	96.6	-	ISRM	S, CN	Class C
C-129-4	Triaxial	2.0	ATM	10.0	10.0	10.0	119.3	-	ISRM	S, C, AC	Class C
C-129-8	Triaxial	2.0	ATM	30.0	30.0	30.0	258.8	-	ISRM	S	Class B
C-129-9	Triaxial	1.97	ATM	20.0	20.0	20.0	198.9	-	ISRM	S	Class B

Golder Associates

TABLE 9 (cont'd)

SUMMARY OF TEST RESULTS, LINGAN SAMPLES

ASPECT NO. 2

SAMPLE NO.	TYPE OF TEST	ASPECT RATIO (L/D)	PORE GAS PRESSURE	INITIAL STRESS LEVEL (MPa)		STRESS LEVEL AT FAILURE (MPa)			APPLIED STRESS RATE	OBSERVED FAILURE MODE	REMARKS
			P(MPa)	σ_3	σ_1	σ_3	σ_1	σ_t			
C-128-2	Triaxial	2.0	ATM	5.0	5.0	5.0	129.2	-	43.7 MPa/s		Class A
C-128-4	Triaxial	2.0	ATM	30.0	30.0	30.0	218.3	-	43.7 MPa/s		Class A
C-129-5	Triaxial	2.0	ATM	15.0	15.0	15.0	172.5	-	43.7 MPa/s		Class A
C-104-7	Triaxial	2.0	ATM	20.0	20.0	20.0	184.6	-	ISRM	S	Class B
C-104-8	Triaxial	2.0	ATM	30.0	30.0	30.0	212.6	-	ISRM	S	Class B

Golder Associates

TABLE 10

SUMMARY OF TEST RESULTS, STRAIN MEASUREMENTS

SAMPLES C-129-1 AND C-129-9, ASPECT NO. 2

a) Sample No. C-129-1 Uniaxial Compression

MAJOR PRINICPAL STRESS σ_1 (MPa)	DEVIATORY STRESS $\sigma_1-\sigma_3$ (MPa)	AXIAL STRAIN $\bar{\varepsilon}_a$ μ	LONGITUDINAL STRAIN $\bar{\varepsilon}_\ell$(1) μ	VOLUMETRIC STRAIN $\varepsilon_v=\bar{\varepsilon}_a+2\bar{\varepsilon}_\ell$ μ
0	0	0	0	0
5	5	-351	- 3	-357
10	10	-696	- 5	-706
15	15	-1080	+ 3	-1074
20	20	-1533	+ 22	-1489
30	30	-2307	+101	-2105
40	40	-3029	+236	-2557
50	50	-3763	+418	-2927
60	60	-4130	+682	-2766
65	65	-4386	+863	-2660
67.1	67.1	-4465	+956	-2553
69.9	69.9	-4624	+1108	-2408
72.7	72.7	-4746	+1291	-2164
75.5	75.5	Failure	Failure	Failure

(1) Average of two gauges

TABLE 10 (cont'd)

b) Sample C-129-9 Triaxial Compression, σ_3=20 MPa

MAJOR PRINCIPAL STRESS σ_1 (MPa)	DEVIATORY STRESS $\sigma_1-\sigma_3$ (MPa)	AXIAL STRAIN $\bar{\varepsilon}_a$(1) μ	LONGITUDINAL STRAIN $\bar{\varepsilon}_\ell$(1) μ	VOLUMETRIC STRAIN $\varepsilon_v=\bar{\varepsilon}_a+2\bar{\varepsilon}_\ell$ μ
20	0	0	0	0
25	5	-154	+10	-134
30	10	-290	+17	-256
35	15	-420	+24	-372
40	20	-553	+35	-483
50	30	-803	+62	-679
60	40	-1042	+96	-850
70	50	-1426	+155	-1116
80	60	-1690	+207	-1276
90	70	-1940	+260	-1420
100	80	-2164	+312	-1540
110	90	-2424	+383	-1658
120	100	-2668	+445	-1778
130	110	-2934	+523	-1888
140	120	-3210	+614	-1982
145	125	-3370	+661	-2048
150	130	-3492	+700	-2092
152	132	-3574	+730	-2114
156	136	-3684	+762	-2160
160	140	-3862	+802	-2258
165	145	-4038	+880	-2278
171	151	-4230	+943	-2344
174	154	-4370	+997	-2376
176	156	-4468	+1033	-2402
179	159	-4550	+1069	-2412
182	162	-4658	+1156	-2346
185	165	-4800	+1224	-2352
188	168	-4906	+1269	-2368
190	170	-4976	+1347	-2282
193	173	-5030	+1403	-2224
196	176	-5176	+1560	-2056
198.9	178.9	Failure	Failure	Failure

(1) Average of two gauges

TABLE 11

SUMMARY OF TEST RESULTS, MULTISTAGE TESTS

SAMPLE C129-11

MAJOR PRINCIPAL STRESS σ_1 (MPa)	DEVIATORY STRESS $\sigma_1-\sigma_3$ (MPa)	AXIAL STRAIN $\bar{\varepsilon}_a$ (avg) μ	LONGITUDINAL STRAIN $\bar{\varepsilon}_\ell$ (avg) μ	VOLUMETRIC STRAIN ε_v μ
Stage 1, $\sigma_3 = 0$				
0	0	0	0	0
5	5	-247	+18	-211
10	10	-592	+60	-472
20	20	-893	+173	-147
30	30	-1145	+220	-705
40	40	-1350	+280	-790
50	50	-1790	+432	-926
52	52	-1863	+462	-939
54	54	-1990	+505	-980
56	56	-2060	+533	-995
58	58	-2295	+614	-1067
60	60	-2400	+669	-1062
62	62	-2480	+702	-1076
64	64	-2554	+744	-1066
66	66	-2694	+790	-1114
68	68	-2770	+843	-1084
70	70	-2834	+878	-1078
72	72	-2937	+933	-1071
74	74	-3030	+987	-1056
*1 set of gauges were broken				
Stage 2, $\sigma_3 = 10$				
10	0	0	0	0
20	10	-196	+48	-100
30	20	-485	+127	-231
40	30	-798	+214	-370
50	40	-1126	+302	-522
55	45	-1320	+356	-608
62	52	-1456	+400	-657
64	54	-1604	+438	-728
66	56	-1682	+460	-762
68	58	-1772	+487	-798
70	60	-1818	+502	-814
72	62	-1886	+530	-828
74	64	-1956	+546	-864
76	66	-2017	+566	-885
79	69	-2126	+602	-922
82	72	-2214	+632	-950
85	75	-2328	+666	-996
87	77	-2404	+693	-1018
90	80	-2490	+718	-1054
93	83	-2583	+756	-1071
96	86	-2677	+792	-1093
99	89	-2790	+836	-1118

TABLE 11 (cont'd)

MAJOR PRINCIPAL STRESS σ_1 (MPa)	DEVIATORY STRESS $\sigma_1 \sigma_3$ (MPa)	AXIAL STRAIN $\bar{\varepsilon}_a$ (avg) μ	LONGITUDINAL STRAIN $\bar{\varepsilon}_\ell$ (avg) μ	VOLUMETRIC STRAIN ε_v μ
Stage 2, σ_3 = 10 (cont'd)				
102	92	-2894	+884	-1126
104	94	-2990	+930	-1130
107	97	-3093	+973	-1147
110	100	-3206	+1025	-1156
113	103	-3305	+1076	-1153
116	106	-3426	+1136	-1154
118	108	-3546	+1199	-1148
Stage 3, σ_3 = 20				
20	0	0	0	0
30	10	-178	+67	-44
40	20	-482	+150	-182
50	30	-818	+250	-318
60	40	-1134	+350	-434
70	50	-1427	+445	-537
80	60	-1739	+546	-647
90	70	-2010	+640	-730
100	80	-2320	+750	-830
110	90	-2610	+856	-898
120	100	-3184	+1114	-956
130	110	-3507	+1262	-983
140	120	-3840	+1353	-1134
150	130	-4282	+1608	-1066
155	135	-4504	+1740	-1074
Stage 4, σ_3 = 30				
30	0	0	0	0
40	10	-242	+62	-118
50	20	-494	+136	-222
60	30	-1160	+360	-440
70	40	-1454	+442	-570
80	50	-1770	+552	-666
100	70	-2350	+748	-854
120	90	-2943	+970	-1003
140	110	-3602	+1260	-1082
160	130	-4407	+1583	-1241
180	150	-5258	+2055	-1148
200	170	-6358	+2760	-838
220	190	-7620	+3780	-60
230	200	-8585	+4980	+1375
240	210	-9900	+6790	+3110

Creep failure (5 seconds) at σ_1 = 240 MPa

σ_3 = 30

TABLE 12

SUMMARY OF TEST RESULTS, MULTISTAGE TESTS

SAMPLE C129-12

MAJOR PRINCIPAL STRESS σ_1 (MPa)	DEVIATORY STRESS $\sigma_1 \sigma_3$ (MPa)	AXIAL STRAIN $\bar{\varepsilon}_a$ (avg) μ	LONGITUDINAL STRAIN $\bar{\varepsilon}_\ell$ (avg) μ	VOLUMETRIC STRAIN ε_v μ
Stage 1, $\sigma_3 = 0$				
0	0	0	0	0
5	5	-121	+16	-139
10	10	-350	+40	-270
15	15	-547	+68	-411
20	20	-346	+108	-530
25	25	-941	+150	-641
30	30	-1132	+196	-740
40	40	-1499	+306	-887
50	50	-1843	+423	-997
52	52	-1921	+458	-1005
54	54	-2005	+494	-1017
56	56	-2085	+532	-1021
58	58	-2251	+596	-1059
60	60	-2330	+636	-1058
62	62	-2394	+670	-1054
64	64	-2472	+708	-1056
66	66	-2557	+756	-1045
68	68	-2634	+796	-1042
70	70	-2706	+842	-1022
72	72	-2773	+876	-1021
Stage 2, $\sigma_3 = 10$				
10	0	0	0	0
20	10	-244	+24	-196
30	20	-555	+92	-371
40	30	-844	+150	-544
50	40	-1130	+233	-664
55	45	-1387	+300	-747
60	50	-1486	+330	-826
62	52	-1549	+352	-845
64	54	-1618	+370	-878
68	58	-1750	+417	-916
70	60	-1785	+427	-931
74	64	-1912	+470	-972
76	66	-1960	+488	-984
78	68	-2026	+504	-1018
80	70	-2093	+523	-1047
85	75	-2211	+573	-1065
87.5	77.5	-2281	+590	-1101
90	80	-2347	+617	-1113
92.5	82.5	-2428	+653	-1122
95	85	-2490	+674	-1142

TABLE 12 (cont'd)

MAJOR PRINCIPAL STRESS σ_1 (MPa)	DEVIATORY STRESS $\sigma_1 \sigma_3$ (MPa)	AXIAL STRAIN $\bar{\varepsilon}_a$ (avg) μ	LONGITUNDIAL STRAIN $\bar{\varepsilon}_\ell$ (avg) μ	VOLUMETRIC STRAIN ε_v μ
Stage 2, σ_3 = 10 (cont'd)				
97.5	87.5	-2576	+714	-1148
100	90	-2657	+751	-1155
102.5	92.5	-2697	+766	-1165
105	95	-2785	+813	-1159
107.5	97.5	-2880	+864	-1182
Stage 3, σ_3 = 20				
20	0	0	0	0
30	10	-286	+62	-162
40	20	-565	+120	-325
50	30	-838	+203	-432
95	75	-2091	+620	-851
100	80	-2209	+648	-913
110	90	-2460	+740	-980
120	100	-2708	+840	-1028
130	110	-3000	+967	-1066
135	115	-3137	+1034	-1069
137.5	117.5	-3237	+1067	-1103
140	120	-3320	+1110	-1100
142.5	122.5	-3428	+1176	-1076
Stage 3, σ_3 = 30				
30	0	0	0	0
40	10	-101	+10	-81
50	20	-482	+106	-270
70	40	-972	+253	-466
100	70	-1712	+483	-746
120	90	-2167	+640	-887
140	110	-2700	+836	-1028
160	130	-3199	+1040	-1119
180	150	-3790	+1322	-1146
200	170	-4473	+1726	-1021
210	180	-4915	+2032	-851
220	190	-5303	+2330	-643

TABLE 13

GAS PERMEABILITY TEST, SAMPLE C-104-4

LINGAN SANDSTONE

AXIAL STRESS: 11.2 MPa
CONFINING STRESS: 10.0 MPa

(Pg) upstream (psi)	(Pg) downstream (psi)	Δt(mins)
1000	0	0
1000	20	1
1007	24	2
1007	31	3
1017	47	5
1017	233	14
1017	369	20
1012	467	25
1023	551	30
1024	640	35
1010	700	40
1011	790	50
1027	900	70
1023	937	81
1023	963	93
1010	991	120
1010	1006	173

Permeability Measurements

Pg(psi)	Q(cm^3/s)	K(cm/s)
1031	0.3448	2.9×10^{-6}
1033	0.3390	2.9×10^{-6}
1035	0.3509	3.0×10^{-6}

TABLE 14

SUMMARY OF TEST RESULTS, ASPECT NO. 3

STRENGTH CHARACTERIZATION OF COLLIERY NO. 26

SAMPLE NO.	TYPE OF TEST	ASPECT RATIO (L/D)	PORE GAS PRESSURE	INITIAL STRESS LEVEL (MPa)		STRESS LEVEL AT FAILURE (MPa)			APPLIED STRESS RATE	OBSERVED FAILURE MODE	REMARKS
			P(MPa)	σ_3	σ_1	σ_3	σ_1	σ_t			
D-165-12	Uniaxial	1.92	ATM	-	-	-	49.0	-	ISRM	AC, SAB	Sample Class C
D-165-15	Triaxial	1.85	ATM	10.0	10.0	10.0	118.0	-	ISRM	S, ICAB	"
D-165-10	Triaxial	1.94	ATM	20.0	20.0	20.0	168.8	-	ISRM	S	"
D-165-9	Triaxial	1.92	ATM	30.0	30.0	30.0	206.3	-	ISRM	S	"

Golder Associates

TABLE 15

SUMMARY OF TEST RESULTS, MULTISTAGE TESTS

SAMPLE D165-11

MAJOR PRINCIPAL STRESS σ_1 (MPa)	DEVIATORY STRESS $\sigma_1-\sigma_3$ (MPa)	AXIAL STRAIN $\bar{\varepsilon}_a$ (avg) μ	LONGITUDINAL STRAIN $\bar{\varepsilon}_\ell$ (avg) μ	VOLUMETRIC STRAIN ε_v μ
Stage 1, $\sigma_3 = 0$				
0	0	0	0	0
Stage 2, $\sigma_3 = 10$				
10	0	0	0	0
20	10	-181	+13	-155
30	20	-389	+27	-335
40	30	-621	+47	-527
50	40	-885	+87	-711
60	50	-1093	+114	-865
70	60	-1346	+166	-1015
80	70	-1601	+225	-1151
85	75	-1739	+251	-1237
90	80	-1953	+305	-1343
95	85	-2186	+362	-1463
100	90	-2356	+413	-1530
105	95	-2496	+457	-1582
110	100	-2657	+501	-1656

NOTE: At 112.5 drastic increase in σ_3 was observed. Also σ_3 ↑ simultaneously with σ_1. It was expected that the sample was at the point of failure or very near to failure. Subsequently σ_3 was increased to 20 MPa and the second stage was repeated.

Stage 3, $\sigma_3 = 20$				
20	0	0	0	0
30	10	-120	+31	-58
40	20	-318	+64	-190
50	30	-520	+94	-332
60	40	-756	+137	-483
70	50	-968	+173	-622
80	60	-1194	+217	-771
100	80	-1637	+318	-1001
120	100	-2090	+426	-1239
134	114	-2484	+564	-1356
137.5	117.5	-2582	+585	-1412
140	120	-2694	+613	-1468
142.5	122.5	-2796	+665	-1466

NOTE: Same phenomenon was observed.

TABLE 15 (cont'd)

MAJOR PRINCIPAL STRESS σ_1 (MPa)	DEVIATORY STRESS $\sigma_1-\sigma_3$ (MPa)	AXIAL STRAIN $\bar{\varepsilon}_a$ (avg) μ	LONGITUDINAL STRAIN $\bar{\varepsilon}_\ell$ (avg) μ	VOLUMETRIC STRAIN ε_v μ
Stage 4, σ_3 = 30				
30	0	0	0	0
40	10	-176	+45	-86
50	20	-450	+64	-322
60	30	-685	+106	-473
70	40	-964	+139	-686
80	50	-1240	+197	-847
100	70	-1740	+312	-1116
120	80	-2220	+442	-1337
140	110	-2686	+564	-1557
160	130	-3190	+743	-1705
170	140	-3400	+1070	-1260

NOTE: Creeping as indicated by strain gauges

TABLE 16

GAS PERMEABILITY TEST, SAMPLE D-165-17

COLLIERY NO. 26 SANDSTONE

	TOTAL STRESS (MPa) σ_3	σ_1	GAS PRESSURE (MPa) (Pq) Upstream	(Pq) Downstream	REMARKS
STAGE 1					
	0	25.1			
	10	10	2.88	0.52	
STAGE 2					
1st Cycle	0	40	2.88	0.88	
	10	10	2.88	0.96	
	5	10	2.88	0.96	
	4	10	2.88	1.09	leakes below 4.0 MPa
2nd Cycle	0	40.1			
	10	10	2.88	1.30	
	5	10	2.88	1.43	
3rd Cycle	0	40.1			
	10	10	2.88	0.78	
	5	10	2.88	0.76	
STAGE 3					
	0	45.2			
	10	10	2.88	1.30	
STAGE 4					
1st Cycle	0	50.2			
	10	10	2.88	1.43	
	5	10	2.88	1.58	
2nd Cycle	10	50.2	2.88	1.38	σ_3 slowly reduced at σ_3=3 MPa, gas leaked and no failure was observed
STAGE 4					
1st Cycle	0	55.2			
	10	10	2.88	1.59	
	5	10	2.88	1.83	
2nd Cycle	5	55.2	2.88	1.45	σ_3 slowly reduced at σ_3=3 MPa, gas leaked and no failure was observed
STAGE 5					
1st Cycle	0	62.8			
	10	10	2.88	1.74	
	5	10	2.88	1.90	
2nd Cycle	5	62.8	2.88	1.47	σ_3 slowly reduced at σ_3=3.5 MPa, gas leaked and no failure was observed

TABLE 16 (cont'd)

GAS PERMEABILITY TEST, SAMPLE D-165-17

COLLIERY NO. 26 SANDSTONE

	TOTAL STRESS (MPa)		GAS PRESSURE (MPa)		REMARKS
	σ_3	σ_1	(Pg) Upstream	(Pg) Downstream	
STAGE 6					
	0	60.3			Upon reloading, sample failed at 60.3 MPa
	10	10	2.88	2.79	
	5	10	2.88	2.81	
	4	10	2.88	2.83	Gas leaked at 3 MPa

TABLE 17

GAS PERMEABILITY TEST, SAMPLE D-165-18

COLLIERY NO. 26 SANDSTONE

TOTAL STRESS MPa			EFFECTIVE STRESS MPa		i	Q	K
σ_1	σ_3	P	σ_1	σ_3		cm^3/s	cm/s
10	10	6.9	3.1	3.1	4939	No flow	0
30	10	6.9	23.1	3.1	4939	No flow	0
30	10	11.0	19.0	-1.0	7837	No flow	0
50.3	10	7.1	43.2	2.9	5082	0.076	8.4×10^{-7}
50.3	20	7.1	43.2	12.9	5082	0.065	7.2×10^{-7}
50.3	25	7.1	43.2	17.9	5082	0.060	6.7×10^{-7}
62.8	10	6.1	56.7	3.9	4366	0.072	9.3×10^{-7}
62.8	10	7.0	55.8	3.0	5009	0.085	9.6×10^{-7}
62.8	20	7.0	55.8	13.0	5009	0.073	8.2×10^{-7}
62.8	25	7.0	55.8	18.0	5009	0.056	6.3×10^{-7}

TABLE 18

SUMMARY OF TEST RESULTS, STRESS CHANGE SIMULATIONS

ASPECT NO. 4, COLLIERY NO. 26 SAMPLES

SAMPLE NO.	TYPE OF TEST	ASPECT RATIO (L/D)	PORE GAS PRESSURE	INITIAL STRESS LEVEL (MPa)		STRESS LEVEL AT FAILURE (MPa)			APPLIED STRESS RATE	OBSERVED FAILURE MODE	REMARKS
			Upstream P(MPa)	σ_3	σ_1	σ_3	σ_1	Downstream Pore Gas Pressure			
D-165-1	Stress Change Simulation	1.90	7.0	20.7	20.7	17.1	233.7	0.7	$R\sigma_1$=43.7 MPa/s $R\sigma_3$=0.7 MPa/s	S, C, AC	Sample Class A
D-165-3	"	1.90	7.0	20.7	20.7	18.2	153.2	1.17	$R\sigma_1$=43.7 MPa/s $R\sigma_3$=0.4 MPa/s	S, S	Sample Class B Two shear planes along
											diagonal. One in sandstone
											and one perpendicular
											along siltstone bedding.
											Slickenside observed on
											the failure plane in
											sandstone.
D-165-8	"	1.90	7.0	20.7	20.7	17.6	81.6	0.0	$R\sigma_1$=43.7 MPa/s $R\sigma_3$=0.8 MPa/s	MS	Sample Class C Approximately 5 shear
											planes along beddings.
D-165-4	"	1.90	9.0	20.7	20.7	11.8	158.9	0.0	$R\sigma_1$=43.7 MPa/s $R\sigma_3$=2.9 MPa/s	S, C, AS	Sample Class C Very little siltstone.
D-165-5	"	1.90	9.0	20.7	20.7	13.7	112.7	0.0	$R\sigma_1$=43.7 MPa/s $R\sigma_3$=3.4 MPa/s	MS	Sample Class C Approximately 7 shear
											planes along beddings.
D-165-16	"	1.90	7.0	20.7	20.7	9.2	175.7	0.2	$R\sigma_1$=43.7 MPa/s $R\sigma_3$=3.3 MPa/s	AS, AC	Sample Class D
D-165-2	"	1.90	9.0	20.7	20.7	10.4	119.4	0.4	$R\sigma_1$=43.7 MPa/s $R\sigma_3$=4.7 MPa/s	MS	Sample Class C
											Failure Plane(5)
											Thick Silt-stone Bedding

Golder Associates

TABLE 18 (cont'd)

SUMMARY OF TEST RESULTS, STRESS CHANGE SIMULATIONS

ASPECT NO. 4, COLLIERY NO. 26 SAMPLES

SAMPLE NO.	TYPE OF TEST	ASPECT RATIO (L/D)	PORE GAS PRESSURE	INITIAL STRESS LEVEL (MPa)		STRESS LEVEL AT FAILURE (MPa)			APPLIED STRESS RATE	OBSERVED FAILURE MODE	REMARKS
			Upstream P(MPa)	σ_3	σ_1	σ_3	σ_1	Downstream Pore Gas Pressure			
D-165-13	Stress Change Simulation	1.90	7.0	20.7	20.7	10.2	113.0	0	$R\sigma_1$=43.7 MPa/s $R\sigma_3$=4.9 MPa/s	MS	Sample Class C
D-165-7	"	1.90	9.0	20.7	20.7	2.7	81.6	0	$R\sigma_1$=43.7 MPa/s $R\sigma_3$=13.3 MPa/s	AS	Sample Class D
D-165-14	"	1.90	7.0	20.7	20.7	5.4	44.0	2.4	$R\sigma_1$=43.7 MPa/s $R\sigma_3$=32.0 MPa/s	S, AS, AC	Sample Class D

Golder Associates

March 1985

841-1287

TABLE 19

UNIAXIAL LOADING UNDER PORE GAS PRESSURE
ASPECT NO. 4, LINGAN SAMPLES

SAMPLE NO.	TYPE OF TEST	ASPECT RATIO (L/D)	PORE GAS PRESSURE	INITIAL STRESS LEVEL (MPa)		STRESS LEVEL AT FAILURE (MPa)			APPLIED STRESS RATE	OBSERVED FAILURE MODE	REMARKS
			P(MPa)	σ_3	σ_1	σ_3	σ_1	σ_t			
C-104-1	Uniaxial	2.26	Upstream 6.2	0	0	0	47.6	-	ISRM	spalling of outer perimeter	Figure 10A, Plate 2
			Downstream 0.02								
C-104-2	Uniaxial	2.26	Upstream 5.24	0	0	0	37.8	-	ISRM	spalling of outer perimeter	Figure 10A, Plate 3
			Downstream 0.01								
C-104-3	Uniaxial	2.26	9.0	0	0	0	49.0	-	ISRM	spalling of outer perimeter	Figure 10B, Plate 4
C-104-5	Uniaxial	2.26	Upstream 6.95								
			Downstream 1.11	0	0	0	58.7	-	ISRM	AS, AC	See Table 20, Plate 5

Golder Associates

TABLE 20

UNIAXIAL LOADING UNDER PORE GAS PRESSURE

SAMPLE NO. C-104-5

LINGAN COLLIERY

	TOTAL STRESS MPa		GAS PRESSURE MPa		TIME (MIN.)	REMARKS
	σ_3	σ_1	(Pg) Up	(Pg) down	Δt	
STAGE 1						
	0	11.2	3.86	C	0	
			3.86	0.1	6	
			3.86	0.14	8	
			3.86	0.17	10	
STAGE 2						
	0	11.2	4.88	0		Increase gas pressure
			4.87	0.19	11	
			4.88	0.21	13	
			4.86	0.25	15	
			4.90	0.32	18	
			4.87	0.37	20	
			4.87	0.52	25	
			4.85	0.68	30	
STAGE 3						
	0	11.2	5.61	0		Increase gas pressure
			5.61	0.73	31	
			5.58	0.79	34	
			5.58	0.85	35	
			5.73	0.90	37	
STAGE 4						
	0	16.8	5.75	0		Increase axial stress
			5.75	0.93	38	
			5.75	1.00	41	
			5.75	1.03	42	
			5.75	1.05	43	
STAGE 5						
	0	19.6	5.77	0		Increase axial stress
			5.77	1.08	44	
			5.78	1.12	45	
			5.78	1.13	48	
STAGE 6		19.6	6.92	0		Increase gas pressure
			6.92	1.13	49	
			6.90	1.12	52	
			6.98	1.11	55	
STAGE 7						
	0	58.7				σ_1 increased to failure

Pg(up) upstream gas pressure (applied from top end of sample)

Pg(down) downstream gas pressure (measured at bottom end of sample)

TABLE 21

RISK ASSESSMENT FOR EJECTION-PRONE SANDSTONES IN RUSSIA[4]

	INDEX CONSIDERED	RISK LEVEL					
		0	0.2	0.4	0.6	0.8	1
Examination of thin sections	% detrital quartz	< 30	30-40	40-50	50-60	60-70	> 70
	% regernated quartz	< 2.5	2.5-5.0	5.0-7.7	7.5-10.0	10.0-12.5	> 12.5
	% argillaceous and micaceous minerals	> 45	45-35	35-25	25-15	15-5	< 5
	Weighted average of grain dimensions (mm)	< 0.12	0.12-0.13	0.13-0.16	0.16-0.2	0.2-0.28	> 0.28
	Extent of intergraular contact (mm)	< 0.1	0.1-0.2	0.2-0.3	0.3-0.4	0.4-0.5	> 0.5
Laboratory measurements	% open pore space	< 2.5	2.5-4.5	4.5-6.5	6.5-8.5	8.5-10.5	> 12
	Tensile strength kg/cm²	>100	100-86	86-72	72-58	58-44	< 40
Percentage of pore space filled by gas (%) (in terms of mass)		< 40	40-50	50-60	60-70	70-80	> 80
Depth (m)		<500	500-700	700-900	900-1100	1100-1300	>1300

Golder Associates

STRESS CHANGE SIMULATIONS
PIER CAP SANDSTONE

FIGURE 1

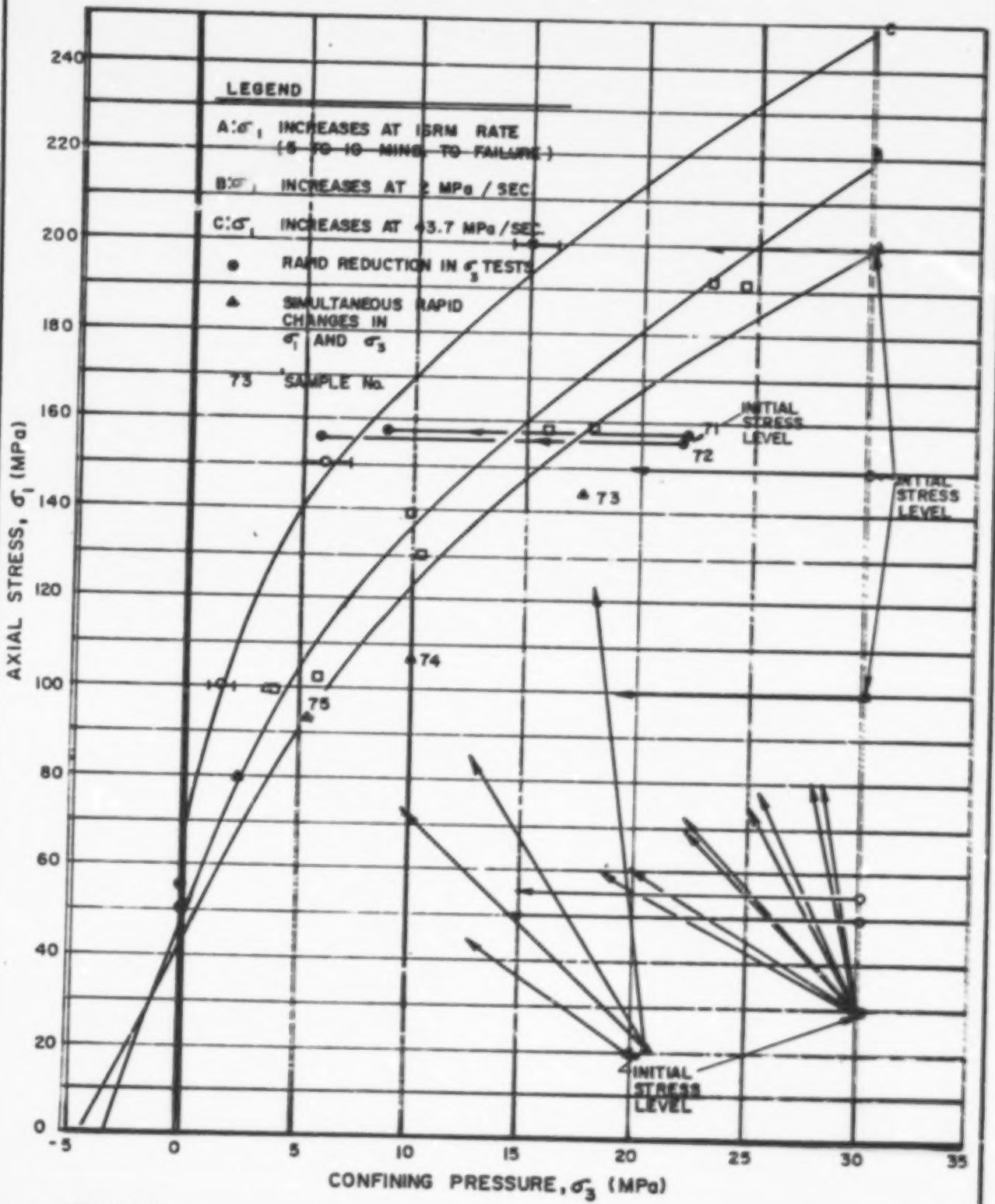

Date MAR 15, 1988

Project 841-1267

Golder Associates

Drawn G.P.

Chkd. E.J.

STRENGTH CHARACTERISTICS
SANDSTONE FROM LINGAN COLLIERY

FIGURE 2

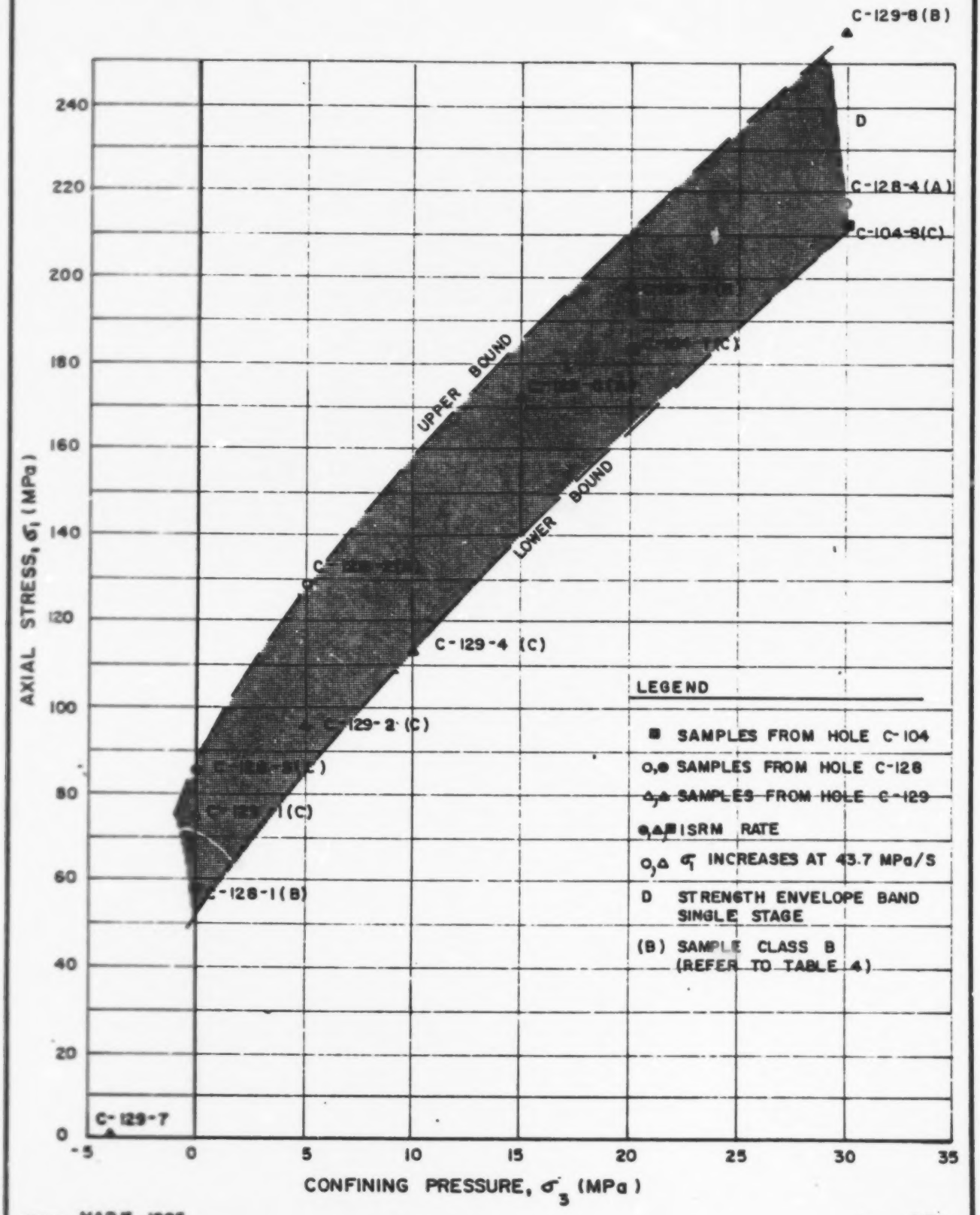

Date MAR 15, 1985
Project 84-1287

Golder Associates

Drawn G.P.
Chkd. GJ

DEVIATOR STRESS VS. AXIAL STRAIN
SAMPLES C-129-1, C-129-9
LINGAN COLLIERY

FIGURE 3

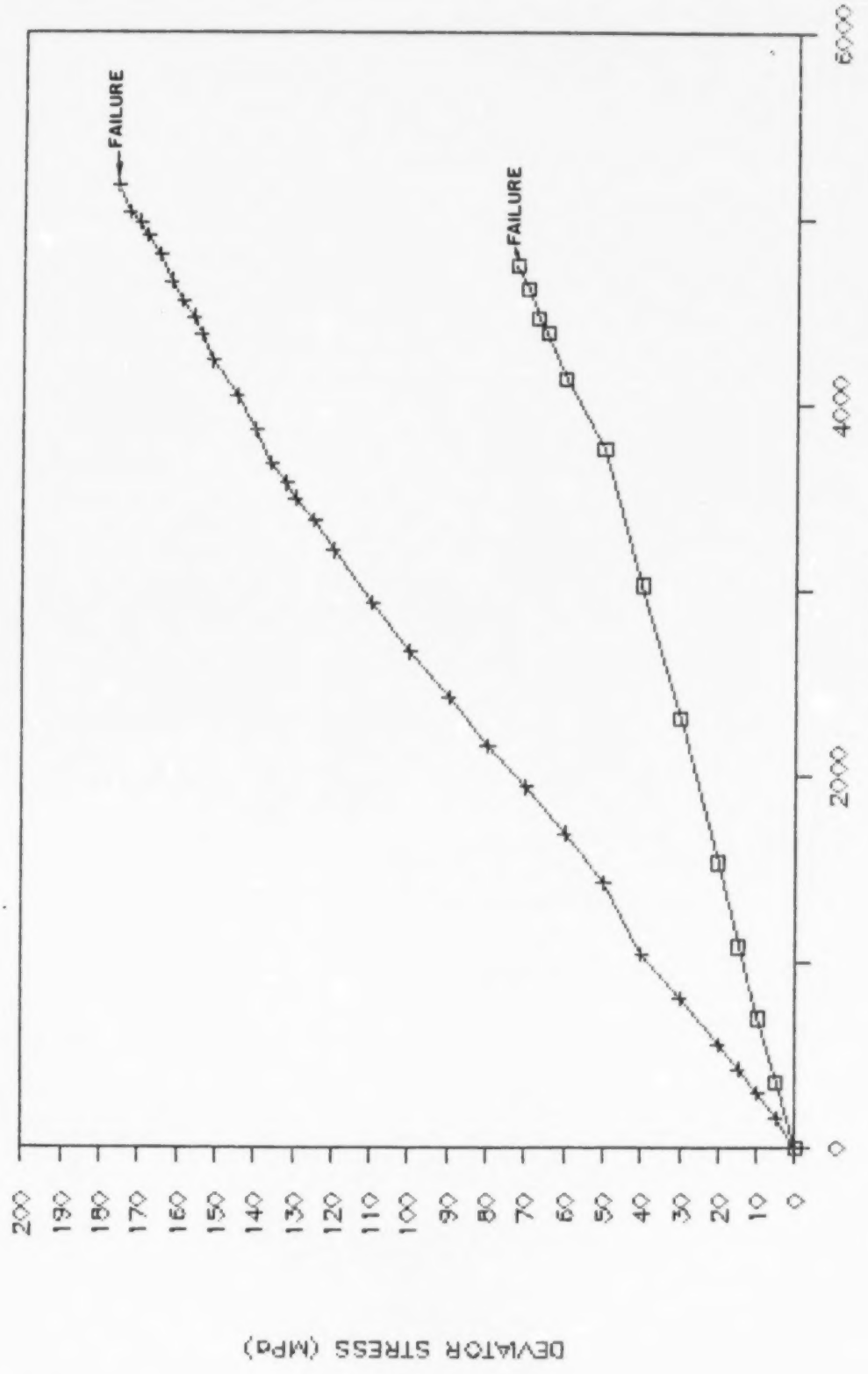

Date MAR. 15, 1985
Project 841-1287

Golder Associates

Drawn G.P.
Chkd.

VOLUMETRIC STRAIN VS. AXIAL STRAIN
SAMPLES C-129-1, C-129-9
LINGAN COLLIERY

FIGURE 4

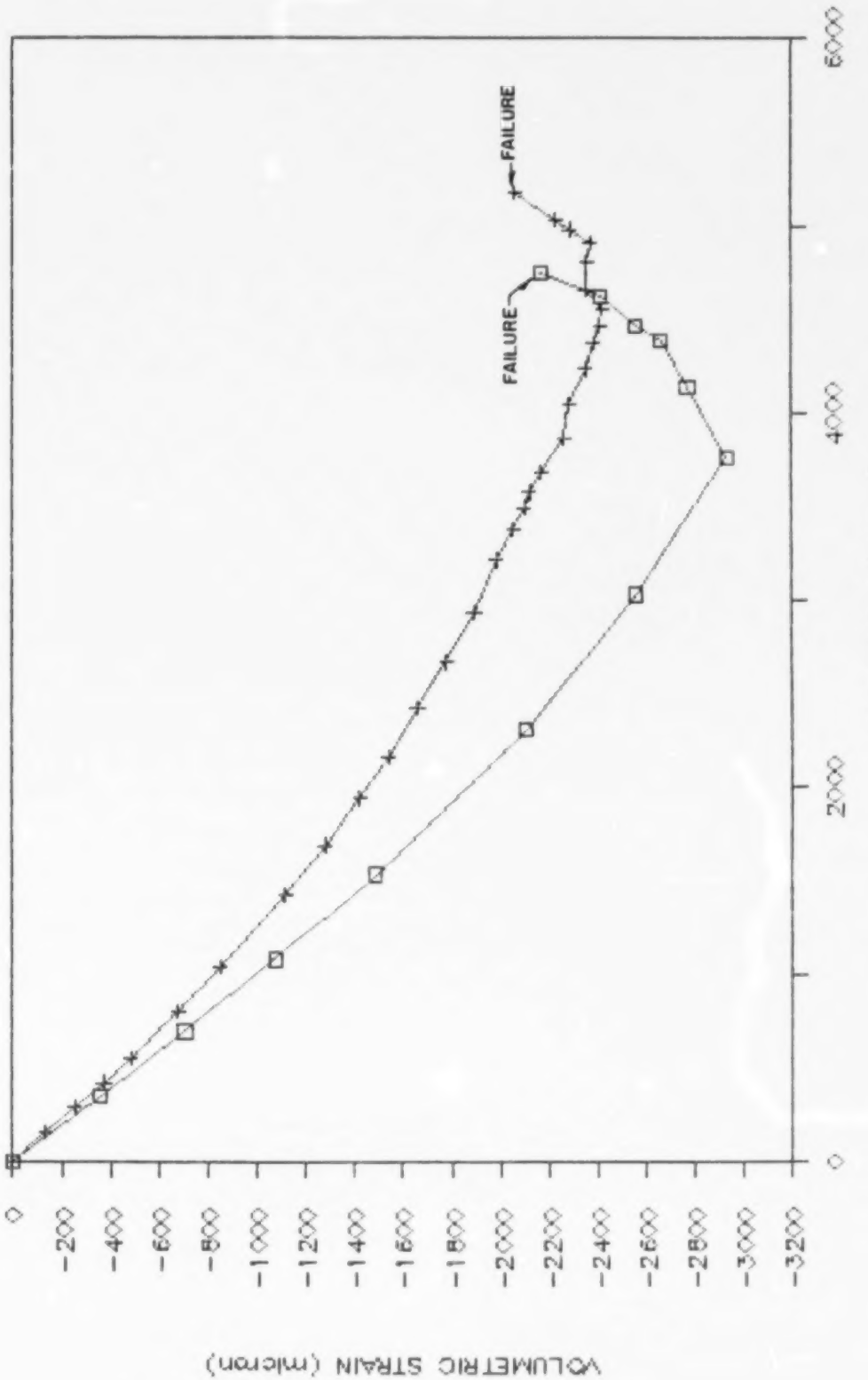

Date MAR.15.1985
Project 841-1287

Golder Associates

Drawn G.P.
Chkd.

MULTISTAGE TRIAXIAL TESTING, SANDSTONE FROM LINGAN COLLIERY

FIGURE 5

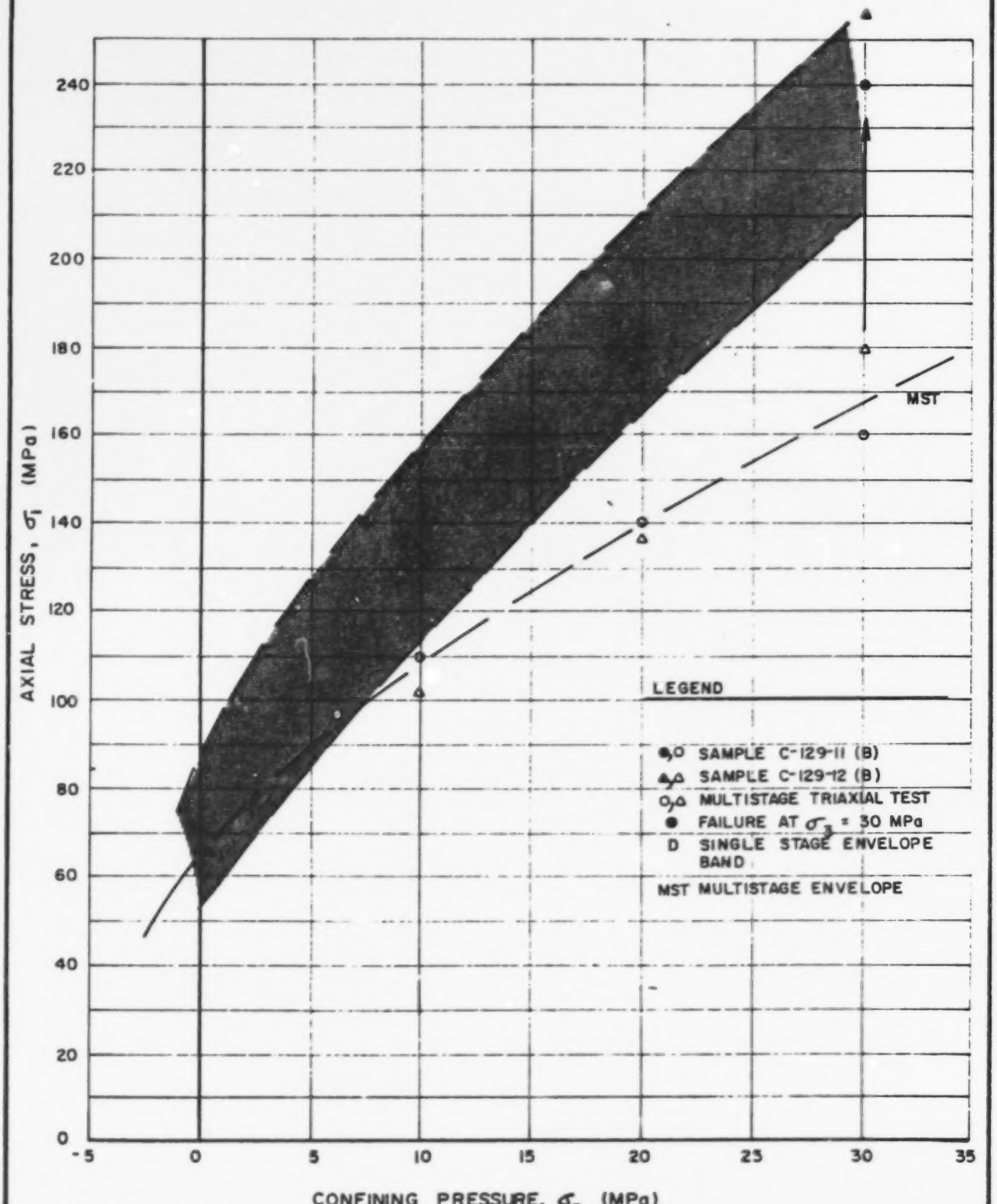

Date MAR.15, 1985
Project 841-1287

Golder Associates

Drawn G.P.
Chkd. ---

STRESS -PERMEABILITY TEST ARRANGEMENT
SAMPLES FROM LINGAN COLLIERY AND COLLIERY No. 26

FIGURE 6

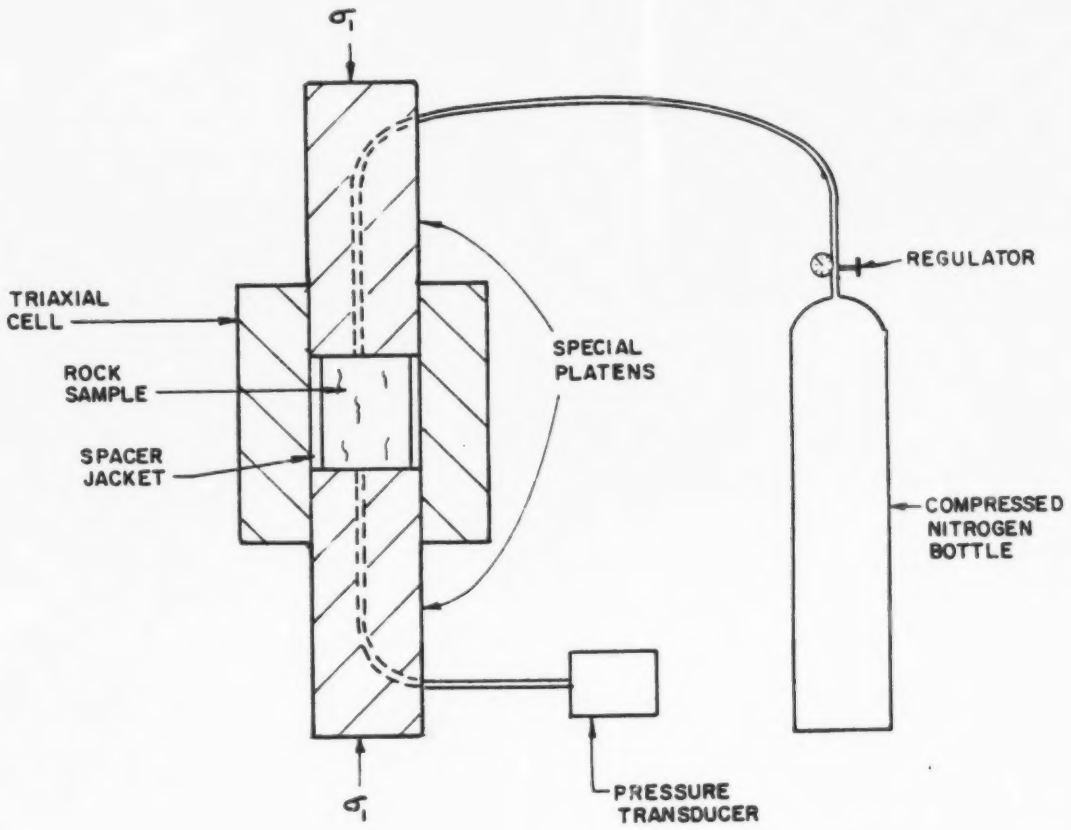

NOT DRAWN TO SCALE

Date MAR.15,1985
Project 841-1287

Golder Associates

Drawn G.P.
Chkd. GJ

STRENGTH CHARACTERISTICS OF SANDSTONE FROM No. 26 COLLIERY

FIGURE 7

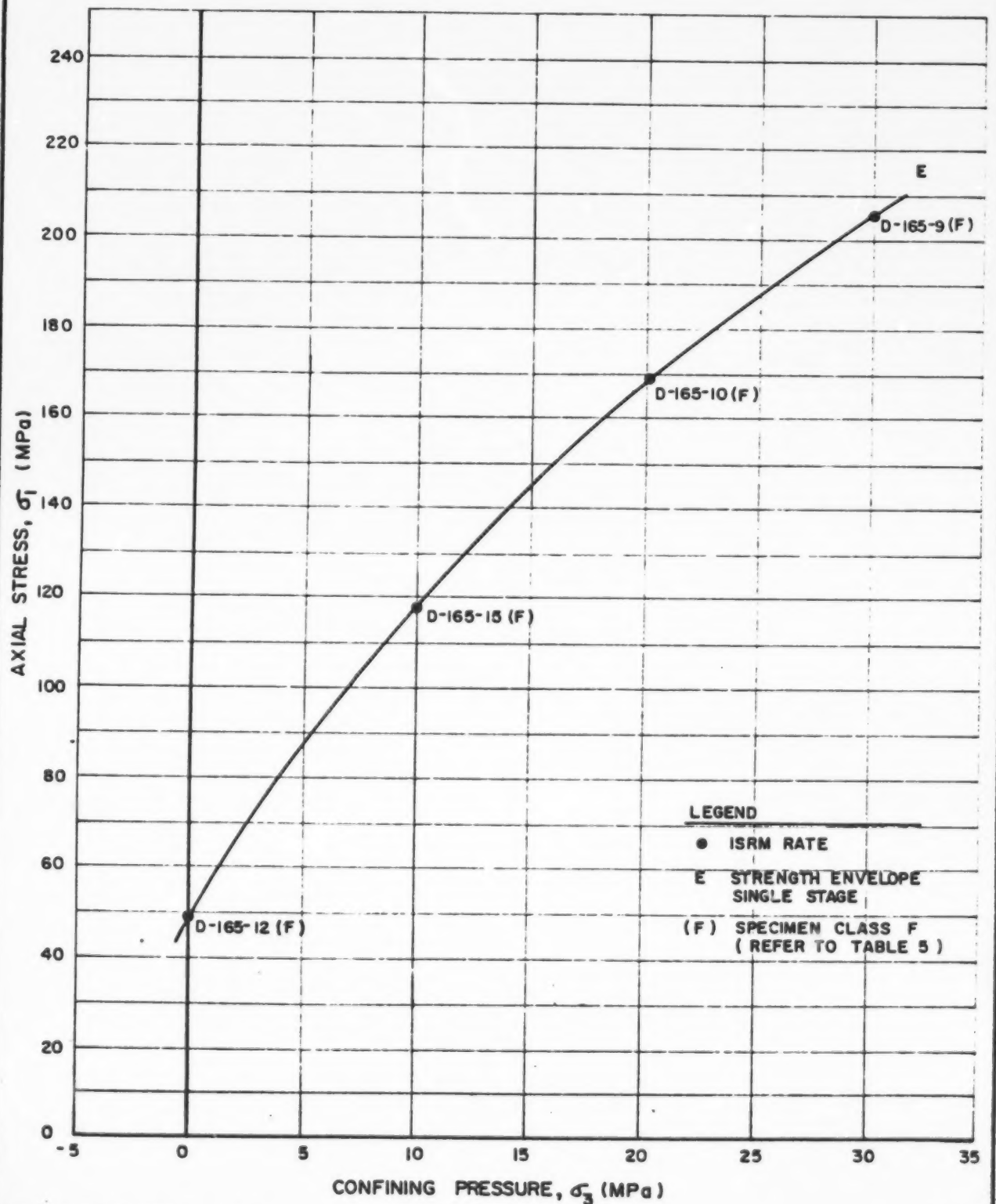

Date MAR. 15, 1985

Project 841-1287

Golder Associates

Drawn G.P.

Chkd. GJ

MULTISTAGE TRIAXIAL TESTING
SANDSTONE FROM No. 26 COLLIERY

FIGURE 8

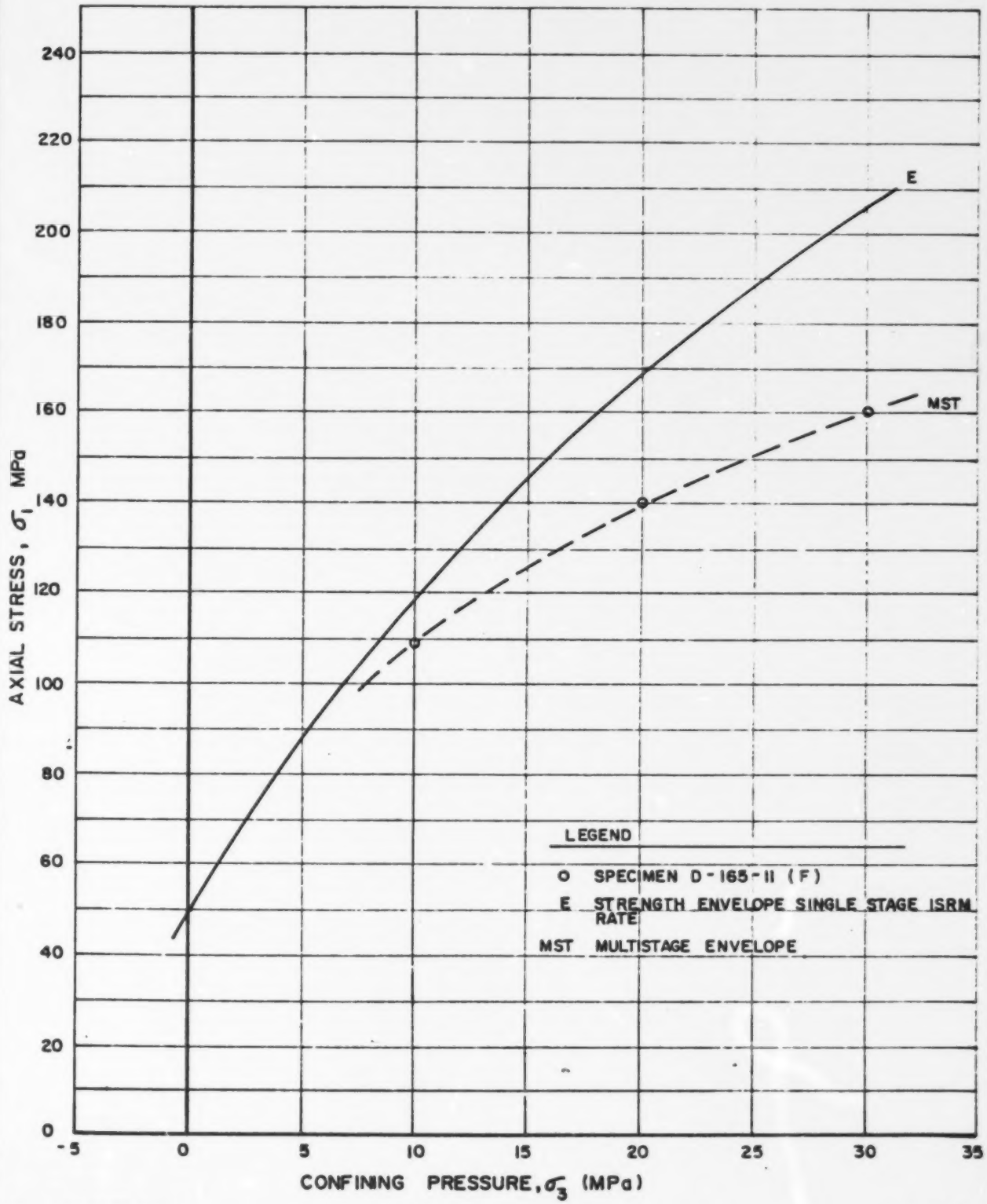

Date MAR. 15, 1985
Project 841-1287

Golder Associates

Drawn G.P.
Chkd. SJC

SIMULATION OF STRESS CHANGES ON No. 26 COLLIERY SANDSTONE

FIGURE 9

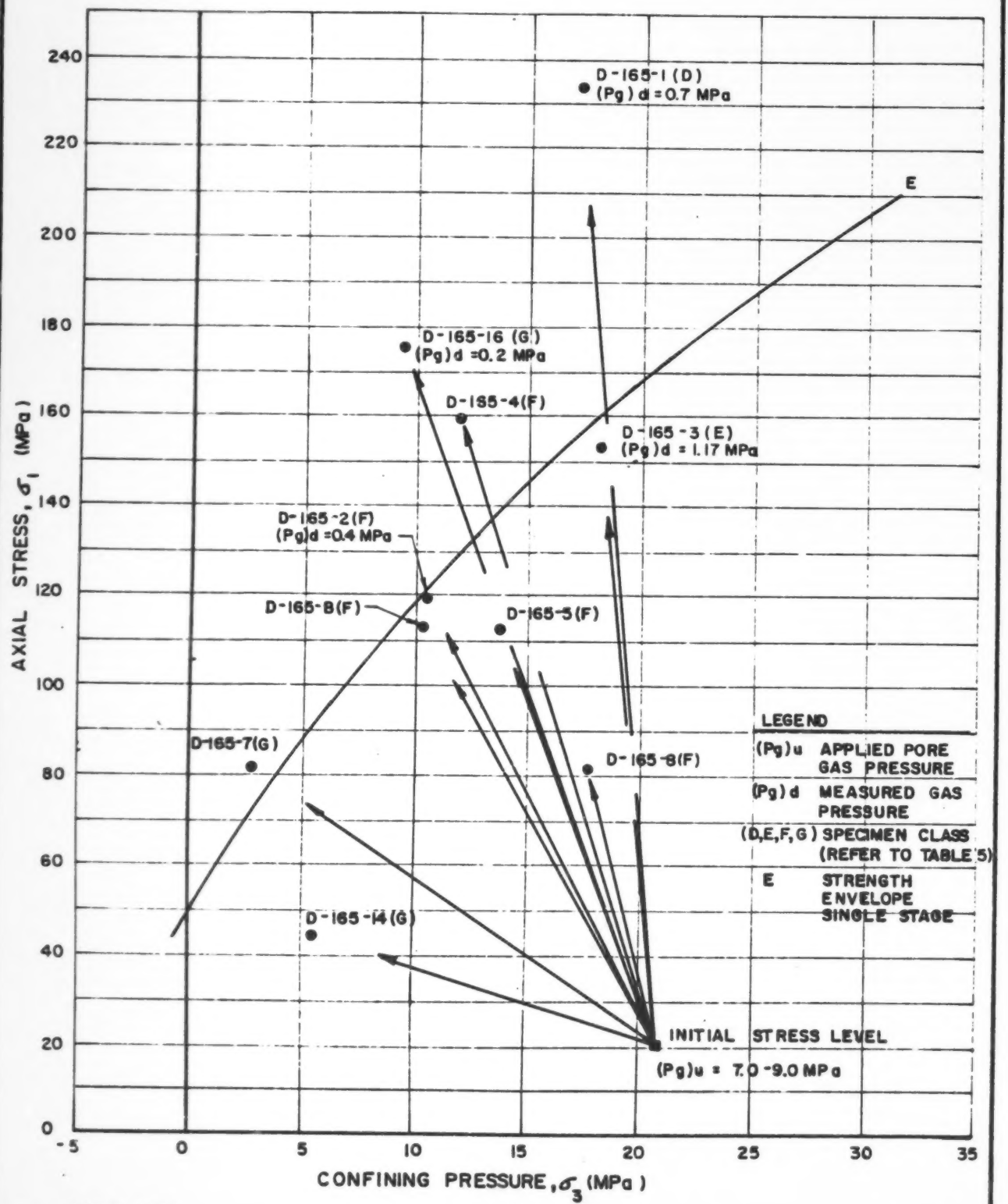

Date MAR 15, 1985

Project 841-1287

Golder Associates

Drawn G.P.

Chkd. C

UNIAXIAL LOADING UNDER PORE GAS PRESSURE, TEST ARRANGEMENT, SAMPLES FROM LINGAN MINE

FIGURE 10

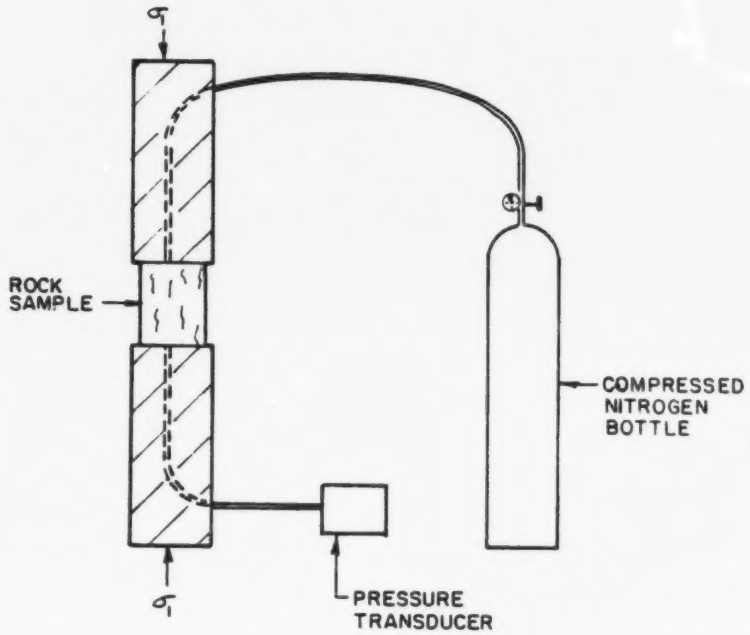

SKETCH A

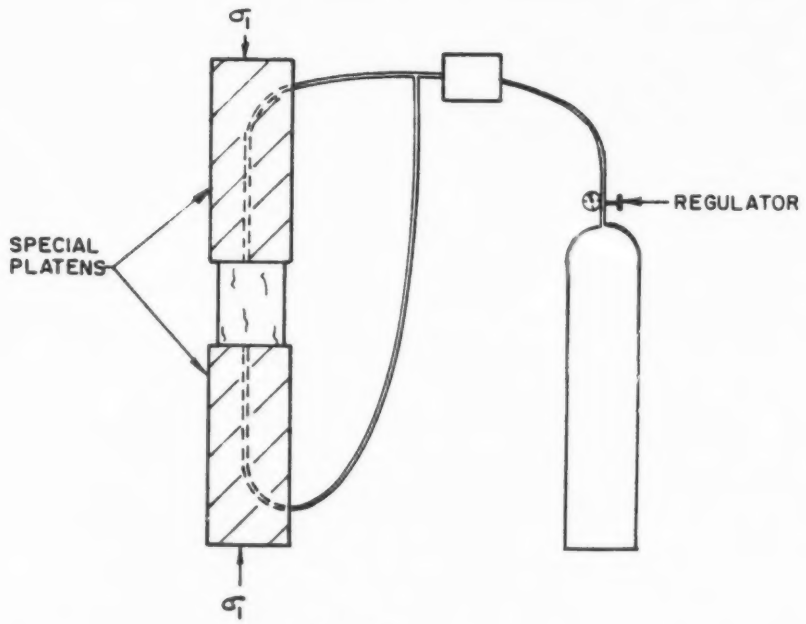

SKETCH B

NOT DRAWN TO SCALE

Date MAR. 15, 1985

Project 841-1287

Golder Associates

Drawn G.P.

Chkd.

PLATE 1: Silicon Rubber Spacer Jacket

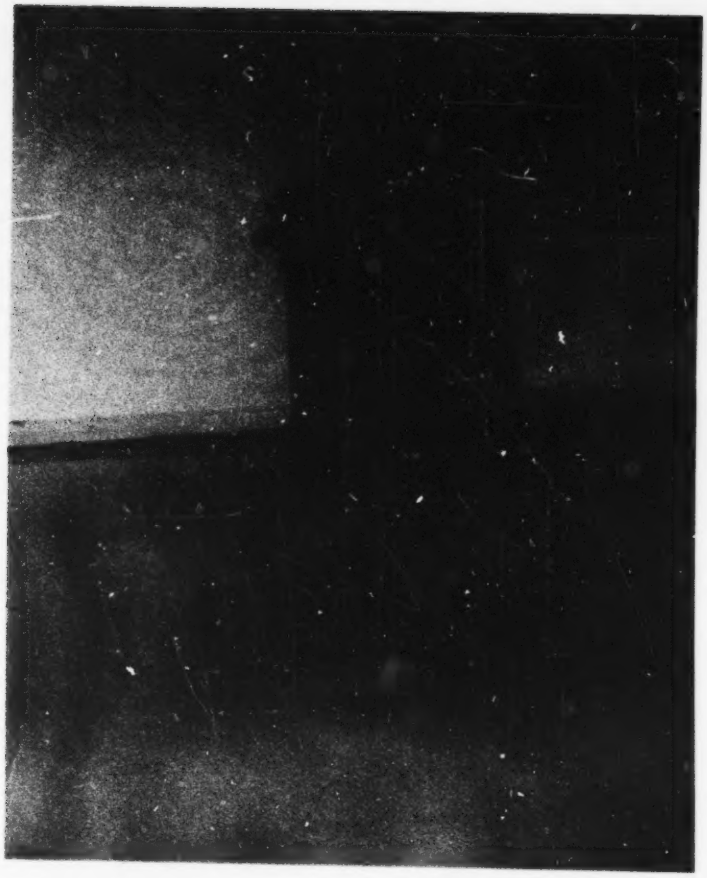

PLATE 2: Sample C-104-1 (ADD-1)

PLATE 3: Sample C-104-2 (ADD-2)

PLATE 4: Sample C-104-3 (ADD-3)

PLATE 5: Sample C-104-5 (ADD-5)

APPENDIX A

MTS σ_3 SERVO-CONTROLLED SYSTEM

Servo-Controlled System for Simultaneous Loading and Unloading

In order to simulate the stress changes around an underground excavation, tests were scheduled in Phase 1 (see Aspects 3 and 4 in Table 1 in Phase 1 report) to incorporate simultaneous changes in the principal stress (σ_1 and σ_3) applied to the specimens. Such changes were achieved by manually controlling the applied stresses.

In order to improve on the procedure of controlling the applied stress levels, a servo-controlled system for regulating the confining pressure in the triaxial cell was designed. An illustration of the main design features of this device is given on Figure A.1.

The controller which will be used to regulate the confining pressure in the traixial cell takes the command signal from the MTS controller (for example, a voltage ramp function), inverts it, and adds a d.c. voltage to it. The fixed d.c. voltage will represent some positive pressure, the amount of confining pressure at the start of the test.

As the test starts, and the axial pressure increases, the confining pressure will decay at the same rate or at a greater or lesser rate (by increasing or decreasing the gain of the amplifier). The controller regulastes the confining pressure by monitoring the pressure to the Hoek cell and dumping the excess oil from the pump into the storage reservoir.

MTS σ_3 SERVO CONTROLLED SYSTEM

FIGURE A.1

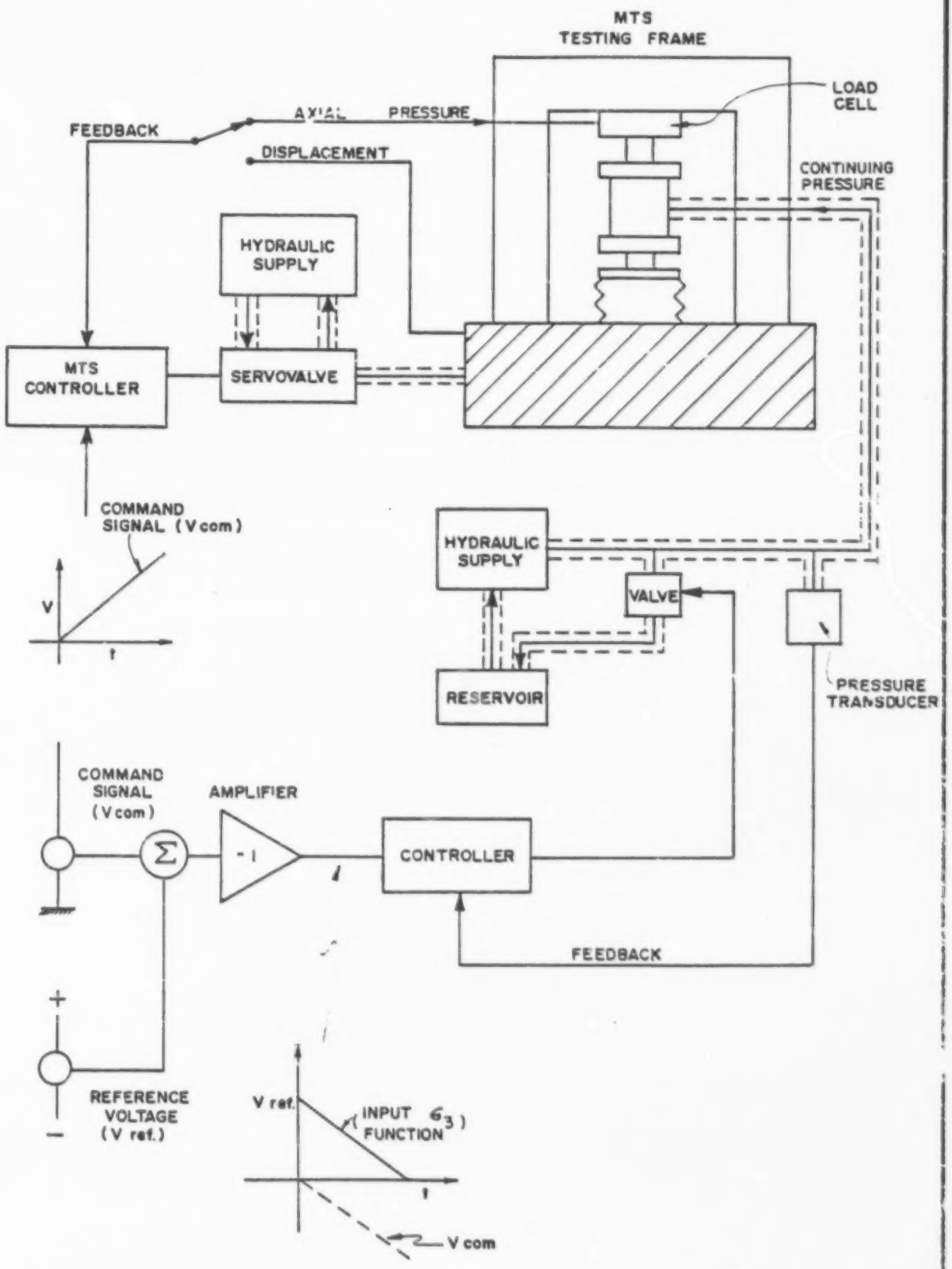

Date DEC. 12, 1984

Project 841-1287

Golder Associates

Drawn L.L.

Chkd.

POOR
QUALITY
ORIGINAL